UNIVERSITY OF CALIFORNIA,
IRVINE

The Function and Mechanism of lncRNA *Jpx* in Mouse X-Chromosome Inactivation

DISSERTATION

submitted in partial satisfaction of the requirements
for the degree of

DOCTOR OF PHILOSOPHY

in Biological Sciences

by

Sarah Lauren Carmona

Dissertation Committee:
Professor Sha Sun, Chair
Professor Kavita Arora
Professor Xing Dai
Professor Grant MacGregor
Professor Zeba Wunderlich

2018

DEDICATION

This dissertation is dedicated to three people, honoring those who supported me most throughout this journey:

Sha Sun

for support in research endeavors;

Debra Mauzy-Melitz

for support in teaching endeavors;

Danny Halim

for support in personal endeavors.

Thank you all for your patience and guidance.

TABLE OF CONTENTS

LIST OF FIGURES

LIST OF TABLES

ACKNOWLEDGMENTS

It takes a village of support to complete a PhD. I would like to express my deepest appreciation for my family, friends, and mentors who have supported me throughout this process.

First and foremost, thank you to my advisor and mentor, Dr. Sha Sun. Throughout the many challenges I have faced in graduate school, Sha has stood by my side and supported me. I truly would not have made it this far without her support and guidance. Thank you also to my thesis committee members Dr. Grant MacGregor, Dr. Kavita Arora, Dr. Zeba Wunderlich, and Dr. Xing Dai. This team of outstanding scientists has been essential to my personal growth and development as a scientist.

Thank you to Dr. Debra Mauzy-Melitz, my teaching advisor and GAANN faculty advisor. Debra has provided me countless opportunities to develop my teaching skills, participate in education research, and grow as a mentor. Her guidance has been fundamental in preparing me for a career after graduate school. Thank you also to my graduate student friends and colleagues in the GAANN fellowship group.

Thank you to my family and friends for your love, support, and understanding throughout this process. I would like to especially recognize my boyfriend Danny Halim, my sisters Shannon and Kaitlyn, my mother Angie and stepfather Terry, and my father Ron and stepmother Luisa. I would also like to thank my fellow graduate students in the department of Developmental and Cell Biology for their friendship and support. I feel so lucky to call this brilliant group of people my friends. We are all in this together.

Finally, I would like to thank the people who have directly contributed to my research. Thank you to past and current members of the Sun Laboratory, especially Heather, Ben, Tristan, and Kathy for their hard work and dedication. Thank you to Jon Neumann and Grant MacGregor of the UCI Transgenic Mouse Facility for assistance in developing transgenic mice, Adeela Syed of the UCI Optical Biology Core Facility for assistance with fluorescence microscopy, and Michael Tram for assistance with mouse genotyping. Financial support was provided by a Graduate Assistance in Areas of National Need (GAANN) fellowship from the US Department of Education, grant number P200A120207.

Text in the thesis abstract, Chapter 2 and Chapter 3 have appeared in the following publication and are used in this thesis under a Creative Commons Attribution (CC BY) license. Citation: Carmona S, Lin B, Chou T, Arroyo K, Sun S (2018) LncRNA *Jpx* induces *Xist* expression in mice using both *trans* and *cis* mechanisms. PLoS Genet 14(5): e1007378. https://doi.org/10.1371/journal.pgen.1007378.

CURRICULIM VITAE

Sarah Lauren Carmona

EDUCATION

University of California, Irvine (UCI) 2013-2018

Doctor of Philosophy, Biological Sciences

Thesis advisor: Dr. Sha Sun

Department of Developmental and Cell Biology

School of Biological Sciences

University of California, San Diego (UCSD) 2009-2013

Bachelor of Science, with Distinction, Human Biology

Minor: Psychology

Honors Thesis advisor: Dr. Douglass Forbes

Division of Biological Sciences

PEER-REVIEWED PUBLICATIONS

- **Carmona, S.,** Lin, B., Chou, T., Arroyo, K., Sun, S. LncRNA *Jpx* induces *Xist* expression in mice using both *trans* and *cis* mechanisms. PLoS Genet. 2018; 14(5): e1007378. https://doi.org/10.1371/ journal.pgen.1007378

- Karner, H. M.*, Webb, C-H.*, **Carmona, S**., Liu, Y., Lin, B., Erhard, M., Chan, D., Baldi, P., Spitale, R. C., Sun, S. Functional conservation of lncRNA *JPX* despite sequence and structural divergence. In Preparation, 2018. * denotes equal contribution.

- **Carmona, S.** and Sun, S. Strategies for lncRNA functional and mechanistic studies in mice. Review Article In Preparation, 2018.

- **Carmona, S.,** Tormanen, K., Mauzy-Melitz, D. Game of Proteins: An Interactive Board Game to Review the Secretory Pathway. In Preparation, 2018.

- Bernis, C., Swift-Taylor, B., Nord, M., **Carmona, S**., Chook, Y. M., Forbes, D. J. Transportin Acts to Regulate Mitotic Assembly Events by Target Binding rather than Ran Sequestration. Mol. Biol. Cell. 2014; 25: 992-1009.

- **Carmona, S**., Bernis, C., Forbes, D. J. Novel Karyopherin Regulation of Mitotic Assembly Events. Undergraduate Honors Thesis, UCSD Biological Sciences. 2013.

- **Carmona, S**. Honors Thesis abstract. UCSD Saltman Quarterly Undergraduate Research Journal. 2013; 10: 41.

RESEARCH EXPERIENCE

Graduate Student Researcher, UC Irvine 09/2013-07/2018

UCI School of Biological Sciences, Department of Developmental and Cell Biology

Thesis advisor: Dr. Sha Sun

- Developed a novel transgenic mouse model to study the function and mechanism of lncRNA *Jpx* in mouse X-Chromosome Inactivation.
- Assisted with other projects in the lab, including protein purification, cloning, and developing transgenic embryonic stem cells.
- Designated lab safety officer, handing all laboratory waste and safety training for new lab members.
- Invited reviewer for PLoS Genetics. Citation: PLOS Genetics 2017 Reviewer and Editorial Board Thank You. PLoS Genet 14(3): e1007265. https://doi.org/10.1371/journal.pgen.1007265

Graduate Student Researcher, Student Rotations, UC Irvine 09/2013-06/2014

Fall Rotation Advisor: Dr. Anand Ganesan, Depts. of Dermatology and Biological Chemistry

- Performed siRNA knockdowns and pigment assays to determine the role of MC1R in melanosomes.
- Prepared and sectioned mouse skin grafts, then performed immunofluorescence to study targets of the ATR pathway.

Spring Rotation Advisor: Dr. Klemens Hertel, Dept. of Microbiology and Molecular Genetics

- Studied the effects of synonymous SNPs on mRNA splicing (in HeLa cells).
- Investigated CRISPR as a method for introducing SNPs in the lab.

Undergraduate Honors Research Assistant, UC San Diego 07/2012-09/2013

UCSD Division of Biological Sciences, Section of Cellular and Developmental Biology

Advisor: Dr. Douglass J. Forbes

- Participated in the divisional honors research program: completed a year of research, wrote a thesis and presented a poster in the student research showcase.

- Conducted research on the role of nuclear transport receptors during mitosis; presented results during regular lab meetings.
- Prepared interphase and mitotic *Xenopus laevis* egg extracts for laboratory use.

Undergraduate Research Assistant, UC San Diego 08/2011-09/2012

UCSD Department of Chemistry and Biochemistry

Advisor: Dr. Patricia Jennings

- Completed cloning and mutagenesis projects; performed detailed analyses and troubleshooting of cloning projects.

LABORATORY SKILLS

Techniques

- Molecular cloning and mutagenesis, DNA sequence analysis
- PCR, RT-qPCR, Western blotting and immunoblotting, DNA, RNA and protein extraction and purification from mouse tissues, cultured cells, or a bacterial system
- siRNA knockdown
- Basic cell culture techniques (HeLa, mouse embryonic stem cells, and mouse fibroblasts)
- Basic mouse care and husbandry
- Mouse Embryonic Fibroblast (mEF) extraction, E13.5
- Mouse embryo extraction, E7.5 and 8.5
- RNA and DNA Fluorescence *in situ* hybridization (FISH)
- GST-pulldown
- Luminescent Cell Viability Assay
- *In vitro* nuclear reconstitution and mitotic spindle reconstitution
- Antibody column purification
- Basic bioinformatic database usage
- Preparation of mouse tissues samples for cryo or paraffin sectioning
- Hematoxylin & Eosin staining
- Preparation of interphase and mitotic *Xenopus laevis* egg extract
- Preparation of competent *E. coli* cells
- Preparation of mouse fibroblast cell lines from embryos

Equipment

- PCR & qPCR machine, centrifuge, spectrophotometer, sonicator, pH meter, tissue homogenizer
- Confocal Microscope (Zeiss LSM 700, 780 and Leica SP8 systems)
- Cs-137 Gamma irradiator

- Multimode detector
- Cryostat and microtome
- Knowledge of High Performance, Fast Protein, and Size Exclusion chromatography equipment

FUNDING SOURCES

Graduate Assistance in Areas of National Need (GAANN) 10/2015-07/2018

US Department of Education

Edward Steinhaus Teaching Award 2015-2016

UCI Ayala School of Biological Sciences

Graduate Student Researcher 2014-2015

University of California, Irvine

PROFESSIONAL SOCIETIES

Genetics Society of America, Member 2016

Society for Developmental Biology, Member 2015-2016

National Society of Collegiate Scholars, Member 2010-2013

CONFERENCES ATTENDED, INC. TALKS AND POSTERS PRESENTED

- Association for Biology Laboratory Education (ABLE), 06/2018. Columbus, OH.
    - Workshop (Tatarakis, D., **Carmona, S**., Lackey, K. and Mauzy-Melitz, D.): You won't believe what these scientists found! Identifying and overcoming misrepresentation of science in mainstream media

- UCI Undergraduate Research Symposium, 05/2018. Irvine, CA.
    - Poster (Arroyo, K., **Carmona, S**., Lin, B., and Sun, S.): Expression of X-linked Genes in Male and Female Mouse Embryonic Fibroblasts

- UCI RNA Symposium, 04/2018. Irvine, CA.

- Society for the Advancement of Biology Education Research (SABER), West Coast Regional Meeting, 01/2018. Irvine, CA.
    - Poster presented (**Carmona, S**., Lackey, K., Tatarakis, D. and Mauzy-Melitz, D.): Strategies for Scientific Success: A Symposium for Graduate and Postdoctoral Professional Development.

- West Coast Epigenetics Day Conference, 12/2017. Irvine, CA.

- Association for Biology Laboratory Education (ABLE), 06/2017. Madison, WI.
    - Workshop (**Carmona, S**., Tormanen, K. (co-authors) and Mauzy-Melitz, D.): Game of Proteins: An Interactive Board Game to Review the Secretory Pathway

- UCI Undergraduate Research Symposium, 05/2017. Irvine, CA.
    - Poster (Lin, B., **Carmona, S**., and Sun, S.): Elucidating lncRNA Jpx Function and Mechanism using Transgenic Mice
    - Poster (Arroyo, K., **Carmona, S**. and Sun, S.): Extraction and Analysis of Transgenic Mouse Embryonic Fibroblasts

- UCI Undergraduate Excellence in Research Symposium, 04/2017. Irvine, CA.
    - Talk (Lin, B., **Carmona, S**., and Sun, S.): Elucidating lncRNA Jpx Function and Mechanism using Transgenic Mice

- Society for Developmental Biology (SDB), West Coast Regional Conference, 03/2017. Yosemite, CA.
    - Talk (Sun, S., Ye, Q., Xu, H., **Carmona, S**., Lin, B., Cang, H.): Epigenetic Inheritance and Sperm Chromatin Visualization

- Project Kaleidoscope (PKAL) Regional Network, Southern California Regional Meeting, 03/2017. San Diego, CA.

- Society for the Advancement of Biology Education Research (SABER), West Coast Regional Meeting, 01/2017. Irvine, CA.

- The Allied Genetics Conference (TAGC), 07/2016. Orlando, FL.
    - Poster (**Carmona, S**., et al.): A Mouse Model for Understanding Epigenetic Gene Regulation by lncRNA
    - Talk (given at the Mouse Trainee Symposium): same as above.

- Association for Biology Laboratory Education (ABLE), 06/2016. Houston, TX.
    - Workshop (**Carmona, S**. and Mauzy-Melitz, D.): Strategies for a Hybrid Classroom: an Online Activity for Understanding Figures from Primary Literature

- UCI Undergraduate Research Symposium, 05/2016. Irvine, CA.
    - Poster (Lin, B., Chou, T., **Carmona, S**., et al.): Expression Profiles of Cancer Associated lncRNAs During Cell Differentiation

- UCI Department of Developmental and Cell Biology Retreat, 04/2016. Dana Point, CA.
    - Poster (**Carmona, S**.): A Mouse Model for Studying *cis* and *trans* Gene Regulation by lncRNA

- Center for Complex Biological Systems (CCBS) Retreat, 03/2016. Los Angeles, CA.
    - Poster (Karner, H., Chiu-Ho, J., **Carmona, S**., and Sun S.): Structure versus Sequence Conservation: Human Long noncoding RNA JPX and its Homology to Murine Jpx

- Southern California Evolutionary Genetics and Genomics (SCalE), Spring Meeting, 03/2014. Los Angeles, CA.
    - Poster (Karner, H., Chiu-Ho, J., **Carmona, S**., and Sun S.): Structure versus Sequence Conservation: Human Long noncoding RNA JPX and its Homology to Murine Jpx

- Abcam West Coast Epigenetics Day Conference, 02/2016. Irvine, CA.

- UCI RNA Symposium, 04/2015. Irvine, CA.

- UCI Department of Developmental and Cell Biology Retreat, 04/2015. Dana Point, CA.
    - Poster (**Carmona, S**., et al.): Elucidating lncRNA function in vivo: Jpx activates mammalian X-chromosome inactivation

- Society for Developmental Biology (SDB), West Coast Regional Conference, 03/2015. Yosemite, CA.
    - Poster (**Carmona, S**., et al.): Elucidating lncRNA function in vivo: Jpx activates mammalian X-chromosome inactivation

- Southern California Evolutionary Genetics and Genomics (SCalE), Fall Meeting, 11/2014. Los Angeles, CA.

- UCI Cancer Research Institute Symposium on Basic Cancer Research, 05/2014. Irvine, CA.

- UCSD Biological Sciences Student Research Showcase, 06/2013. La Jolla, CA.
    - Poster (**Carmona, S**., et al.): Novel Karyopherin Regulation of Mitotic Assembly Events

- American Association for the Advancement of Science (AAAS) General Meeting, 02/2010. San Diego, CA.

AWARDS & HONORS

- Charlie Drewes Waiver of Registration Grant for the 2017 ABLE Conference, 04/2017
- Selected Presenter for the 2016 TAGC Mouse Trainee Symposium, International Mammalian Genome Society (IMGS), 07/2016

- Edward Steinhaus Teaching Award, 06/2015
- Honorable Mention, NSF Graduate Research Fellowship Program, 2014-15
- UCI Cellular and Molecular Biosciences Graduate Dean Recruitment Fellowship (GDRF) Award, 02/2013
- Bachelor's Degree conferred with College Honors and Distinction in Biological Sciences, 06/2013
- UCSD Biological Sciences Student Research Showcase, poster winner for the Section of Cellular and Developmental Biology, 06/2013
- UCSD Sixth College Award for Excellence in Writing and Public Speaking, 12/2012
- San Diego Foundation Scholar (Reuben H. Fleet Scholarship), 2012-13
- Alumni Leadership Scholar (Brutten Scholarship), 2011-13

TEACHING EXPERIENCE

Developmental and Cell Biology Teaching Assistant, UC Irvine 01/2015-06/2018

- Teaching assistant for Bio Sci D104 (Developmental Biology): led a discussion/ office hours, wrote test questions, proctored and graded exams, monitored discussion board, assisted professor in-class.
- Teaching assistant for Bio Sci 75 (Human Development: Conception to Birth): gave a guest lecture on mitosis and meiosis, administered case study activities in class, held office hours, wrote test questions, proctored and graded exams, monitored discussion board, managed grade book and iclicker records.
- Teaching assistant for Bio Sci 100 (Scientific Writing): held office hours, wrote test questions, created seating chart, proctored and graded exams, monitored Piazza discussion board, monitored and graded assignments on Peerceptiv and Turnitin platforms, led an in-class discussion on experimental design, created an online activity for understanding figures from primary research articles
- Teaching assistant for Bio Sci 93 (DNA to Organisms): held weekly discussion sessions and office hours, developed active learning in-class activities, proctored and graded exams and quizzes, monitored Piazza discussion board, and assisted professor in-class.

GAANN Fellowship, UC Irvine 10/2015-07/2018

- Created an online activity for understanding figures from primary research articles (in conjunction with teaching assistant work for the Bio100 course). This work was selected and presented as a talk/ workshop at the Association for Biology Laboratory Education (ABLE) national meeting in 2016.
- Assisted in revising and teaching a lecture on data analysis and linear regression for an undergraduate upper division biology course (team taught with other GAANN fellows).
- Assisted in planning and leading the 2nd Annual GAANN Strategies for Scientific Success symposium to engage undergraduates in scientific research and encourage them to join research labs. Specifically, I created an activity entitled "What Career is Right for

You?" based on the AAAS MyIDP. I also coordinated a career speakers panel, which invited community members in various scientific fields to discuss their career in a Q&A panel.
- Assisted in planning and leading the 2nd Annual GAANN Strategies for Scientific Success: Amplify your Career Portfolio symposium. Specifically, I developed and presented two activities: one on developing hybrid lecture courses, and one on individual development planning.

Sun Laboratory, UC Irvine 08/2014-07/2018

- Mentored 4 undergraduates for Bio 199; mentored our lab manager in molecular cloning: directly mentored students (one-on-one teaching of biological concepts and lab skills), oversaw projects, assisted with troubleshooting, assisted undergraduates with their project proposals and poster presentations.
- Mentored a local high school student on basic laboratory techniques (summer, 2016) and lab etiquette.
- Mentored one undergraduate for UCI Excellence in Research; that student won the Robert Ernst Prize for Excellence in Research in the Biological Sciences.

Center for Excellence in Writing and Communication, UC Irvine 04/2018

- Received training on effective responses to student writing.

Division of Teaching Excellence and Innovation, UC Irvine 09/2017-12/2017

- Received formal teaching pedagogy training. Achieved CIRTL Associate status.

Forbes and Jennings Laboratories, UC San Diego 07/2012-09/2013

- Mentored 4 undergraduates on basic lab techniques for Bio199. Assisted in teaching cloning and basic molecular biology to new members of the Forbes lab.

Mathematics Tutor, Simi Valley, CA 2006-2009

Private Tutor, Simi Valley High School

- Tutored Geometry, Algebra I and Algebra II students of all high school grade levels and abilities.

OTHER EXPERIENCE

Pre-Medical Student Intern, Thousand Oaks, CA 06-09/2010

Office of Drs. Hayashi, Dahms, Durand, Pattee, & Vercillo.

Intern to Dr. Pierre Durand, Jr., Orthopedic Surgeon, Sports Medicine

- Observed surgeries, engaged in constant patient contact, prepared injections, and analyzed both MRI and X-Ray images.

EXTRACURRICULAR & OUTREACH ACTIVITIES

Department of Developmental and Cell Biology

Elected Student Government Member, 10/2016-07/2018

- Graduate Student Representative, 2017-18
- Social Committee Representative, 2016-17

Laguna Beach Unified School District

Volunteer, 07/2017-07/2018

- Volunteer for the Breakers Advance workshop. Hosted laboratory tours, explored different cells under the microscope, and held a hands-on pipetting and dilutions workshop

American Association of University Women (AAUW)

Volunteer, 06/2013-06/2017

- Volunteer for UCI and UCSD Tech Trek! Math and Science Camp for Eighth-grade girls. At UCSD, spoke as a professional woman in science, presented a poster regarding my undergraduate research, and held a Q&A session for common myths in everyday science and health. At UCI, hosted laboratory tours, explored different cells under the microscope, and held a hands-on pipetting and dilutions workshop.

University of California, Irvine Mathematics Department

Volunteer, 04/2016

- Volunteer for the Math CEO program, where I led middle school students through a hands-on DNA extraction from fruit.

Irvine Unified School District

Volunteer, 09/2013-12/2015

- Volunteer for the District Science Fair and for Ask-A-Scientist Night.
- Volunteer for the District Middle School Career Conference, where I presented an interactive version of Hanahan and Weinberg's Hallmarks of Cancer manuscripts (2000 & 2011) and spoke about careers in science.

Saddleback Valley Unified School District

Bio-Rad Science Ambassador, 02/2015-02/2016

- Volunteer with Trabuco Hills High School, where I preformed DNA extraction from cheek cells with biology students (materials provided by Bio-Rad Science Ambassador outreach program).

UCI MB&B STEM Education Group

Member, 09/2013-1/2016

- Monthly group hosted by the UCI Molecular Biology and Biochemistry Department which discusses STEM teaching methods and curricula in K-12 and university education.

American Cancer Society

Volunteer, 2003-2014

- Team Captain for UCI Relay For Life
- Former Team Development chair of UCSD Relay For Life
- Former Survivorship chair of UCSD Colleges Against Cancer, 2012-13
- Former Treasurer of UCSD Colleges Against Cancer, 2011-12
- Provided musical entertainment for Simi Valley and Moorpark Relay For Life

UCSD and UCI Wind Ensemble

Piccolo/ Principal Flute, 09/2009-06/2018

- Principal flute and piccolo player for the UCI Wind Ensemble, and previously for the UCSD Wind Ensemble.
- Shown continual presence for over ten years in various school, honor, and family bands.

The Pre-Medical Association of Students for Service (P.A.S.S.)

Member, 2009-2012

- Publicity Chair, 2010-11
- Co-President and Treasurer, 2011-12
- Spanning three years, I performed over 65 hours of medical-related community service in San Diego. As club co-president, I organized service events and handled club finances.

ABSTRACT OF THE DISSERTATION

The Function and Mechanism of lncRNA *Jpx* in Mouse X-Chromosome Inactivation

By

Sarah Lauren Carmona

Doctor of Philosophy in Biological Sciences

University of California, Irvine, 2018

Assistant Professor Sha Sun, Chair

Long noncoding RNA (lncRNA) have been identified in all eukaryotes but the functions and mechanisms of many lncRNA are unknown, and remain challenging to study *in vivo*. Mammalian X-Chromosome Inactivation (XCI) is regulated by lncRNA and has emerged as a model system in which to study lncRNA function. The "master regulator" of XCI is lncRNA *Xist*, which coordinates epigenetic silencing one of the two X chromosomes in females. While the primary *Xist* activating factor has been under debate, the lncRNA *Jpx* has emerged as a proposed activator. However, *Jpx*'s function and mechanism have been unclear due to conflicting findings in mouse embryonic stem cell models.

I hypothesized that *Jpx* activates *Xist* expression *in vivo*, and that it would do so using both *trans* and *cis* genetic mechanisms. To test this, I utilized two transgenes, Tg(Jpx) and Tg(Jpx, Xist), to develop a novel *Jpx* transgenic mouse model and study the function of *Jpx* in mouse XCI. I found that transgenic *Jpx* mice were viable and fertile, although transgenic male viability was lower in certain Tg(Jpx) lines. Using RT-qPCR and Fluorescence *in situ* Hybridization (FISH) in mouse embryonic fibroblasts (mEFs) and post-implantation embryos, I observed a dose-dependent relationship between *Jpx* copy number and *Xist* expression in

transgenic mice. This suggests that *Jpx* is sufficient to activate *Xist* expression *in vivo.* Further, I analyzed *Jpx*'s allelic origin with RNA and DNA FISH and observed *Jpx* using both *trans* and *cis* mechanisms to activate *Xist* expression. RT-qPCR showed reduced X-linked gene expression in male and female Tg(Jpx) mEFs, suggesting that ectopic *Xist* can induce XCI. The presence of XCI in the male may explain the reduction in transgenic male viability. Overall, I have demonstrated that *Jpx* is a *trans*- and *cis*-acting *Xist* activator in mice. In the discussion, I have provided suggestions for future studies, including live cell imaging of the *Jpx* transcript and development of a *Jpx* knockout mouse model. The work presented here provides a framework for lncRNA functional studies in mice, and will help us understand how lncRNA regulate eukaryotic gene expression.

Chapter 1

Introduction

1.1 Sex determination and dosage compensation

Sex is determined using multiple methods within the animal kingdom. For some species, such as certain fish and reptiles, environmental cues like egg incubation temperature will determine the sex of the offspring (Crews, 2003; Warner and Shine, 2008). Other species such as flies, worms, and mammals, rely on a pair of sex chromosomes for sex determination (Payer and Lee, 2008). In mammals, these sex chromosomes are the X and Y. Female mammals have two X chromosomes (XX) while males have one X and one Y chromosome (XY). These X and Y sex chromosomes originated as a pair of autosomes, but diverged through acquisition of a sex-determining gene on one of the two chromosomes (Charlesworth, 1996; Graves, 2006). Over the course of evolution, the X and Y chromosomes have further accumulated sex-specific mutations and become divergent, leading to an inherent imbalance of sex-linked gene products between genders. This genetic inequality is mitigated by dosage compensation, a process which balances gene products between sexes. Dosage compensation is not required for animals with alternative methods of sex determination, such as environmental cues. However, these animals are more sensitive to minute changes in their environment. Therefore, chromosomal sex determination is a more robust method of ensuring the viability of male and female animals. As such, several dosage compensation systems have evolved to balance sex-linked gene products in different animal species.

Flies, worms, and mammals have developed unique methods of dosage compensation (Cline and Meyer, 1996; Lucchesi et al., 2005). In Drosophila, males (XY) upregulate expression

of X-linked genes two-fold to match that of females (XX). Inversely, C. Elegans hermaphrodites (XX) downregulate expression of X-linked genes on one X chromosome to match that of males (XO). In eutherian mammals, dosage compensation is achieved by X-Chromosome Inactivation (XCI) (Payer and Lee, 2008). In this process, females (XX) transcriptionally silence one X chromosome to balance their X-linked gene products with males (XY). It is essential for animal survival that these dosage compensation systems function properly. If the compensation mechanism is compromised, the genetically unbalanced animal will not be viable.

In both the fly and mammalian systems, dosage compensation is coordinated by long noncoding RNA (lncRNA). Mammalian XCI has become a model system for understanding the structure, function, and regulation of lncRNA since multiple lncRNA regulate this process. In particular, the lncRNA *Xist* has been described as the 'master regulator' of XCI because it is the primary factor that coordinates X-linked gene silencing (Froberg et al., 2013; Payer and Lee, 2008).

1.2 Epigenetic regulation by long noncoding RNA

LncRNA: an overview

Human and mouse transcriptome analyses have painted a fascinating picture of mammalian gene regulation, and revealed that the majority of transcribed genes do not encode protein (Birney et al., 2007; Carninci et al., 2006; Djebali et al., 2012; Okazaki et al., 2002). Previously thought to be transcriptional noise, noncoding RNA are now recognized for their epigenetic gene regulatory potential (Mattick, 2007). In the last 10 years, long noncoding RNA

(lncRNA) have become a major research focus as the number of identified and functionally annotated lncRNA has grown.

LncRNA are defined as non-protein coding transcripts longer than 200 nucleotides (Derrien et al., 2012). They share many similarities to mRNA, including transcription by RNA Polymerase II (Guttman et al., 2009). They also undergo transcriptional processing events such as splicing, 5' capping, and 3' polyadenylation (Quinn and Chang, 2016). One defining feature present in mRNA but lacking in lncRNA is an open reading frame (ORF) indicating the translation start site (Dinger et al., 2008). LncRNA genes can arise *de novo* in the genome, or evolve from pseudogenes (Carvunis et al., 2012; Tautz and Domazet-lošo, 2011; Zheng et al., 2007). In the latter case, a protein coding gene loses its coding potential, but gains a functional role in gene regulation as a noncoding transcript. Evidence for pseudogenization can be found in the mammalian X-inactivation center (Xic), where a cluster of lncRNA genes have evolved functional roles in X-Chromosome Inactivation (XCI) (Jégu et al., 2017). Most notably, the *Xist* gene has acquired a central role in directing epigenetic silencing of X-linked genes during XCI (Fig. 1.1) (Duret et al., 2006; Penny et al., 1996). While lncRNA are generally expressed at lower levels compared to mRNA, they exhibit much greater cell-, tissue-, and developmental stage-specificity (Cabili et al., 2011; Derrien et al., 2012). Functional roles for lncRNA are now being analyzed within the context of epigenetics, animal development, and human disease (Batista and Chang, 2013; Khorkova et al., 2015). To this end, lncRNA have become important biomarkers for specific cancers, and their expression levels can help determine prognosis (Chen et al., 2013; Qi and Du, 2013; Wapinski and Chang, 2011).

Many lncRNA have been identified at this point, yet functional annotation has been ascribed to few (Mallory and Shkumatava, 2015). LncRNA genes generally exhibit poor

conservation at the primary sequence level (Cabili et al., 2011; Hezroni et al., 2015; Wang et al., 2004), so a direct connection between lncRNA sequence, structure and function is often unclear (Johnsson et al., 2014). Instead, RNA secondary structures have been shown to define functional outcomes (Ilik et al., 2012; Novikova et al., 2012a; Smola et al., 2016). Secondary structures, such as stem-loops, are generally conserved and have been identified as functionally relevant in the mammalian *Xist* (Fang et al., 2015; Liu et al., 2017; Smola et al., 2016) and Drosophila *roX1* lncRNA (Byron et al., 2010; Ilik et al., 2012; Quinn et al., 2014). These secondary structures can be predicted by computational analyses (Burge et al., 2013; Volders et al., 2013), or experimental techniques (Guo et al., 2016). Little is known about the role of tertiary structure in lncRNA function (Novikova et al., 2012b).

Functional outcomes have been characterized for few lncRNA (Mallory and Shkumatava, 2015). At this time, lncRNA have been described as able to bind RNA, DNA, and protein. They can act as scaffolds, conformational switches, or guides which lead proteins to target genes (Mercer and Mattick, 2013). The genetic or molecular mechanisms which these lncRNA use to enact their function are even less understood.

Model systems for assaying lncRNA function and mechanism

The majority of our knowledge regarding lncRNA structure, function and mechanism has come from computational modeling, biochemical probing, cultured cell studies, and mouse models. Several lncRNA are commonly used as models systems to understand how lncRNA may regulate gene expression, including mammalian *Xist, H19, Hotair,* and the Drosophila *roX1/2*.

The lncRNA *Xist* is the primary factor that coordinates X-Chromosome Inactivation (XCI) to achieve dosage compensation in mammals (Froberg et al., 2013; Payer and Lee, 2008). XCI has served as an excellent model system in which to study lncRNA function, mechanism, and regulation. This is because multiple lncRNA are involved in XCI, thereby demonstrating several functional roles for lncRNA. *Xist*, for example, interacts directly with the SHARP protein and Polycomb Repressive Complex 2 (PRC2) subunits (Chu et al., 2015; McHugh et al., 2015). These interactions can be used to study lncRNA-protein interactions. XCI also allows for analysis of lncRNA promoters, developmental timing, and mechanism of action. The *Xist* gene is regulated by other lncRNA, such as *Jpx* and *Tsix*, and proteins such as NANOG and RNF12 (van Bemmel et al., 2016; Jégu et al., 2017). Regulatory mechanisms at the *Xist* gene locus therefore provide an avenue to study specific lncRNA mechanisms, and how lncRNA and proteins may work together to coordinate gene expression. Finally, *Xist* is an imprinted gene, so XCI provides the opportunity to study epigenetic inheritance (Peters and Robson, 2008).

Differentiation of female mouse embryonic stem cells (mESCs) is commonly used to model XCI (Lee, 2010). Undifferentiated ESCs begin with two active X chromosomes and, through differentiation, undergo XCI to silence one X by about differentiation day 12. Different stages of XCI can be isolated for study during this differentiation process, allowing for lncRNA functional studies at the relevant time point during development. Since lncRNA are highly cell-, tissue-, and developmental stage-specific, this model system allows for study of lncRNA in the proper context. Thus, mammalian XCI is an excellent model system in which to study lncRNA function and mechanism.

Other lncRNA systems can also provide valuable functional insight for lncRNA, and help us further understand specific functions for lncRNA in XCI. For example, the gene encoding

lncRNA *H19* is an imprinted gene expressed from the maternal allele (Bartolomei et al., 1991). *H19* functions both in controlling fetal growth (Gabory et al., 2009) and as a tumor suppressor gene (Yoshimizu et al., 2008). Studies using lncRNA *H19* as a model have uncovered the existence of an imprinting control element (Gabory et al., 2009; Ripoche et al., 1997). This has helped us understand how epigenetics are inherited, and why the maternal and paternal copies of a gene may not be functionally identical (Gabory et al., 2010). Further, research on *H19* will ultimately help us understand imprinting mechanisms, such as those used by *Xist* in extraembryonic tissues.

Next, the lncRNA *Hotair* has been used as a model to study lncRNA mechanism, especially *cis*- and *trans*-diffusible gene regulatory roles. *Hotair* was initially characterized as a *trans*-acting lncRNA affecting homeobox (*Hox*) gene expression and development of the spine and wrist (Li et al., 2013; Rinn et al., 2007). However, recent reports which re-analyzed *Hotair* function in mice found a *cis*-acting mechanism with separate spinal morphology (Amandio et al., 2016). These conflicting mechanistic findings are discussed in greater detail in Chapter 4. Since *Hotair* is a relatively small, 2-exon lncRNA whose deletion shows obvious morphological defects in mice, *Hotair* has served as an attractive model system for lncRNA functional studies. These findings will help us understand lncRNA genetic mechanisms and can be applied to mechanistic roles for lncRNA in the Xic (such as *Jpx*) during *Xist* activation.

Finally, the lncRNA *roX1* and *roX2* regulate dosage compensation in male Drosophila (Ilik and Akhtar, 2009). Although these lncRNA differ in size and sequence, they are functionally redundant (Franke and Baker, 1999; Stuckenholz et al., 2003). This allows for study of functional cooperation by lncRNA. Fly dosage compensation also offers an abundance of lncRNA-protein interactions as the *roX* lncRNA must bind to MSL proteins to form the dosage

compensation complex and direct gene silencing. In terms of dosage compensation mechanisms, Drosophila balance X-linked gene expression by a two-fold increase X-linked genes in the male (Ilik and Akhtar, 2009). Interestingly, the mammalian system also experiences a two-fold increase of X-linked gene expression of the single X in the male and of the active X in the female (Payer and Lee, 2008). This X-linked upregulation takes place by an unknown mechanism and is likely necessary to balance X-linked gene dosage with that of autosomes. Therefore, understanding how flies achieve X-linked gene balance may uncover new insight into mammalian dosage compensation.

Together, these model systems provide a framework in which to understand the functional roles and mechanisms of action for unknown lncRNA. However, many questions regarding specific lncRNA function persist within each model. In particular, the regulatory mechanisms controlling *Xist* expression in XCI has remained unclear. Another lncRNA, *Jpx*, has emerged as a potential *Xist* activation factor, but its role in XCI has been under debate based on conflicting data from mouse embryonic stem cell models. In this thesis, I address this controversy by establishing the first transgenic mouse model in which to study the function and mechanism of lncRNA *Jpx* at the organismal level.

1.3 Mammalian X-Chromosome Inactivation

XCI: an overview

Mammalian X-Chromosome Inactivation (XCI) balances X-linked gene dosage between males and females by epigenetic silencing of one X chromosome in females. The process was discovered by Mary Lyon, who predicted the random inactivation and heterochromatinization of

a single X-Chromosome in female mice (observed as a Barr Body) (Lyon, 1961, 1971). Since its initial characterization, two forms of XCI have been characterized in mouse and embryonic stem cell (ESC) models: random XCI (rXCI) in the embryo proper and imprinted XCI (iXCI) in extraembryonic tissues (Wutz, 2011). The process can be conceptualized beginning in spermatogenesis, where the single X chromosome in the male is silenced for iXCI. The zygote inherits this silenced paternal X chromosome (Xp). Upon differentiation into a blastocyst, Xp undergoes a reactivation process in the inner cell mass. Shortly after, one of the two X chromosomes will randomly be selected for inactivation for rXCI. While the majority of XCI research has concentrated on rXCI in the embryo proper, many questions remain regarding this process. For example, what mechanisms control X chromosome reactivation? Once both X chromosomes are active in the early epiblast, what is the trigger for rXCI? Then, how is gene silencing regulated and what determines which genes escape inactivation? Meanwhile in the trophoblast, Xp remains silenced for the duration of gestation. While less is known about iXCI, the process shares some mechanisms with rXCI including coordinated gene silencing by *Xist*.

Both lncRNA and proteins contribute to XCI, but the 'master regulator' of XCI is lncRNA *Xist* (Fig. 1.1) (Brockdorff et al., 1992; Brown et al., 1992; Jégu et al., 2017). The *Xist* gene is located in the X inactivation center (Xic) near the center of the X chromosome. Other lncRNA genes involved in XCI flank the *Xist* gene. The mouse *Xist* transcript is 15kb (Brockdorff et al., 1992) (human *XIST* is 17kb (Brown et al., 1992)) and can be divided into functional regions characterized by repeating sequences. For example, the repeat A (RepA) sequence within *Xist*'s 5' region recruits the Polycomb Repressive Complex 2 (PRC2) during XCI (Zhao et al., 2008). Once transcribed, the *Xist* lncRNA recruits and binds to the PRC2 complex. This process is facilitated by the bivalent DNA- and RNA-binding protein YY1, which

binds to *Xist* at its repeat C region (RepC) on the chromatin and the transcript (Jeon and Lee, 2011). *Xist* then spreads across the X chromosome in *cis* (on the same chromosome from which it is transcribed) (van Bemmel et al., 2016), recruiting the PRC2 complex in the process. PRC2 then adds H3K27me3 and other histone marks to induce chromatin condensation and long-term gene silencing (Gaydos et al., 2014). Thus, *Xist* regulates epigenetic silencing of an X chromosome by coordinating the addition of repressive histone marks at specific gene loci. This activity ensures long-term, stable gene silencing throughout the animal's lifetime.

During spreading, *Xist* utilizes the three-dimensional architecture of the X chromosome to efficiently spread across the length of the X in *cis* (on the same chromosome) (Engreitz et al., 2013). *Xist* interacts with many proteins during this process (Chu et al., 2015; McHugh et al., 2015), including nuclear lamin proteins which it uses to anchor the condensing X and create a silencing compartment (Nora et al., 2012). Silencing begins with gene-rich regions near the *Xist* transcription site in the Xic. *Xist*-mediated silencing is more efficient at short ranges from the Xic (Loda et al., 2017), which is likely based on transcript half-life. Later, gene-poor regions are pulled into the silencing compartment. Four separate models exist to describe how escaping genes avoid silencing (Jégu et al., 2017), including physically separating escapee genes from the *Xist* "core" (Chow et al., 2010).

Xist's expression must be tightly regulated due to its fantastic gene silencing potential. Activation and inhibition of *Xist* expression are coordinated by lncRNA and proteins neighboring *Xist* in the Xic. The primary *Xist* inhibitory factor is the lncRNA *Tsix* (Lee and Lu, 1999). *Tsix* prevents *Xist* transcription in several ways, including modifying the *Xist* chromatin structure; recruiting DNA methyltransferase (Dnmt3a) to prevent *Xist* gene expression; and by blocking recruitment of PRC2 to newly transcribed *Xist* (Sado et al., 2005; Stavropoulos et al., 2001; Sun

et al., 2006; Zhao et al., 2008). *Tsix* itself is under regulation by lncRNA *Xite* and the chromatin insulating factor REX1 (Navarro et al., 2010; Ogawa and Lee, 2003).

Intriguingly, deleting *Tsix* from male mouse embryonic stem cells does not lead to *Xist* upregulation (Lee and Lu, 1999). This suggests that "competence factors" are necessary for activating *Xist*, in addition to the "blocking factors" which inhibit *Xist* expression. Two *Xist* activating factors have been proposed: the lncRNA *Jpx* and the E3 Ubiquitin ligase RNF12.

1.4 *Xist* activating factors and their mechanisms

Xist activation and the number of XCI events in a cell are determined by the ratio of X chromosomes to autosomes (X:A) (Barakat and Gribnau, 2012). The cell calculates this ratio by counting the number of X-encoded "numerators" and autosomal-encoded "denominators." A normal female cell will have two X chromosomes and two of each autosome, leading to a single XCI event on one of the two X chromosomes. Male cells, on the other hand, have one X chromosome per each pair of autosomes. With a ratio of 0.5, a male does not activate *Xist* expression and initiate XCI. Using this ratio, the cell is able to compensate for certain chromosomal abnormalities, such as the XXY karyotype in patients with Klinefelter's syndrome. In this case, the cell will initiate XCI on one of the two X chromosomes to balance X-linked gene dosage. Chromosome and gene copy numbers therefore play large roles in orchestrating *Xist* activation.

A "Two Factors Model" has been used to describe *Xist* activation on a molecular level, in which competence factors induce XCI on the future inactive X (Xi) while blocking factors inhibit XCI on the future active X (Xa) (Lee and Lu, 1999; Starmer and Magnuson, 2009; Sun et

al., 2013). The two competence factors that have been described in the most detail are lncRNA *Jpx* and protein RNF12. Due to conflicting observations between research groups, the primary *Xist* activating factor is under debate. As discussed below, both *Jpx* and RNF12 appear to activate *Xist* expression based on mESC models. However, RNF12 has recently been described as unnecessary for *Xist* expression in the mouse embryo (Shin et al., 2014). In this thesis, I provide transgenic mouse models to investigate the role of *Jpx* in mouse XCI, and resolve the debate regarding *Jpx* as an *Xist* activating factor *in vivo.*

The role of RNF12 in XCI

RNF12 (also called RLIM) is an E3 Ubiquitin ligase that has been shown to activate *Xist* expression in mESC models (Barakat et al., 2011). The *Rnf12* gene is located approximately 500kb upstream of *Xist*. *Rnf12* is expressed prior to XCI, correlating with a decrease in the pluripotency factor NANOG and subsequent *Xist* activation (Barakat et al., 2011). To promote *Xist* expression, RNF12 targets and Ubiquitinates REX1, a chromatin insulating factor which blocks *Xist* expression by binding to the *Xist* promoter (Fig. 1.2) (Gontan et al., 2012). Once tagged with Ubiquitin, REX1 is removed from the *Xist* promoter and degraded by the proteasome. Interestingly, deleting *Rnf12* from mESCs did not prevent XCI. In both heterozygous and homozygous *Rnf12* deletion mutants, *Xist* expression could still be detected from differentiating mESCs (Barakat et al., 2011; Jonkers et al., 2009). XCI was delayed, however, suggesting that RNF12 does indeed play a role in XCI initiation. RNF12's role in XCI has also been described by several conditional knockout studies in the mouse embryo (Shin et al., 2010, 2014; Wang et al., 2017). The knockout was performed by using a *Sox2*-driven Cre recombinase to conditionally delete *Rnf12* from the mouse epiblast. With this method, *Rnf12*

activity was specifically deleted in the embryo proper, where random XCI takes place; imprinted XCI in extraembryonic tissues was unaffected. These knockout studies have characterized RNF12 as a competency factor specifically for imprinted XCI. Random XCI proceeds in an RNF12-independent manner (Wang et al., 2017). The mechanistic differences between *Xist* activation in rXCI and iXCI are unknown, and will require further investigation. Thus, while RNF12 has been described as an *Xist*-activating factor in mESC models, careful study in the mouse has revealed that RNF12 does not specifically activate *Xist* in rXCI.

The role of Jpx *in XCI*

The lncRNA *Jpx* has also been proposed as an *Xist* activator in mESCs and, based on the work presented in this thesis, has been shown to activate *Xist* expression in the mouse. The *Jpx* gene (Just Proximal to *Xist*; also called *Enox*) is approximately 10kb upstream of *Xist*, is transcribed in the opposite direction, and contains no open reading frame (Chow et al., 2003; Chureau et al., 2002; Johnston et al., 2002). Initial studies found that *Jpx* was not developmentally regulated and was not expressed exclusively in either sex, implying that *Jpx* was a pseudogene. However, a later study which inserted an *Xist*-*Tsix*-*Xite* transgene into mESCs was unable to activate *Xist* (Lee et al., 1999). *Xist* expression could only be restored when the transgene included the region upstream of *Xist* (including *Jpx*). In addition, a chromosome conformation capture study reported *Jpx* within *Xist*'s chromatin hub, implying a functional role in *Xist* regulation (Tsai et al., 2008). These studies led to speculation that *Jpx* may be an *Xist* activating factor.

Jpx is expressed in both female and male ESCs, and its expression in females increases approximately 10- to 20-fold over the course of ESC differentiation (Tian et al., 2010). *Jpx* is specifically expressed prior to *Xist* expression, suggesting that it is indeed developmentally regulated. During XCI, *Jpx* escapes inactivation by *Xist* since it is continuously expressed from both alleles in the female cell. This is consistent with RNA Fluorescence *in situ* Hybridization (FISH) experiments, which showed *Jpx* adjacent to the *Xist* RNA cloud instead of inside it (a characteristic of genes escaping XCI) (Clemson et al., 2006; Namekawa et al., 2010). *Jpx* is relatively conserved in its 5' region (Chureau et al., 2002), and a heterozygous deletion of the 5' region—including *Jpx*'s first two exons and a CpG island in its promoter region—is lethal to female ESCs (Tian et al., 2010). *Jpx* knockout cells displayed morphological abnormalities, which increased in severity after initiation of XCI on differentiation day 4. The cells also failed to induce *Xist* expression and therefore did not undergo XCI. This viability phenotype could be rescued by addition of a BAC transgene containing *Jpx*. These data suggest that *Jpx* is necessary for proper *Xist* expression. In contrast, a deletion of *Rnf12* does not prevent XCI, but instead delays XCI by two days (Jonkers et al., 2009). The cell must be sensitive to *Jpx* copy number, since one endogenous copy of *Jpx* was not sufficient to rescue the effect in the heterozygous mutant. Interestingly, deleting *Jpx* has no effect on male ESC viability (Tian et al., 2010). This suggests a female specific effect, consistent with a role for *Jpx* in female XCI. Therefore, *Jpx* and *Tsix* likely hold antagonistic roles in activating and repressing *Xist* expression, respectively.

Jpx has been shown to influence *Xist* expression in mESCs using both *trans* and *cis* genetic mechanisms (Fig. 1.2). *Jpx*'s *trans* mechanism was demonstrated when the *Jpx* deletion phenotype was rescued with a BAC transgene (Tian et al., 2010). In this experiment, the *Jpx* transgene integrated into an autosome but was able to rescue endogenous *Xist* expression.

Therefore, *Jpx* must be a *trans*-diffusible molecule. This finding is in alignment with the discovery that a *trans*-diffusible molecule is necessary for *Xist* activation (Barakat et al., 2014). Further, posttranscriptional knockdown of *Jpx* RNA with small hairpin RNA (shRNA) recapitulates the deletion phenotype, suggesting that *Jpx* is a noncoding RNA that functions in *trans* to influence *Xist* expression and XCI. Additionally, *Jpx* was shown to act in *cis* by allele-specific RT-qPCR in *Jpx* knockout cell lines. A small subpopulation of cells survived *Jpx* knockout and completed differentiation. Allele-specific PCR then revealed an allelic skewing of *Xist* activation, and *Xist* was specifically expressed from the X chromosome with the remaining *Jpx* allele (Tian et al., 2010). Therefore, *Jpx* is able to function using both *trans* and *cis* mechanisms to activate *Xist* expression in mESCs.

It is puzzling why the remaining *Jpx* gene in the heterozygous knockout cells could not activate *Xist* in *trans* to avoid cell death. This would suggest that the cell is sensitive to *Jpx* copy number and gene dosage. *Jpx* has been shown to influence *Xist* in a dose-dependent manner, since a *Jpx* transgene retrofitted with a strong promoter can induce a corresponding increase in *Xist* expression (Sun et al., 2013). This activity may be explained by *Jpx*'s molecular mechanism within *Xist* activation (Fig. 1.2). *Jpx* has been shown to bind the zinc-finger protein CTCF, primarily with *Jpx*'s first three exons (Sun et al., 2013). The *Xist* promoter region contains three binding sites for CTCF (Navarro et al., 2006; Pugacheva et al., 2005), and CTCF occupancy is inversely correlated to *Xist* expression (Sun et al., 2013). Specifically, CTCF binds *Xist*'s P2 promoter and blocks its transcription (Sun et al., 2013). To initiate *Xist* expression, *Jpx* binds this CTCF and removes it from the *Xist* promoter (Fig. 1.2). *Jpx* and the *Xist* P2 promoter compete for CTCF binding. When *Jpx* is inactive, CTCF occupies the P2 promoter. However, when *Jpx* is highly expressed at the start of XCI, *Jpx* binds CTCF and frees the P2 promoter to allow *Xist*

transcription. Thus, *Jpx* functions in a dose-dependent manner to directly bind CTCF and remove it from the *Xist* promoter, allowing *Xist* transcription to proceed.

Interestingly, a separate study has reported conflicting results on *Jpx*'s function and mechanism in mESCs. While the aforementioned study performed a targeted deletion of *Jpx* (including the promoter and first few exons), a separate study deleted a large, 500kb deletion of the genomic region upstream of *Xist* (Barakat et al., 2014). However, despite deleting both *Jpx* and *Rnf12*, no major viability defect was observed. *Xist* expression was significantly decreased in these *Jpx-Rnf12* double knockout compared to a knockout of *Rnf12* by itself. A transgene containing *Rnf12* was able to rescue *Xist* expression only up to approximately 65% of the wildtype levels, suggesting that *Jpx* is needed for full activation of *Xist* in female mESCs. The same group later introduced a transgene containing both *Jpx* and *Ftx* (another gene proximal to *Jpx*, and reported to positively influence *Xist* expression (Chureau et al., 2011)) into mESCs (Barakat et al., 2014). This transgene failed to induce *Xist* expression, although *Jpx* expression levels were not reported. Nevertheless, this group reported a minor, *cis* role for *Jpx* in *Xist* activation. Since publication of this conflicting data in 2014, the XCI community has questioned whether *Jpx* holds a functionally significant role as an *Xist* activator.

The efficacy of ex vivo *functional studies for lncRNA*

The conflicting arguments for *Jpx*'s function in XCI have all been based on experiments performed in mESC models. However, culture conditions have been shown to influence data output within XCI research. Retinoic Acid (RA) is commonly used to induce cell differentiation in culture (Breitman et al., 1980). But differentiating ESCs with RA has been shown to skew

XCI in several ways. RA represses OCT4, which in turn leads to increased *Xist* expression in the wrong context (such as in male cells, which normally do not express any *Xist*) (Ahn and Lee, 2010). RA also directs ESC lineage to specify *Rlim* (the gene encoding RNF12) pathways. Normally over the course of differentiation, ESCs will follow an *Rlim*-independent pathway during random XCI in the embryo. Meanwhile in embryonic tissues, imprinted XCI is *Rlim*-dependent. RA directs ESC differentiation such that cells always follow an *Rlim*-dependent pathway in both tissues (Wang et al., 2017). Oxygen levels in culture also affect XCI (Lengner et al., 2010). Embryos are typically exposed to low oxygen levels in utero, about 2-8% (Fischer and Bavister, 1993), but cells grown in culture generally experience greater oxygen levels. When cultured in 7.5% O_2, differentiating ESCs showed approximately a two-fold increase in *Xist* expression in *Rlim*-dependent tissues (Wang et al., 2017). XCI kinetics were also affected, as imprinted XCI happened slower than in wildtype ESC differentiation. These examples indicate that differentiating ESCs are highly sensitive to culture conditions, and specific environmental cues can skew XCI in mESCs.

It is known that *ex vivo* (cultured cell) studies may not accurately model *in vivo* (live animal) systems. For example, as noted with RNF12, observations on RNF12's role as an *Xist* activator were conflicting between mESC and live animal models. RNF12 was required to activate *Xist* expression in differentiating mESCs (Barakat et al., 2011, 2014). Yet in a mouse model, RNF12 was not required for *Xist* expression and random XCI in the mouse embryo (Shin et al., 2014). Several functional studies of other lncRNA also reflect differences between cultured cell and live animal models. Studies which examined the role of *H19* in cancer cells reported conflicting results, both oncogenic (Barsyte-lovejoy et al., 2006; Matouk et al., 2007) and tumor suppressor (Dao et al., 1999; Frevel et al., 1999). Only upon deletion of *H19* in a

mouse did a tumor suppressor role become clear (Yoshimizu et al., 2008). In another example, the role of lncRNA *Malat1* had been extensively characterized in several cancer cell lines, and was found to regulate cell cycle progression, apoptosis and cancer metastasis (Gutschner et al., 2013). However, three independent studies deleting *Malat1* from mice found no contribution of *Malat1* to cancer phenotypes (Eissmann et al., 2012; Nakagawa et al., 2012; Zhang et al., 2012). Therefore, while culturing cells is a faster, cheaper alternative to animal models, it may not accurately reflect lncRNA function at the organismal level. Based on the conflicting arguments on *Jpx*'s function in mESCs, I decided to test if *Jpx* would have a functional role as an *Xist* activator in mice.

1.5 Establishment of transgenic mouse models to determine *Jpx*'s function and mechanism *in vivo*

Experimental design for the Jpx *transgenic mouse models*

The debate on *Jpx*'s function and mechanism within the mESC model system prompted analysis of *Jpx* in a mouse model. Prior to the work presented in this thesis, no mouse model existed for analyzing *Jpx*'s function *in vivo*. Therefore, to resolve *Jpx*'s function and mechanism *in vivo*, I developed a transgenic mouse model using two *Jpx* transgene constructs. Based on *Jpx*'s proposed mechanism in mESCs, several points were taken into consideration when designing the *Jpx* mouse model. First, I decided not to delete *Jpx* in the mouse. In one study, a *Jpx* deletion in mESCs was haploinsufficient and led to death of female ES cells during differentiation (Tian et al., 2010). I therefore hypothesized that a mouse which was missing even one copy of *Jpx* would not be viable. On the other hand, increasing *Jpx* copy number by addition

of a transgene had led to an increase in *Xist* expression in mESCs (Sun et al., 2013). No obvious morphological phenotype was reported in these ES cells. Therefore, in order to develop a viable model for initial study of *Jpx* in the mouse, I chose a gain-of-function approach and established transgenic *Jpx* mice.

In the present study, I added extra copies of the *Jpx* gene into the mouse genome to develop transgenic *Jpx* mice. This gain-of-function mouse model was designed to answer several questions. First, how does increasing *Jpx* copy number affect mouse viability? What is *Jpx*'s role in mouse XCI? Do *Jpx* and *Xist* maintain the same dose-dependent relationship *in vivo* as observed *ex vivo*? Which genetic mechanisms (*trans* or *cis*) might *Jpx* use to influence *Xist*? Does *Jpx* have a role in mouse development outside of XCI?

To address these questions, I developed transgenic mice by integrating BAC transgenes into mouse pronuclei. The two transgenes, termed Tg(Jpx) and Tg(Jpx, Xist), were developed by subcloning a region of the Xic (containing either *Jpx* or *Jpx* and *Xist* together) into BAC vectors, which are vectors capable of handling large DNA constructs. These regions were subcloned to specifically study function of the *Jpx* gene, either in isolation or coupled with its proposed target *Xist* (Fig. 3.1). The subcloning process is described further in Chapter 2 and (Sun et al., 2015). To mimic an increase in gene copy number from the same animal origin, endogenous sequences (those identical to the normal genes on the X chromosome) were used in the transgenes. However, one issue with this approach is that transgenic sequences were indistinguishable from the endogenous. Therefore, since the transcripts were identical, RT-qPCR or RNA Fluorescence *in situ* Hybridization (FISH) alone could not distinguish endogenous from transgenic expression. As described in Chapter 3, corresponding RNA and DNA FISH had to be performed using a combination of fluorescent probes to demonstrate transgenic *Jpx* expression. The transgene also

contained the regions just up- and down-stream of *Jpx* to ensure inclusion of *Jpx*'s endogenous promoter and any necessary regulatory regions. While Doxycycline-inducible systems have been used to study *Xist* function in transgenic human iPSCs (Jiang et al., 2013), the inducible system may not mimic wildtype expression levels. Therefore, to ensure that all endogenous machinery was influencing *Jpx* expression in my transgenic mice, I used endogenous *Jpx* sequences and promoters within the transgenes.

When generating transgenic mice, the transgene can be integrated randomly or at a targeted site. For this mouse model, I chose the traditional route and generated mice by pronuclear injection of transgenic DNA. While faster and cheaper, pronuclear injection also leads to random integration of transgenic DNA into the mouse genome (Ohtsuka et al., 2012). Frequently, multiple copies of the transgene are integrated into the same locus. Therefore, multiple transgenic mouse lines had to be analyzed in this study to rule out a positional effect (due to the transgene integration site or a repeat-induced gene silencing effect). Yet, random integration of multiple transgene copies into the mouse genome was also necessary for the experimental design of this study. Random integration predicts autosomal integration, rather than on a sex chromosome, which allowed for analysis of *Jpx*'s genetic mechanism. Specifically, I analyzed the *trans* effect of *Jpx* on endogenous *Xist* loci (for Tg(Jpx)), and the *cis* effect of *Jpx* on transgenic *Xist* at the transgenic integration site (for Tg(Jpx, Xist)). The integration of multiple transgene copies at a single site also allowed for analysis of a dose-dependent relationship between *Jpx* copy number and resulting *Xist* expression. Once transgenic lines were established, I performed RT-qPCR and FISH on transgenic embryonic fibroblasts and post-implantation embryos to study the function of *Jpx in vivo*.

The Tg(Jpx) and Tg(Jpx, Xist) transgenes can model Jpx *'s* trans *and* cis *genetic mechanisms*

In addition to testing a functional role for *Jpx* in *Xist* activation and XCI, the *Jpx* transgenic mice were designed to analyze *Jpx*'s genetic mechanism. Genetic mechanism defines the spatial relationship between a lncRNA's gene locus and the target gene locus, and is classified as *cis* or *trans* (Lee, 2012; Wray et al., 2003). Alternatively, molecular mechanisms typically describe biochemical processes, involving proteins or other binding partners. A *cis* genetic mechanism describes lncRNA activity at proximal distances, usually in the same locus or on the same chromosome. In my model, Tg(Jpx, Xist) depicts *Jpx* activity in *cis*, since *Jpx* can act locally on nearby transgenic *Xist*. Many lncRNA function in *cis*, with the lncRNA gene locus antisense or adjacent to its target gene (Guil and Esteller, 2012; Kapranov et al., 2007; Lee, 2012). *Xist* is classically defined as using a *cis* mechanism when targeting and silencing genes on the X chromosome (van Bemmel et al., 2016). During early embryonic development, at the start of XCI, one X chromosome in females is randomly chosen to be inactivated. *Xist* is then transcribed from and spreads along this chromosome in *cis* (Wutz et al., 2002). Importantly, *Xist* only functions in *cis* such that the remaining, active X chromosome, is unaffected. *Xist* retains a *cis* mechanism even when placed in a different chromosomal environment by means of a transgene (Lee and Jaenisch, 1997; Lee et al., 1996). In one study, the Xic (including the *Xist* gene) was inserted into one copy of chromosome 21 in human trisomy 21 induced pluripotent stem cells (iPSCs) (Jiang et al., 2013). When induced by Doxycycline, *Xist* coated the chromosome in *cis* and silenced genes on chromosome 21. Thus, when the Tg(Jpx, Xist) transgene is inserted into an autosomal locus, I expect that transgenic *Xist* RNA will induce autosomal gene silencing in *cis*, around the transgene insertion site.

Alternatively, a *trans* genetic mechanism describes lncRNA activity at distal loci. Typically, lncRNA which act in *trans* must move or diffuse across the nucleus from their site of transcription to the target locus. In my model, Tg(Jpx) depicts *Jpx* activity in *trans*, since the transcript must travel from the autosomal insertion site to endogenous *Xist* loci. In other systems, the lncRNA *Hotair* has been used to illustrate lncRNA activity in *trans*, since it is transcribed from the mouse *HoxC* cluster and can affect *HoxD* gene expression (Rinn et al., 2007). Interestingly, a more recent study which re-evaluated *Hotair*'s mechanism in mice has suggested that *Hotair* acts in *cis*, and described no activity *trans* (Amandio et al., 2016). *Jpx*'s genetic mechanism in mESCs has similarly been under debate. First, a heterozygous *Jpx* deletion results in female cell death unless rescued by a *Jpx* transgene (Tian et al., 2010). This would suggest that *Jpx* functions in *trans* to activate *Xist* expression. Interestingly, the few cells which survived cell death (without the transgene rescue) had activated *Xist* specifically on the chromosome with the remaining *Jpx* gene, as determined by allele-specific PCR. This suggests that *Jpx* is able to activate *Xist* using *cis* mechanisms. Therefore, experiments which can specifically isolate and test a lncRNA's *trans* or *cis* mechanism will be necessary to fully resolve both *Hotair*'s and *Jpx*'s mechanism of action.

With the Tg(Jpx) transgenic mouse model, I have provided the means to resolve *Jpx*'s *trans* mechanism *in vivo*. Based on random insertion of the transgene, I would expect Tg(Jpx) to integrate into an autosome. Transgenic *Jpx* therefore must act in *trans* if it affects endogenous *Xist* expression. The Tg(Jpx, Xist) transgene is also able to model *trans* activity, since transgenic *Jpx* has the option to activate *Xist* expression at endogenous sites (*trans* activity) or within the transgene (*cis* activity). Neither the *trans* nor *cis* mechanisms can be studied independently in Tg(Jpx, Xist), since both mechanisms are possible. While Tg(Jpx, Xist) can provide evidence of

cis activity, future work will be required to observe *Jpx*'s *cis* activity in isolation. Therefore, with these mouse models, Tg(Jpx) can model *Jpx*'s *trans* mechanism within *Xist* activation, while Tg(Jpx, Xist) can model *Jpx* activity in *trans* and *cis*. Using these mouse models, I have demonstrated that *Jpx* is able to activate *Xist* expression in mice using both *trans* and *cis* mechanisms.

Figure 1.1: *Xist* activity within mammalian X-Chromosome Inactivation. Cells in the female epiblast undergo X-Chromosome Inactivation (XCI) to balance X-linked gene expression between male and female individuals. At the start of XCI, *Jpx* is expressed from the future inactive X chromosome (Xi) and activates *Xist* expression, while *Tsix* is expressed from the future active X chromosome (Xa) and represses *Xist*. As development and XCI proceed, *Xist* is expressed and spreads along Xi in *cis*. *Xist* recruits PRC2 to stably silence X-linked genes through repressive histone marks. By the end of XCI, genes on Xi have been silenced while genes on Xa remain active.

Figure 1.1

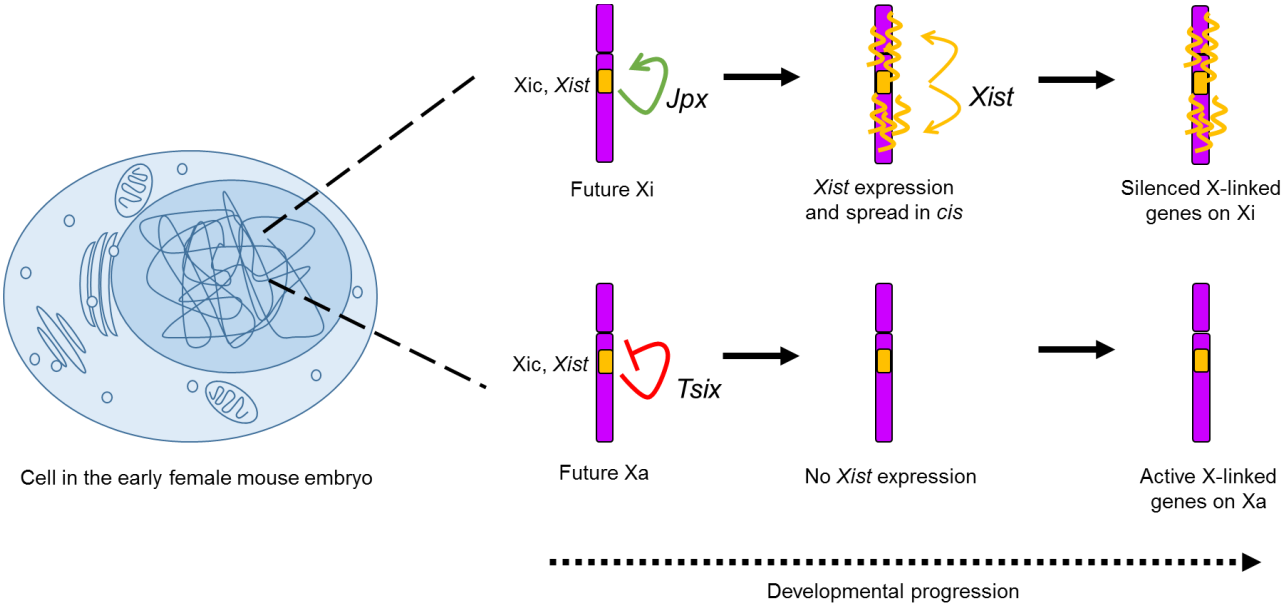
Xic, Xist
Jpx
Xist
Future Xi
Xist expression
and spread in cis
Silenced X-linked
genes on Xi
Xic, Xist
Tsix
Future Xa
No Xist expression
Active X-linked
genes on Xa
Cell in the early female mouse embryo
Developmental progression

Figure 1.2: Genetic and Molecular Mechanisms of *Jpx* and RNF12 at the *Xist* locus. A) Molecular mechanisms of *Jpx* and RNF12. Based on mESC studies, RNF12 activates *Xist* expression using *trans* mechanisms (from a separate chromosomal locus). Meanwhile, *Jpx* is able to activate *Xist* expression in *cis* (at the same chromosomal locus) and in *trans*. B) Genetic mechanisms of *Jpx* and RNF12. *Xist* expression is blocked by multiple chromatin insulator proteins, including REX1 and CTCF. To initiate XCI, RNF12 Ubiquitinates REX1 for degradation by the proteasome. Concurrently, *Jpx* binds to CTCF and removes it from the *Xist* promoter, allowing *Xist* transcription to proceed.

Figure 1.2

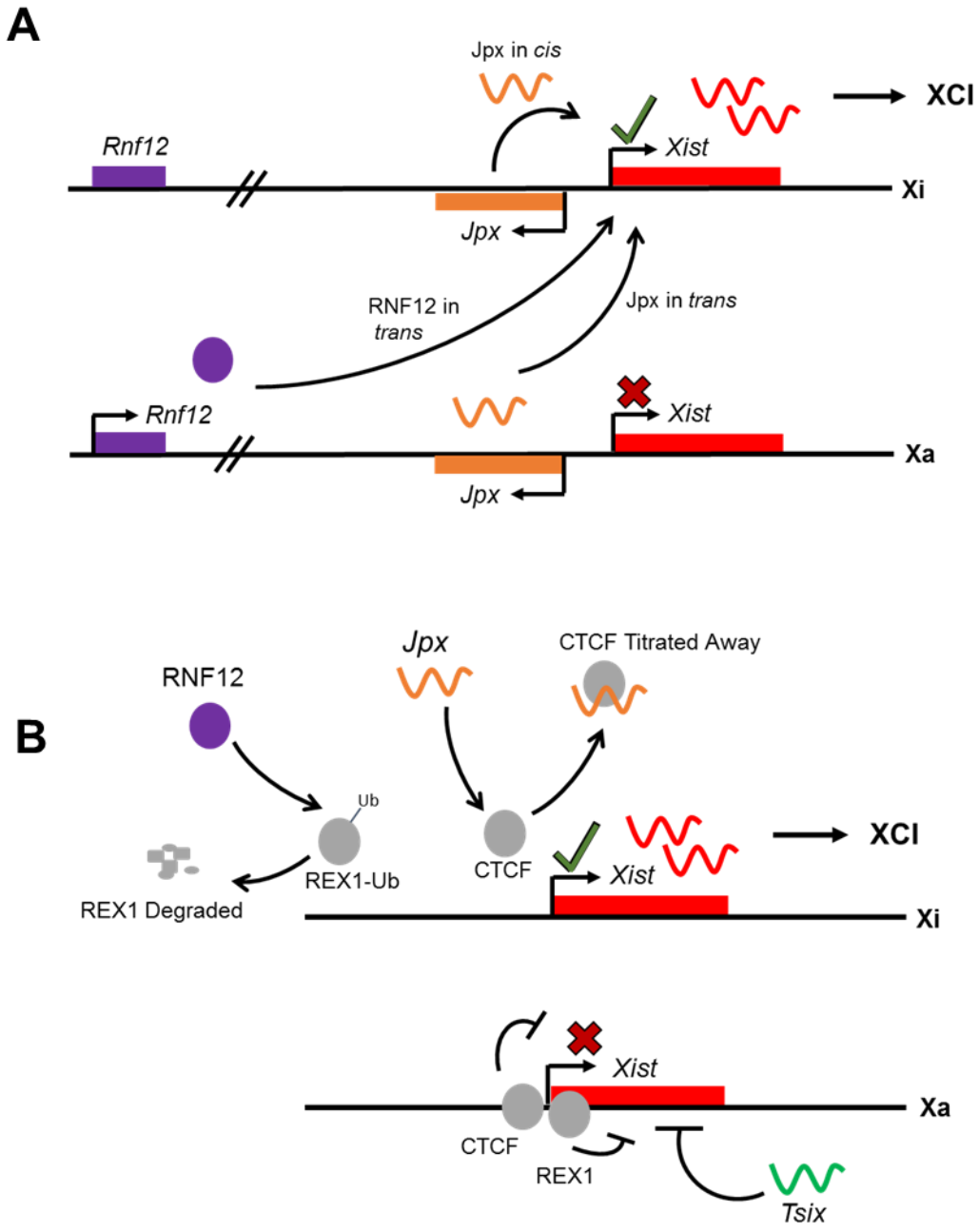
A
Jpx in cis
XCI
Rnf12
Xist
Xi
Jpx
RNF12 in trans
Jpx in trans
Rnf12
Xist
Xa
Jpx
B
RNF12
Jpx
CTCF Titrated Away
Ub
REX1-Ub
CTCF
Xist
XCI
REX1 Degraded
Xi
Xist
Xa
CTCF
REX1
Tsix

1.6 References

Ahn, J.Y., and Lee, J.T. (2010). Retinoic acid accelerates downregulation of the Xist repressor, Oct4, and increases the likelihood of Xist activation when Tsix is deficient. BMC Dev. Biol. *10*, 1–14.

Amandio, A.R., Necsulea, A., Joye, E., Mascrez, B., and Duboule, D. (2016). Hotair Is Dispensible for Mouse Development. PLoS Genet. *12*, 1–27.

Barakat, T.S., and Gribnau, J. (2012). X chromosome inactivation in the cycle of life. Development *139*, 2085–2089.

Barakat, T.S., Gunhanlar, N., Pardo, C.G., Achame, E.M., Ghazvini, M., Boers, R., Kenter, A., Rentmeester, E., Grootegoed, J.A., and Gribnau, J. (2011). RNF12 Activates Xist and Is Essential for X Chromosome Inactivation. PLoS Genet. *7*, 1–12.

Barakat, T.S., Loos, F., Van Staveren, S., Myronova, E., Ghazvini, M., Grootegoed, J.A., and Gribnau, J. (2014). The trans-activator RNF12 and cis-acting elements effectuate X chromosome inactivation independent of X-pairing. Mol. Cell *53*, 965–978.

Barsyte-lovejoy, D., Lau, S.K., Boutros, P.C., Andrulis, I.L., Tsao, M.S., Penn, L.Z., Khosravi, F., and Jurisica, I. (2006). The c-Myc Oncogene Directly Induces the H19 Noncoding RNA by Allele-Specific Binding to Potentiate Tumorigenesis. Cancer Res. *66*, 5330–5338.

Bartolomei, M.S., Zemel, S., and Tilghman, S.M. (1991). Parental imprinting of the mouse H19 gene. Nature *351*, 153–155.

Batista, P.J., and Chang, H.Y. (2013). Long noncoding RNAs: Cellular address codes in development and disease. Cell *152*, 1298–1307.

van Bemmel, J.G., Mira-Bontenbal, H., and Gribnau, J. (2016). Cis- and trans-regulation in X inactivation. Chromosoma *125*, 41–50.

Birney, E., Stamatoyannopoulos, J.A., Dutta, A., Guigó, R., Gingeras, T.R., Margulies, E.H., Weng, Z., Snyder, M., Dermitzakis, E.T., Thurman, R.E., et al. (2007). Identification and analysis of functional elements in 1% of the human genome by the ENCODE pilot project. Nature *447*, 799–816.

Breitman, T.R., Selonick, S.E., and Collins, S.J. (1980). Induction of differentiation of the human promyelocytic leukemia cell line (HL-60) by retinoic acid. Proc. Natl. Acad. Sci. *77*, 2936–2940.

Brockdorff, N., Ashworth, A., Kay, G.F., McCabe, V.M., Norris, D.P., Cooper, P.J., Swift, S., and Rastan, S. (1992). The product of the mouse Xist gene is a 15 kb inactive X-specific transcript containing no conserved ORF and located in the nucleus. Cell *71*, 515–526.

Brown, C.J., Hendrich, B.D., Rupert, J.L., Lafrenière, R.G., Xing, Y., Lawrence, J., and Willard, H.F. (1992). The human XIST gene: Analysis of a 17 kb inactive X-specific RNA that contains conserved repeats and is highly localized within the nucleus. Cell *71*, 527–542.

Burge, S.W., Daub, J., Eberhardt, R., Tate, J., Barquist, L., Nawrocki, E.P., Eddy, S.R., Gardner, P.P., and Bateman, A. (2013). Rfam 11.0 : 10 years of RNA families. Nucleic Acids Res. *41*, 226–232.

Byron, K., Cervantes, M.C., Wang, J.T.L., and Park, Y. (2010). Mining roX1 RNA in Drosophila Genomes using Covariance Models. Int. J. Comput. Biosci. *1*, 22–32.

Cabili, M.N., Trapnell, C., Goff, L., Koziol, M., Tazon-Vega, B., Regev, A., and Rinn, J.L. (2011). Integrative annotation of human large intergenic noncoding RNAs reveals global properties and specific subclasses. Genes Dev. *25*, 1915–1927.

Carninci, P., Kasukawa, T., Katayama, S., Gough, J., Frith, M.C., Maeda, N., Oyama, R., Ravasi, T., Lenhard, B., Wells, C., et al. (2006). The Transcriptional Landscape of the Mammalian Genome. Science (80-.). *309*, 1559–1563.

Carvunis, A.-R., Rolland, T., Wapinski, I., Calderwood, M.A., Yildirim, M.A., Hidalgo, C.A., Barbette, J., Santhanam, B., Brar, G.A., Simonis, N., et al. (2012). Proto-genes and de novo gene birth. Nature *487*, 370–374.

Charlesworth, B. (1996). The evolution of chromosomal sex determination and dosage compensation. Curr. Biol. *6*, 149–162.

Chen, G., Wang, Z., Wang, D., Qiu, C., Liu, M., Chen, X., Zhang, Q., Yan, G., and Cui, Q. (2013). LncRNADisease: A database for long-non-coding RNA-associated diseases. Nucleic Acids Res. *41*, 983–986.

Chow, J.C., Hall, L.L., Clemson, C.M., Lawrence, J.B., and Brown, C.J. (2003). Characterization of expression at the human XIST locus in somatic, embryonal carcinoma, and transgenic cell lines. Genomics *82*, 309–322.

Chow, J.C., Ciaudo, C., Fazzari, M.J., Mise, N., Servant, N., Glass, J.L., Attreed, M., Avner, P., Wutz, A., Barillot, E., et al. (2010). LINE-1 Activity in Facultative Heterochromatin Formation during X Chromosome Inactivation. Cell *141*, 956–969.

Chu, C., Zhang, Q.C., da Rocha, S.T., Flynn, R.A., Bharadwaj, M., Calabrese, J.M., Magnuson, T., Heard, E., and Chang, H.Y. (2015). Systematic Discovery of Xist RNA Binding Proteins. Cell *161*, 404–416.

Chureau, C., Prissette, M., Bourdet, A., Cattolico, L., Jones, L., Avner, P., and Duret, L. (2002). Comparative Sequence Analysis of the X-Inactivation Center Region in Mouse, Human, and Bovine. Genome Res. *12*, 894–908.

Chureau, C., Chantalat, S., Romito, A., Galvani, A., Duret, L., Avner, P., and Rougeulle, C. (2011). Ftx is a non-coding RNA which affects Xist expression and chromatin structure within the X-inactivation center region. Hum. Mol. Genet. *20*, 705–718.

Clemson, C.M., Hall, L.L., Byron, M., Mcneil, J., and Lawrence, J.B. (2006). The X chromosome is organized into a gene-rich outer rim and an internal core containing silenced nongenic sequences. Proc. Natl. Acad. Sci. *103*, 7688–7693.

Cline, T.W., and Meyer, B.J. (1996). VIVE LA DIFFERENCE: Males vs Females in Flies vs Worms. Annu. Rev. Genet. *30*, 637–702.

Crews, D. (2003). Sex determination: where environment and genetics meet. Evol. Dev. *5*, 50–55.

Dao, D., Walsh, C.P., Yuan, L., Gorelov, D., Feng, L., Hensle, T., Nisen, P., Yamashiro, D.J., Bestor, T.H., and Tycko, B. (1999). Multipoint analysis of human chromosome 11p15/mouse distal chromosome 7: inclusion of H19/IGF2 in the minimal WT2 region, gene specificity of H19 silencing in Wilms' tumorigenesis and methylation hyper-dependence of H19 imprinting. Hum. Mol. Genet. *8*, 1337–1352.

Derrien, T., Johnson, R., Bussotti, G., Tanzer, A., Djebali, S., Tilgner, H., Guernec, G., Martin, D., Merkel, A., Knowles, D.G., et al. (2012). The GENCODE v7 catalog of human long noncoding RNAs : Analysis of their gene structure , evolution , and expression. Genome Res. *22*, 1775–1789.

Dinger, M.E., Pang, K.C., Mercer, T.R., and Mattick, J.S. (2008). Differentiating protein-coding and noncoding RNA: Challenges and ambiguities. PLoS Comput. Biol. *4*.

Djebali, S., Davis, C.A., Merkel, A., Dobin, A., Lassmann, T., Mortazavi, A., Tanzer, A., Lagarde, J., Lin, W., Schlesinger, F., et al. (2012). Landscape of transcription in human cells. Nature *489*, 101–108.

Duret, L., Chureau, C., Samain, S., Weissenbach, J., and Avner, P. (2006). The Xist RNA Gene Evolved in Eutherians by Pseudogenization of a Protein-Coding Gene. Science (80-.). *312*, 1653–1655.

Eissmann, M., Gutschner, T., Hämmerle, M., Günther, S., Caudron-Herger, M., Gross, M., Schirmacher, P., Rippe, K., Braun, T., Zörnig, M., et al. (2012). Loss of the abundant nuclear non-coding RNA MALAT1 is compatible with life and development. RNA Biol. *9*, 1076–1087.

Engreitz, J.M., Pandya-Jones, A., McDonel, P., Shishkin, A., Sirokman, K., Surka, C., Kadri, S., Xing, J., Goren, A., Lander, E.S., et al. (2013). The Xist lncRNA exploits three-dimensional genome architecture to spread across the X chromosome. Science *341*, 1237973.

Fang, R., Moss, W.N., Rutenberg-schoenberg, M., and Simon, M.D. (2015). Probing Xist RNA Structure in Cells Using Targeted Structure-Seq. PLOS Genet. *11*, 1–29.

Fischer, B., and Bavister, B.D. (1993). Oxygen tension in the oviduct and uterus of rhesus monkeys, hamsters and rabbits. J. Reprod. Fertil. *99*, 673–679.

Franke, A., and Baker, B.S. (1999). The rox1 and rox2 RNAs are essential components of the compensasome, which mediates dosage compensation in Drosophila. Mol. Cell *4*, 117–122.

Frevel, M.A.E., Sowerby, S.J., Petersen, G.B., and Reeve, A.E. (1999). Methylation Sequencing Analysis Refines the Region of H19 Epimutation in Wilms Tumor. J. Biol. Chem. *274*, 29331–29340.

Froberg, J.E., Yang, L., and Lee, J.T. (2013). Guided by RNAs: X-inactivation as a model for lncRNA function. J. Mol. Biol. *425*, 3698–3706.

Gabory, A., Ripoche, M., Digarcher, A. Le, Watrin, F., Ziyyat, A., Forné, T., Jammes, H., Ainscough, J.F.X., Surani, M.A., Journot, L., et al. (2009). H19 acts as a trans regulator of the imprinted gene network controlling growth in mice. Development *136*, 3413–3421.

Gabory, A., Jammes, H., and Dandolo, L. (2010). The H19 locus: Role of an imprinted non-coding RNA in growth and development. BioEssays *32*, 473–480.

Gaydos, L.J., Wang, W., and Strome, S. (2014). H3K27me and PRC2 transmit a memory of repression across generations and during development. Science (80-.). *345*, 1515–1518.

Gontan, C., Achame, E.M., Demmers, J., Barakat, T.S., Rentmeester, E., van IJcken, W., Grootegoed, J.A., and Gribnau, J. (2012). RNF12 initiates X-chromosome inactivation by targeting REX1 for degradation. Nature *485*, 386–390.

Graves, J.A.M. (2006). Sex Chromosome Specialization and Degeneration in Mammals. Cell *124*, 901–914.

Guil, S., and Esteller, M. (2012). Cis-acting noncoding RNAs: friends and foes. Nat. Struct. Mol. Biol. *19*, 1068–1075.

Guo, X., Gao, L., Wang, Y., Chiu, D.K.Y., Wang, T., and Deng, Y. (2016). Advances in long noncoding RNAs: identification, structure prediction and function annotation. Brief. Funct. Genomics *15*, 38–46.

Gutschner, T., Hämmerle, M., and Diederichs, S. (2013). MALAT1 - A paradigm for long noncoding RNA function in cancer. J. Mol. Med. *91*, 791–801.

Guttman, M., Amit, I., Garber, M., French, C., Lin, M.F., Feldser, D., Huarte, M., Zuk, O., Carey, B.W., Cassady, J.P., et al. (2009). Chromatin signature reveals over a thousand highly conserved large non-coding RNAs in mammals. Nature *458*, 223–227.

Hezroni, H., Koppstein, D., Schwartz, M.G., Avrutin, A., Bartel, D.P., and Ulitsky, I. (2015). Principles of Long Noncoding RNA Evolution Derived from Direct Comparison of Transcriptomes in 17 Species. Cell Rep. *11*, 1110–1122.

Ilik, I., and Akhtar, A. (2009). roX RNAs: Non-coding regulators of the male X chromosome in flies. RNA Biol. *6*, 113–121.

Ilik, I.A., Quinn, J.J., Georgiev, P., Tavares-cadete, F., Maticzka, D., Toscano, S., Wan, Y., Spitale, R.C., Luscombe, N., Backofen, R., et al. (2012). Tandem Stem-Loops in roX RNAs Act Together to Mediate X Chromosome Dosage Compensation in Drosophila. Mol. Cell *51*, 156–173.

Jégu, T., Aeby, E., and Lee, J.T. (2017). The X chromosome in space. Nat. Rev. Genet. *18*, 377–389.

Jeon, Y., and Lee, J.T. (2011). YY1 Tethers Xist RNA to the inactive X nucleation center. Cell *146*, 119–133.

Jiang, J., Jing, Y., Cost, G.J., Chiang, J.-C., Kolpa, H.J., Cotton, A.M., Carone, D.M., Carone, B.R., Shivak, D.A., Guschin, D.Y., et al. (2013). Translating dosage compensation to trisomy 21. Nature *500*, 296–300.

Johnsson, P., Lipovich, L., Grandér, D., and Morris, K. V. (2014). Evolutionary conservation of long non-coding RNAs; Sequence, structure, function. Biochim. Biophys. Acta - Gen. Subj. *1840*, 1063–1071.

Johnston, C.M., Newall, A.E., Brockdorff, N., and Nesterova, T.B. (2002). Enox, a novel gene that maps 10 kb upstream of Xist and partially escapes X inactivation. Genomics *80*, 236–244.

Jonkers, I., Barakat, T.S., Achame, E.M., Monkhorst, K., Kenter, A., Rentmeester, E., Grosveld, F., Grootegoed, J.A., and Gribnau, J. (2009). RNF12 Is an X-Encoded Dose-Dependent Activator of X Chromosome Inactivation. Cell *139*, 999–1011.

Kapranov, P., Cheng, J., Dike, S., Nix, D.A., Duttagupta, R., Willingham, A.T., Stadler, P.F., Hertel, J., Hackermüller, J., Hofacker, I.L., et al. (2007). RNA Maps Reveal New RNA Classes and a Possible Function for Pervasive Transcription. Science (80-.). *316*, 1484–1489.

Khorkova, O., Hsiao, J., and Wahlestedt, C. (2015). Basic biology and therapeutic implications of lncRNA. Adv. Drug Deliv. Rev. *87*, 15–24.

Lee, J.T. (2010). The X as Model for RNA' s Niche in Epigenomic Regulation. Cold Spring Harb. Perspect. Biol.

Lee, J.T. (2012). Epigenetic regulation by long noncoding RNAs. Science (80-.). *338*, 1435–1439.

Lee, J.T., and Jaenisch, R. (1997). Long-range cis effects of ectopic X-inactivation centres on a mouse autosome. Nature *386*, 275–279.

Lee, J.T., and Lu, N. (1999). Targeted Mutagenesis of Tsix Leads to Nonrandom X Inactivation. Cell *99*, 47–57.

Lee, J.T., Strauss, W.M., Dausman, J.A., and Jaenisch, R. (1996). A 450 kb Transgene Displays Properties of the Mammalian X-Inactivation Center. Cell *86*, 83–94.

Lee, J.T., Lu, N., and Han, Y. (1999). Genetic analysis of the mouse X inactivation center defines an 80-kb multifunction domain. Proc. Natl. Acad. Sci. *96*, 3836–3841.

Lengner, C.J., Gimelbrant, A.A., Erwin, J.A., Cheng, A.W., Guenther, M.G., Welstead, G.G., Alagappan, R., Frampton, G.M., Xu, P., Muffat, J., et al. (2010). Derivation of Pre-X Inactivation Human Embryonic Stem Cells under Physiological Oxygen Concentrations. Cell *141*, 872–883.

Li, L., Liu, B., Wapinski, O.L., Tsai, M.C., Qu, K., Zhang, J., Carlson, J.C., Lin, M., Fang, F., Gupta, R.A., et al. (2013). Targeted Disruption of Hotair Leads to Homeotic Transformation and Gene Derepression. Cell Rep. *5*, 3–12.

Liu, F., Somarowthu, S., and Pyle, A.M. (2017). Visualizing the secondary and tertiary architectural domains of lncRNA RepA. Nat. Chem. Biol. *13*, 282–289.

Loda, A., Brandsma, J.H., Vassilev, I., Servant, N., Loos, F., Amirnasr, A., Splinter, E., Barillot, E., Poot, R.A., Heard, E., et al. (2017). Genetic and epigenetic features direct differential efficiency of Xist-mediated silencing at X-chromosomal and autosomal locations. Nat. Commun. *8*.

Lucchesi, J.C., Kelly, W.G., and Panning, B. (2005). Chromatin Remodeling in Dosage Compensation. Annu. Rev. Genet. *39*, 615–653.

Lyon, M. (1961). Gene action in the X-chromosome of the mouse (mus musculus L.). Nature

190, 576–581.

Lyon, M. (1971). Possible Mechanisms of X Chromosome Inactivation. Nat. New Biol. *232*, 229–232.

Mallory, A.C., and Shkumatava, A. (2015). LncRNAs in vertebrates: Advances and challenges. Biochimie *117*, 3–14.

Matouk, I.J., Degroot, N., Mezan, S., Ayesh, S., Abu-lail, R., Hochberg, A., and Galun, E. (2007). The H19 Non-Coding RNA Is Essential for Human Tumor Growth. PLoS One *2*, e845, 1–15.

Mattick, J.S. (2007). A new paradigm for developmental biology. J. Exp. Biol. *210*, 1526–1547.

McHugh, C.A., Chen, C.-K., Chow, A., Surka, C.F., Tran, C., McDonel, P., Pandya-Jones, A., Blanco, M., Burghard, C., Moradian, A., et al. (2015). The Xist lncRNA interacts directly with SHARP to silence transcription through HDAC3. Nature *521*, 232–236.

Mercer, T.R., and Mattick, J.S. (2013). Structure and function of long noncoding RNAs in epigenetic regulation. Nat. Struct. Mol. Biol. *20*, 300–307.

Nakagawa, S., Ip, J.Y., Shioi, G., Tripathi, V., Zong, X., Hirose, T., and Prasanth, K. V. (2012). Malat1 is not an essential component of nuclear speckles in mice. RNA *18*, 1487–1499.

Namekawa, S.H., Payer, B., Huynh, K.D., Jaenisch, R., and Lee, J.T. (2010). Two-Step Imprinted X Inactivation: Repeat versus Genic Silencing in the Mouse. Mol. Cell. Biol. *30*, 3187–3205.

Navarro, P., Page, D.R., Avner, P., and Rougeulle, C. (2006). Tsix-mediated epigenetic switch of a CTCF-flanked region of the Xist promoter determines the Xist transcription program. Genes Dev. *20*, 2787–2792.

Navarro, P., Oldfield, A., Legoupi, J., Festuccia, N., Dubois, A., Attia, M., Schoorlemmer, J., Rougeulle, C., Chambers, I., and Avner, P. (2010). Molecular coupling of Tsix regulation and pluripotency. Nature *468*, 457–461.

Nora, E.P., Lajoie, B.R., Schulz, E.G., Giorgetti, L., Okamoto, I., Servant, N., Piolot, T., van Berkum, N.L., Meisig, J., Sedat, J., et al. (2012). Spatial partitioning of the regulatory landscape of the X-inactivation centre. Nature *485*, 381–385.

Novikova, I. V., Hennelly, S.P., and Sanbonmatsu, K.Y. (2012a). Structural architecture of the human long non-coding RNA, steroid receptor RNA activator. Nucleic Acids Res. *40*, 5034–5051.

Novikova, I. V., Hennelly, S.P., and Sanbonmatsu, K.Y. (2012b). Sizing up long non-coding RNAs: Do lncRNAs have secondary and tertiary structure? Bioarchitecture *2*, 189–199.

Ogawa, Y., and Lee, J.T. (2003). Xite, X-Inactivation Intergenic Transcription Elements that Regulate the Probability of Choice. Mol. Cell *11*, 731–743.

Ohtsuka, M., Miura, H., Sato, M., Kimura, M., Inoko, H., and Gurumurthy, C.B. (2012). PITT: Pronuclear Injection-Based Targeted Transgenesis, a Reliable Transgene Expression Method in Mice. Exp. Anim. *61*, 489–502.

Okazaki, Y., Furuno, M., Kasukawa, T., Adachi, J., Bono, H., Kondo, S., Nikaido, I., Osato, N., Saito, R., Suzuki, H., et al. (2002). Analysis of the mouse transcriptome based on functional annotation of 60,770 full-length cDNAs. Nature *420*, 563–573.

Payer, B., and Lee, J.T. (2008). X Chromosome Dosage Compensation: How Mammals Keep the Balance. Annu. Rev. Genet. *42*, 733–772.

Penny, G., Kay, G., Sheardown, S., Rastan, S., and Brockdorff, N. (1996). Requirement for Xist in X chromosome inactivation. Nature *379*, 131–137.

Peters, J., and Robson, J.E. (2008). Imprinted noncoding RNAs. Mamm. Genome *19*, 493–502.

Pugacheva, E.M., Tiwari, V.K., Abdullaev, Z., Vostrov, A.A., Flanagan, P.T., Quitschke, W.W., Loukinov, D.I., Ohlsson, R., and Lobanenkov, V. V (2005). Familial cases of point mutations in the XIST promoter reveal a correlation between CTCF binding and pre-emptive choices of X chromosome inactivation. Hum. Mol. Genet. *14*, 953–965.

Qi, P., and Du, X. (2013). The long non-coding RNAs, a new cancer diagnostic and therapeutic gold mine. Mod. Pathol. *26*, 155–165.

Quinn, J.J., and Chang, H.Y. (2016). Unique features of long non-coding RNA biogenesis and function. Nat. Rev. Genet. *17*, 47–62.

Quinn, J.J., Ilik, I.A., Qu, K., Georgiev, P., Chu, C., Akhtar, A., and Chang, H.Y. (2014). Revealing long noncoding RNA architecture and functions using domain-specific chromatin isolation by RNA purification. Nat. Biotechnol. *32*, 933–940.

Rinn, J.L., Kertesz, M., Wang, J.K., Squazzo, S.L., Xu, X., Brugmann, S.A., Goodnough, L.H., Helms, J.A., Farnham, P.J., Segal, E., et al. (2007). Functional Demarcation of Active and Silent Chromatin Domains in Human HOX Loci by Noncoding RNAs. Cell *129*, 1311–1323.

Ripoche, M.A., Kress, C., Poirier, F., and Dandolo, L. (1997). Deletion of the H19 transcription unit reveals the existence of a putative imprinting control element. Genes Dev. *11*, 1596–1604.

Sado, T., Hoki, Y., and Sasaki, H. (2005). Tsix Silences Xist through Modification of Chromatin Structure. Dev. Cell *9*, 159–165.

Shin, J., Bossenz, M., Chung, Y., Ma, H., Byron, M., Taniguchi-Ishigaki, N., Zhu, X., Jiao, B., Hall, L.L., Green, M.R., et al. (2010). Maternal Rnf12/RLIM is required for imprinted X-chromosome inactivation in mice. Nature *467*, 977–981.

Shin, J., Wallingford, M.C., Gallant, J., Marcho, C., Jiao, B., Byron, M., Bossenz, M., Lawrence, J.B., Jones, S.N., Mager, J., et al. (2014). RLIM is dispensable for X-chromosome inactivation in the mouse embryonic epiblast. Nature *511*, 86–89.

Smola, M.J., Christy, T.W., Inoue, K., Nicholson, C.O., Friedersdorf, M., Keene, J.D., Lee, D.M., Calabrese, J.M., and Weeks, K.M. (2016). SHAPE reveals transcript-wide interactions, complex structural domains, and protein interactions across the Xist lncRNA in living cells. Proc. Natl. Acad. Sci. U. S. A. 201600008.

Starmer, J., and Magnuson, T. (2009). A new model for random X chromosome inactivation. Development *136*, 1–10.

Stavropoulos, N., Lu, N., and Lee, J.T. (2001). A functional role for Tsix transcription in blocking Xist RNA accumulation but not in X-chromosome choice. Proc. Natl. Acad. Sci. U. S. A. *98*, 10232–10237.

Stuckenholz, C., Meller, V.H., and Kuroda, M.I. (2003). Functional Redundancy Within roX1, a Noncoding RNA Involved in Dosage Compensation in Drosophila melanogaster. Genetics *164*, 1003–1014.

Sun, B.K., Deaton, A.M., and Lee, J.T. (2006). A Transient Heterochromatic State in Xist Preempts X Inactivation Choice without RNA Stabilization. Mol. Cell *21*, 617–628.

Sun, S., Del Rosario, B.C., Szanto, A., Ogawa, Y., Jeon, Y., and Lee, J.T. (2013). Jpx RNA Activates Xist by Evicting CTCF. Cell *153*, 1537–1551.

Sun, S., Payer, B., Namekawa, S., An, J.Y., Press, W., Catalan-Dibene, J., Sunwoo, H., and Lee, J.T. (2015). Xist imprinting is promoted by the hemizygous (unpaired) state in the male germ line. Proc. Natl. Acad. Sci. *112*, 14415–14422.

Tautz, D., and Domazet-lošo, T. (2011). The evolutionary origin of orphan genes. Nat. Rev. Genet. *12*, 692–702.

Tian, D., Sun, S., and Lee, J.T. (2010). The long noncoding RNA, Jpx, Is a molecular switch for X chromosome inactivation. Cell *143*, 390–403.

Tsai, C.L., Rowntree, R.K., Cohen, D.E., and Lee, J.T. (2008). Higher order chromatin structure at the X-inactivation center via looping DNA. Dev. Biol. *319*, 416–425.

Volders, P., Helsens, K., Wang, X., Martens, L., Gevaert, K., Vandesompele, J., and Mestdagh, P. (2013). LNCipedia : a database for annotated human lncRNA transcript sequences and structures. Nucleic Acids Res. *41*, 246–251.

Wang, F., McCannell, K.N., Bošković, A., Zhu, X., Shin, J.D., Yu, J., Gallant, J., Byron, M., Lawrence, J.B., Zhu, L.J., et al. (2017). Rlim-Dependent and -Independent Pathways for X Chromosome Inactivation in Female ESCs. Cell Rep. *21*, 3691–3699.

Wang, J., Zhang, J., Zheng, H., Li, J., Liu, D., Li, H., Samudrala, R., Yu, J., and Wong, G.K.-S. (2004). Mouse transcriptome: Neutral evolution of 'non-coding' complementary DNAs. Nature *431*, 1–2.

Wapinski, O., and Chang, H.Y. (2011). Long noncoding RNAs and human disease. Trends Cell Biol. *21*, 354–361.

Warner, D.A., and Shine, R. (2008). The adaptive significance of temperature-dependent sex determination in a reptile. Nature *451*, 566–569.

Wray, G.A., Hahn, M.W., Abouheif, E., Balhoff, J.P., Pizer, M., Rockman, M. V, and Romano, L.A. (2003). The Evolution of Transcriptional Regulation in Eukaryotes. Mol. Biol. Evol. *20*, 1377–1419.

Wutz, A. (2011). Gene silencing in X-chromosome inactivation: advances in understanding facultative heterochromatin formation. Nat. Rev. Genet. *12*, 542–553.

Wutz, A., Rasmussen, T.P., and Jaenisch, R. (2002). Chromosomal silencing and localization are

mediated by different domains of Xist RNA. Nat. Genet. *30*, 167–174.

Yoshimizu, T., Miroglio, A., Ripoche, M., Gabory, A., Vernucci, M., Riccio, A., Terris, B., Dandolo, L., and Colnot, S. (2008). The H19 locus acts in vivo as a tumor suppressor. Proc. Natl. Acad. Sci. *105*, 12417–12422.

Zhang, B., Arun, G., Mao, Y.S., Lazar, Z., Hung, G., Bhattacharjee, G., Xiao, X., Booth, C.J., Wu, J., Zhang, C., et al. (2012). The lncRNA malat1 is dispensable for mouse development but its transcription plays a cis-regulatory role in the adult. Cell Rep. *2*, 111–123.

Zhao, J., Sun, B.K., Erwin, J.A., Song, J.-J., and Lee, J.T. (2008). Polycomb Proteins Targeted by a Short Repeat RNA to the Mouse X Chromosome. Science (80-.). *322*, 759–756.

Zheng, D., Frankish, A., Baertsch, R., Kapranov, P., Reymond, A., Choo, S.W., Lu, Y., Denoeud, F., Antonarakis, S.E., Snyder, M., et al. (2007). Pseudogenes in the ENCODE regions : Consensus annotation, analysis of transcription, and evolution. Genome Res. *17*, 839–851.

Chapter 2

Materials and Methods

2.1 Materials and Methods

Ethics Statement

Mice were housed at the University of California, Irvine and handled according to Institutional Animal Care and Use Committee (IACUC) guidelines. Animal Use Protocol number: 2013-3109.

Transgenic embryonic stem cells

The Tg(Jpx, Xist) transgene was subcloned from BAC 388K20, a BAC8 transgene (Augui et al., 2007; Sun et al., 2015) via ET-Cloning. The transgene was introduced into male (J1) and female (16.7) ES cells by electroporation, and positive clones were picked under neomycin antibiotic (G418, Geneticin, Gibco, Life Technology) selection. DNA FISH was used to confirm stable transgene integration. Control cells were obtained from a parallel electroporation procedure using a pSKYneo+ plasmid, which does not contain any X chromosome sequence but provides the same neomycin resistance to selected clones. Mouse ES cells were differentiated as described previously (Sun et al., 2013). Briefly, female ES cells were grown on male embryonic fibroblast feeders and in the presence of Leukemia Inhibitory Factor (LIF). To differentiate ES cells into Embryoid Bodies (EBs), LIF was removed from the media. Cells were imaged every 4 days from 0-12 days of differentiation.

Generation of transgenic mice

The Tg(Jpx) and Tg(Jpx, Xist) transgene constructs were subcloned from a BAC8 transgene (Augui et al., 2007; Sun et al., 2015). DNA was purified using a Macherey-Nagel NucleoBond Xtra BAC kit. Pronuclear injection of DNA into B6SJLF1/J donor embryos was performed at the UCI Transgenic Mouse Facility. Transgenic founder animals were crossed with C57BL/6J wildtype mice to establish individual transgenic lines. Crosses performed were WT/WT x TG/WT (TG: Transgenic; founders of both sexes were obtained and used as transgenic donors). Mice were identified as transgenic by genomic PCR on toe DNA digested overnight in 100uL Lysis buffer + Proteinase K. Two primer sets were used in PCR: BAC8 (primes to the vector sequence to determine if the mouse is transgenic (Sun et al., 2015)) and UBEX/Y (primes to the UBEX or UBEY gene to determine mouse sex (Senner et al., 2011)). For primer sequences, see Table 3.1.

Quantitative PCR

To determine transgene copy number, genomic DNA was isolated and purified from lysed toe tissue and primed for genomic *Jpx* and *Xist* genes. Presence of the transgene was also confirmed by priming to the BAC8 vector (Sun et al., 2015). Transgene copy number was determined by normalizing the genomic *Jpx* and *Xist* copy numbers to the X-linked *Hprt* gene (internal control) and comparing to the wildtype male or female samples. To measure RNA expression, cultured E13.5 mEFs or minced embryo tissue (E7.5/ 8.5) were homogenized in TRIzol Reagent (Invitrogen); chloroform and isopropanol were used to extract and precipitate RNA; and the RNA was treated with TURBO DNaseI (Life Technology) before reverse transcription with Maxima Reverse Transcriptase (Thermo Fisher). For E7.5 tissues with very low RNA yield, reverse transcription was instead performed using a SuperScript III Reverse Transcriptase (Thermo Fisher). qRT-PCR was then performed on a BioRad CFX96 Real-Time

PCR system. *Jpx* and *Xist* primers targeted mature transcripts. *Gapdh* expression was used as an internal control (Payer et al., 2013). For primer sequences, see Table 3.1.

Mouse embryonic fibroblast (mEF) extraction

Mouse mating was timed such that embryos were extracted on embryonic day 13.5 (E13.5). Once the pregnant dame was sacrificed, her uterine horns were removed and placed in PBS 1x on ice. Each pup was then removed from the uterus, placenta, and finally the yolk sac. Using forceps, each pup's head was removed and used for genotyping (with the BAC8 and UBEX/Y primers). The organs (lungs, heart, liver, GI tract) were removed and the body cavity (containing fibroblasts) was diced and stored overnight in 0.25% Trypsin-EDTA (Gibco, Life Technologies) at 4ºC. The next day, tissue chunks were digested for 20 minutes at 37ºC and filtered through a 70μm nylon Falcon cell strainer (Fisher). The cells were then plated on a 10cm plate and passaged once to select for live mEFs. Half of the culture was then resuspended in TRIzol Reagent for RNA extraction and qRT-PCR while the other half was cryopreserved or cultured further for FISH.

Post-implantation embryo extraction

Mouse mating was timed such that embryos were extracted on embryonic day 7.5 (E7.5) or day 8.5 (E8.5) as described in (Behringer et al., 2014). Briefly, whole embryos were isolated from the pregnant mother's uterus and separated from the decidua. If present, Reichert's membrane was removed by quickly placing the embryo in 0.25% Trypsin-EDTA, then pulling the sticky membrane apart with forceps. Using a scalpel and a dissecting microscope, the embryo was cut to separate the embryo proper from the extra-embryonic tissues. For embryos used in FISH, the embryo proper was minced well with the scalpel and soaked in 0.25% Trypsin-EDTA

(Gibco, Life Technologies) for approximately 1 hour at 4°C. The embryonic tissues were then digested for 10 minutes at 37°C and homogenized via pipetting, then cytospun onto two slides per embryo and fixed in 4% paraformaldehyde. For embryos used in qRT-PCR, the embryo proper was homogenized directly in TRIzol Reagent (Invitrogen). RNA was extracted as described above. E8.5 RNA was treated with TURBO DNaseI (Life Technologies) before reverse transcription with Maxima Reverse Transcriptase (Thermo Fisher Scientific). E7.5 RNA was reverse transcribed using SuperScript III First Strand Synthesis kit (Thermo Fisher Scientific). qRT-PCR was then performed as described above.

Fluorescence in situ *Hybridization (FISH)*

Fluorescent Cyanine3 (Enzo Life Sciences) and Fluorescein (eEnzyme) probes were made using a Nick Translation Kit (Roche) and column purified (GE Healthcare). RNA FISH, DNA FISH, and combined RNA-DNA FISH were performed as described in (Lee and Lu, 1999; Namekawa and Lee, 2011; Zhang et al., 2007). For each procedure, cells were cytospun onto slides and fixed in 4% paraformaldehyde. Cells grown in culture were diluted to 100,000 cells per spot on the slide. Early embryo samples were split in half after digestion with Trypsin/ homogenization and spun onto two slides, each with one spot of cells.

RNA FISH: probes incubated with cells on slides for 16 hrs at 37°C, and FISH images were collected on a Zeiss LSM 700 or LSM 780 confocal microscope and analyzed with Volocity software (PerkinElmer); the cell positions for each RNA FISH image were recorded so that the same cells were imaged for the sequential DNA FISH. DNA FISH: cells on the same slides were treated with RNase A to degrade RNA, followed by treatment with 70% formamide 2XSSC at 80°C to denature DNA; probes hybridized 16 hrs at 42°C and DNA FISH images were collected on the same microscope and analyzed with Volocity.

Combined RNA-DNA FISH: performed as described previously (Lee and Lu, 1999). Briefly, slides were treated with 70% formamide 2XSSC at 80^{o}C to denature DNA, without any RNase A treatment, followed by probe hybridization for 16 hrs at 42^{o}C. Combined RNA-DNA FISH images were collected on a Nikon Eclipse 90i microscope and analyzed with Volocity.

Statistical analyses

Binomial test: compare transgenic and wildtype mouse viability; Female vs. Male and TG vs. WT outcomes are expected at equal ratios based on the breeding scheme WT/WT x TG/WT; N mice used is listed in Fig. 3.2C. Paired student *t*-test: compare female and male average viability ratios; N mice used is listed in Fig. 3.2C. One tailed, unpaired student *t*-test: compare WT and TG expression levels; analysis performed on average expression of ≥2 mEF littermates (N. animals in each category, see Fig. 3.2E); Standard error of the mean is also displayed in Figures 3.2D, 3.5B, 3.5C, 3.9D, 3.9E. Chi-square test: compare number of cells with and without *Jpx* or *Xist* RNA clouds in transgenic and wildtype mEFs; N cells and clouds counted is listed in Figs. 3.8B and 3.9A.

Reagent and Mouse Strain Availability

Sperm from the 10 transgenic mouse strains have been cryopreserved with the UCI Transgenic Mouse Facility. Two TG/WT males were provided for each line. Their fertility and ability to pass on the transgene was checked by mating the males with a WT/WT female and genotyping the pups. Transgenic lines can be reconstituted with the TMF by microinjecting sperm into B6SJLF1/J oocyte donors and backcrossing the lines with C57BL/6J, as was done to develop the line initially.

Generation of transgenic Jpx-*PP7 ES Cells*

In preparation for live cell imaging, the endogenous *Jpx* gene was tagged with the PP7 repeat region in female *Tsix* TST +/- ES cells. The X^{129} chromosome in this line has a mutated copy of the *Tsix* gene, and will always induce *Xist* and undergo XCI (Ogawa et al., 2008). Endogenous *Jpx* was targeted using CRISPR with two separate guide RNA specific for genomic mouse *Jpx*. ES cells were transfected with the CRISPR/ Cas9 machinery using the following schema: transfection with donor DNA, followed by transfection with guide RNA and Cas9 the following day. Two samples underwent an additional round of transfection, either repeated over the course of two days or a single day of donor DNA + guide RNA and Cas9 transfection. The donor DNA plasmid contained the PP7 sequence surrounded by homologous sequences to *Jpx*'s Exon 3. Transfection was performed with Lipofectamine 2000 (Thermo Fisher) and 2.5μg donor DNA. Cas9 then cut the endogenous DNA at Exon 3 and inserted the PP7 donor DNA via homologous recombination. Individual colonies were picked to select for homogenous clones and were grown on 24-well plates until confluent. Half of the colony was then cryo preserved for future growth while the other half was spun down and reserved for RNA extraction and RT-qPCR.

2.2 References

Augui, S., Filion, G.J., Huart, S., Nora, E., Guggiari, M., Maresca, M., Stewart, A.F., and Heard, E. (2007). Sensing X Chromosome Pairs Before X Inactivation via a Novel X-Pairing Region of the Xic. Science (80-.). *318*, 1632–1637.

Behringer, R., Gertsenstein, M., Nagy, K.V., and Nagy, A. (2014). Isolating Postimplantation Embryos. In Manipulating the Mouse Embryo, 4th Edition, pp. 159–166.

Lee, J.T., and Lu, N. (1999). Targeted Mutagenesis of Tsix Leads to Nonrandom X Inactivation. Cell *99*, 47–57.

Namekawa, S.H., and Lee, J.T. (2011). Detection of nascent RNA, single-copy DNA and protein localization by immunoFISH in mouse germ cells and preimplantation embryos. Nat. Protoc. *6*, 270–284.

Ogawa, Y., Sun, B.K., and Lee, J.T. (2008). Intersection of the RNA interference and X-inactivation pathways. Science (80-.). *320*, 1336–1341.

Payer, B., Rosenberg, M., Yamaji, M., Yabuta, Y., Koyanagi-Aoi, M., Hayashi, K., Yamanaka, S., Saitou, M., and Lee, J.T. (2013). Tsix RNA and the germline factor, PRDM14, link X reactivation and stem cell reprogramming. Mol. Cell *52*, 805–818.

Senner, C.E., Nesterova, T.B., Norton, S., Dewchand, H., Godwin, J., Mak, W., and Brockdorff, N. (2011). Disruption of a conserved region of Xist exon 1 impairs Xist RNA localisation and X-linked gene silencing during random and imprinted X chromosome inactivation. Development *138*, 1541–1550.

Sun, S., Del Rosario, B.C., Szanto, A., Ogawa, Y., Jeon, Y., and Lee, J.T. (2013). Jpx RNA Activates Xist by Evicting CTCF. Cell *153*, 1537–1551.

Sun, S., Payer, B., Namekawa, S., An, J.Y., Press, W., Catalan-Dibene, J., Sunwoo, H., and Lee, J.T. (2015). Xist imprinting is promoted by the hemizygous (unpaired) state in the male germ line. Proc. Natl. Acad. Sci. *112*, 14415–14422.

Zhang, L.F., Huynh, K.D., and Lee, J.T. (2007). Perinucleolar Targeting of the Inactive X during S Phase: Evidence for a Role in the Maintenance of Silencing. Cell *129*, 693–706.

Chapter 3

LncRNA *Jpx* induces *Xist* expression in mice using both *trans* and *cis* mechanisms

3.1 Abstract

Mammalian X chromosome dosage compensation balances X-linked gene products between sexes and is coordinated by the long noncoding RNA (lncRNA) *Xist*. Multiple *cis* and *trans*-acting factors modulate *Xist* expression; however, the primary competence factor responsible for activating *Xist* remains a subject of dispute. The lncRNA *Jpx* is a proposed competence factor, yet it remains unknown if *Jpx* is sufficient to activate *Xist* expression in mice. Here, we utilize a novel transgenic mouse system to demonstrate a dose-dependent relationship between *Jpx* copy number and ensuing *Jpx* and *Xist* expression. By localizing transcripts of *Jpx* and *Xist* using RNA Fluorescence *in situ* Hybridization (FISH) in mouse embryonic cells, we provide evidence of *Jpx* acting in both *trans* and *cis* to activate *Xist*. Our data contribute functional and mechanistic insight for lncRNA activity in mice, and argue that *Jpx* is a competence factor for *Xist* activation *in vivo*.

3.2 Author Summary

Long noncoding RNA (lncRNA) have been identified in all eukaryotes but mechanisms of lncRNA function remain challenging to study *in vivo*. A classic model of lncRNA function and mechanism is X-Chromosome Inactivation (XCI): an essential process which balances X-linked gene expression between male and female mammals. The "master regulator" of XCI is lncRNA *Xist*, which is responsible for silencing one of the two X chromosomes in females. Another lncRNA, *Jpx*, has been proposed to activate *Xist* gene expression in mouse embryonic

stem cells; however, no mouse models exist to address *Jpx* function *in vivo*. In this study, we developed a novel transgenic mouse system to demonstrate the regulatory mechanisms of lncRNA *Jpx*. We observed a dose-dependent relationship between *Jpx* copy number and *Xist* expression in transgenic mice, suggesting that *Jpx* is sufficient to activate *Xist* expression *in vivo*. In addition, we analyzed *Jpx*'s allelic origin and have provided evidence for *Jpx* inducing *Xist* transcription using both *trans* and *cis* mechanisms. Our work provides a framework for lncRNA functional studies in mice, which will help us understand how lncRNA regulate eukaryotic gene expression.

3.3 Introduction

Mammalian gender is determined by a pair of sex chromosomes (females are XX while males are XY), leading to an inherent imbalance of X-linked gene products between the sexes. Gene dosage is compensated by X-Chromosome Inactivation (XCI), a process which transcriptionally silences one X chromosome in females during early embryonic development (Payer and Lee, 2008). XCI is primarily carried out by a cluster of long noncoding RNA (lncRNA) located on the X chromosome in a region known as the X-inactivation center (Xic) (Horvath et al., 2011; Lee, 2012). The master regulator of XCI is the lncRNA *Xist*, which coordinates X-linked gene silencing by spreading across the future inactive X (X_i) (Brockdorff et al., 1992; Brown et al., 1992).

How *Xist* is selectively activated in female individuals, but not in males, remains an essential, unresolved question in the field. A "Two Factors Model" has been used to describe XCI initiation and *Xist* regulation, in which competence factors trigger XCI on X_i while blocking

factors prevent XCI on the active X (X_a) (Lee and Lu, 1999; Starmer and Magnuson, 2009; Sun et al., 2013). To determine the number of XCI events, the cell counts the number of X chromosomes relative to autosomes – the X:A ratio (Barakat and Gribnau, 2012). Male cells (X:A = 1:2) typically do not induce XCI while female cells (X:A = 2:2) normally induce one XCI event. When the X:A ratio is disturbed, for example in genetic aneuploidies such as a male XXY (X:A = 2:2), the male cell initiates an XCI event to maintain proper X chromosome dosage (Barakat and Gribnau, 2012). Chromosome counting involves a genetic component, as the X chromosome count and subsequent XCI events must be influenced by a *trans*-diffusible factor (Barakat et al., 2014; Sun et al., 2013). A Self-Enhanced Transport (SET) model has also been proposed to describe XCI activation, in which *Xist* exhibits an ultrasensitive (switch-like) response to a competence factor followed by a self-enhanced positive feedback mechanism to maintain *Xist* expression at the initiation of XCI (Li et al., 2016a).

While the primary *Xist* activating factor is under debate, two competence factors have been described. One candidate is E3-Ubiquitin ligase RNF12 (also known as RLIM), which activates *Xist* expression by targeting and degrading the *Xist* blocking-factor REX1 (Gontan et al., 2012). In mouse embryonic stem cell (mESC) models that recapitulate XCI during embryonic development, *Rnf12* expression correlates with downregulation of the pluripotency factor NANOG and subsequent *Xist* activation (Barakat et al., 2011). However, deleting *Rnf12* from mESCs does not prevent XCI from occurring. In one study, a heterozygous *Rnf12* deletion reduced the rate of XCI initiation, but *Xist* RNA clouds were still detected in differentiating mESCs (Jonkers et al., 2009). A later study achieved a homozygous *Rnf12* deletion yet still detected sporadic *Xist* expression from mESCs (Barakat et al., 2011). Further, when *Rnf12* was conditionally deleted from mouse embryos, no effect on *Xist* expression or XCI was observed

(Shin et al., 2014). In mice, RNF12 has since been shown to control *Xist* activation during imprinted XCI, a form of XCI in extraembryonic tissues which does not involve the same X-chromosome counting process as random XCI in the embryo (Shin et al., 2010, 2014). A most recent study characterizing *Rnf12* and XCI in mouse extraembryonic tissues and embryo proper revealed *Rnf12* downregulation prior to random XCI in the embryo. (Wang et al., 2017). Together, these studies suggest that additional X-encoded factors can activate *Xist* expression and initiate XCI in mESCs and in the mouse embryo.

Another proposed *Xist* activator is *Jpx*, a functional lncRNA whose gene is located just proximal to *Xist*. *Jpx* escapes inactivation and has been found to activate *Xist* expression by binding to and removing CTCF protein from the *Xist* promoter (Sun et al., 2013; Tian et al., 2010). *Jpx* appears necessary for XCI in a mESC model, in which a heterozygous *Jpx* deletion compromised the overall *Jpx* and *Xist* expression and led to lethality in differentiating female ES cells (Tian et al., 2010). Intriguingly, the surviving female cells maintained *Xist* induction preferentially associated with the remaining *Jpx* allele in *cis* (on the same chromosome). Importantly, a transgene containing *Jpx*, Tg(Jpx), was able to restore *Xist* expression and rescue the female cell viability, supporting a *trans*-acting role of *Jpx* for *Xist* activation in mESCs (Tian et al., 2010). Using the mESC system, another study reported a large deletion of a 500kb genomic region upstream of *Xist*, which includes both *Jpx* and *Rnf12* but nevertheless caused no major defects to the cells (Barakat et al., 2014). Interestingly, the overall *Xist* expression was significantly decreased in the heterozygous Δ(*Jpx-Rnf12*) differentiating mES cells compared to the cells with heterozygous deletion of *Rnf12* by itself. A transgene containing *Rnf12* was able to rescue the *Xist* expression in these heterozygous Δ(*Jpx-Rnf12*) cells but only up to ~65% of the

wildtype level (Barakat et al., 2014). These observations suggest that *Jpx* is needed for full activation of *Xist* in mESCs.

Further, when the Tg(Jpx) transgene was inserted into wildtype mESCs, *Xist* was ectopically expressed in both male and female cells, indicating that *Jpx* itself is capable of activating *Xist* in *trans* (Sun et al., 2013). However, a different transgene (containing *Jpx* and *Ftx*) failed to induce *Xist* expression in mESCs (Barakat et al., 2014; Monkhorst et al., 2009), although *Jpx* expression levels in these cells were not noted. The current debate on an active role of *Jpx* in XCI, and the effects of transgenic *Jpx* on *Xist* expression in mESCs, prompts the establishment and characterization of *Jpx* transgenic mouse models. In this study, we provide findings from novel transgenic mice to elucidate the relationship between *Jpx* and *Xist* activities *in vivo.*

Specifically, to test if *Jpx* is a competence factor for *Xist* activation in mice, we asked if additional copies of *Jpx* would induce *Xist* expression *in vivo*. We further questioned what genetic mechanism *Jpx* acts through: a *trans* (distal) or *cis* (local) regulatory control. We utilized a pair of overlapping transgene constructs to develop a novel transgenic mouse model, in which we monitored the *Xist* response to *Jpx* expression from a *trans* (on a different chromosome) or *cis* (on the same chromosome or within the transgene) origin. By characterizing phenotypic consequences of the transgenes, particularly expression patterns of *Jpx* and *Xist* in mouse embryonic cells, we determined the function and genetic mechanism of *Jpx* on *Xist* activation *in vivo*.

3.4 Results

Jpx *transgenes induce* Xist *expression in mESCs using both* trans *and* cis *mechanisms*

Two transgene constructs have been generated to characterize the regulatory interaction between *Jpx* and *Xist* in mice: Tg(Jpx) is a 90kb BAC that contains the *Jpx* gene and flanking genomic DNA; Tg(Jpx, Xist) is a 120kb BAC that includes both *Jpx* and *Xist* genes in their endogenous *cis* positioning (Fig. 3.1A). Using mESC models, a previous study inserted Tg(Jpx) into an autosome and observed ectopic *Xist* upregulation from the X chromosome in both female and male mESCs, suggesting a *trans* mechanism for *Jpx* in activating *Xist* (Sun et al., 2013). The same Tg(Jpx), when introduced in the *Jpx*-deletion mESCs, was capable of rescuing the *Xist* and cell viability defect, which is also consistent with the proposed *trans* activity of *Jpx* (Tian et al., 2010). In the present study, we first introduced Tg(Jpx, Xist) into mESCs to test possible mechanisms of *Xist* activation by *Jpx*. As shown in Figure 3.1, a single-copy Tg(Jpx, Xist) insertion in an autosome was sufficient to induce ectopic *Xist* upregulation in female ESCs. Expression of both endogenous and transgenic *Xist* were observed, suggesting both *trans*- and *cis*- effects of *Jpx* in activating *Xist*. Such effects were detected in multiple independent transgenic mESC lines, including both female and male cells carrying single-copy Tg(Jpx, Xist) insertion (Fig. 3.7). Stable integration of the transgene into a random autosomal site was verified by combined RNA-DNA Fluorescence *in situ* Hybridization (FISH) as in Figure 3.1B.

In particular, we describe the *Xist* expression pattern observed in Tg(Jpx, Xist) female mESCs upon differentiation. Combined RNA-DNA FISH was performed to visualize the characteristic *Xist* RNA "cloud" associated with the "pinpoint" DNA locus (Lee and Lu, 1999; Tian et al., 2010). As shown in Figure 3.1B, upregulation of *Xist*, observed as an enlarged domain (green *Xist* cloud), was associated with the endogenous DNA locus (red *Xpct* pinpoint). By Day 2 of mESC differentiation, significantly more *Xist* clouds were observed in Tg(Jpx, Xist)

cells compared to control cells (Figs. 3.1C and 3.7A). In a small subset of cells we observed three distinct *Xist* clouds: one at each endogenous site and one at the transgenic integration site. These results support that Tg(Jpx, Xist) is functionally active in mESCs. Furthermore, ectopic *Xist* expression as two clouds at both endogenous sites demonstrate a *trans*- effect from the autosomal-integrated Tg(Jpx, Xist). In addition, an *Xist* cloud from the Tg(Jpx, Xist) transgene suggests the activation of *Xist* by its upstream *Jpx* located in *cis* within the same transgene. Such *Xist* upregulation was observed in multiple transgenic female cell lines, up to differentiation day 8 (Figs. 3.7 B-D), suggesting stable activation of the transgenic *Xist*. Ectopic *Xist* upregulation and transgenic *Xist* expression were also observed in male mESCs transfected with Tg(Jpx, Xist) (Fig. 3.7A, 3.7E, and 3.7F). Therefore, effects of Tg(Jpx, Xist) in mESCs indicate both *trans*- and *cis*- acting roles of *Jpx* on *Xist*.

Jpx *transgenes cause reduced viability of transgenic male mice*

By introducing Tg(Jpx) or Tg(Jpx, Xist) as transgenes in mice, we next asked if *Jpx* would be sufficient to induce *Xist* expression and whether increasing *Jpx* gene copy number leads to any observable abnormality in live animals. Transgenic mice were generated by microinjecting BAC DNA into mouse pronuclei and were recovered as founder animals for independent lines. Figure 3.2A summarizes a total of ten transgenic mouse lines obtained, five for Tg(Jpx) and five for Tg(Jpx, Xist), with copies of transgenes randomly integrated in the genome. All transgenic founder mice appeared morphologically normal, fertile, and were able to transmit the transgene to the next generation. Stable integration and inheritance of the transgenes were verified by genotyping offspring along five generations of outcrossing. For each transgenic line, a single autosomal integration site was detected by DNA FISH localizing the transgene in

mouse fibroblasts, as exampled in Figures 3.3 and 3.4. Five representative lines, with transgene copy numbers ranging from one to fifteen, were characterized to address the regulatory effects of *Jpx* on *Xist* in this study.

Transgenic animals of both sexes were born in each line, yet with variable frequencies as compared to wildtype littermates. In Figure 3.2B, we plotted the ratios of transgenic to wildtype (TG : WT) animals born within each line and found an overall difference between the male (TG/WT ratio average = 0.81) and female (TG/WT ratio average = 1.00). A paired student *t*-test indicated a significantly lower representation of transgenic males (the one-tailed $P = 0.01$). The male viability defect was most obvious in two independent Tg(Jpx) lines, 95.4 and 95.8, in which nearly 50% fewer transgenic males were born (Figs. 3.2B and 3.2C). A male-specific viability defect suggests possible influence to the X chromosome: transgenic *Jpx* may be activating the single endogenous *Xist* on the only male X chromosome. Ectopic activation of *Xist* may lead to inappropriate silencing of X-linked essential genes in the male. By contrast, the same effect to endogenous *Xist* in the female could be modulated between its two X's, thus minimizing the potentially deleterious consequence of silencing both X chromosomes.

Transgene copy number is positively correlated with Jpx *and* Xist *expression*

We compared *Jpx* and *Xist* expression levels in five transgenic lines with different copy numbers of the transgene. To specifically focus on gene activities in embryonic tissues, we isolated mouse embryonic fibroblasts (mEFs) from embryonic day 13.5 (E13.5). As shown in Figure 3.2D, both *Jpx* and *Xist* transcript levels increased with increasing transgene copy number, reflecting a dose-dependent gene regulation. At the same time, higher *Jpx* levels

correlated with increased *Xist* expression, suggesting positive regulation of *Jpx* on *Xist* in these transgenic animals. In particular, *Xist* expression was detected in male mEFs of transgenic lines 95.4, 93.7, 04.2 and 05.2, whereas wildtype males normally have no *Xist* expression in any somatic cell (Fig. 3.2D). A control qRT-PCR reaction performed without reverse-transcriptase (RT minus) confirmed that *Xist* amplification detected in the Tg(Jpx) male was indeed of *Xist* RNA (Fig. 3.8A). We also noted variability in *Jpx* and *Xist* expression between littermate animals of the same genotype, and between litters of the same lineage (Fig. 3.2D, standard errors). Thus, littermates of wildtype and transgenic animals were used for all comparisons, except for noted situations (Fig. 3.2E; denoted by '+') when wildtype littermates were not available and an average of wildtype samples was used in analysis.

In Tg(Jpx, Xist) transgenic animals, increased *Xist* expression was observed from both females and males in line 05.2. While this ectopic *Xist* likely derives from the transgene, the transcripts cannot be distinguished from endogenous *Xist* by nucleotide sequence or the qRT-PCR assay in this analysis. In contrast, Tg(Jpx) does not contain *Xist*, and thus the observed induction of *Xist* expression in 95.4 and 93.7 transgenic males must be exclusively *trans*-activation of the endogenous *Xist* (the only copy on the male X chromosome) by the transgenic *Jpx* (from the autosomal Tg(Jpx)). Therefore, these data demonstrate that increasing *Jpx* gene copies induces *Xist* expression in mice, and that transgenic *Jpx* can activate the endogenous *Xist* in *trans*.

Jpx *utilizes a* trans *mechanism to activate* Xist *expression in Tg(Jpx) mice*

To clearly distinguish between transgenic and endogenous gene activation, we performed sequential RNA and DNA FISH on Tg(Jpx) E13.5 mEFs. This technique allowed independent visualization of *Jpx* and *Xist* transcripts and of the genomic transgene integration site (Fig. 3.3A). Sequential FISH on the same cell allowed us to associate an RNA cloud with its corresponding DNA locus on the endogenous or transgenic allele (Figs. 3.3A and 3.3B: closed arrowhead, endogenous; open arrowhead, transgenic). On its own, DNA FISH was also used to confirm the correct ploidy and X chromosome number in each cell. In high transgene copy lines (such as line 93.7), the transgenic DNA locus often appeared much larger and was distinct from the smaller endogenous loci, as visualized by the '*Jpx*+*Xist*' probe (Fig. 3.3A, middle column). To confirm endogenous alleles when the transgene was not obvious, we used a second probe, '*Rnf12*,' to target the X chromosome outside the transgene sequence (Fig. 3.1A), which co-localized with endogenous *Jpx* and *Xist* but not with the transgenic allele (Fig. 3.3A, right column). Taken together, sequential RNA and DNA FISH allowed us to identify the expression pattern of *Jpx* and *Xist* in Tg(Jpx) mEFs.

Wildtype mEFs typically displayed *Jpx* RNA FISH foci larger than a single pinpoint, which we denote as a dot-like 'cloud' to signify the expression of *Jpx* from the gene locus. As shown in Figure 3.3, wildtype female mEFs displayed one *Jpx* RNA cloud and one *Xist* RNA cloud, each corresponding to an endogenous gene locus; wildtype male mEFs displayed one *Jpx* RNA cloud at the endogenous *Jpx* gene locus and showed no *Xist* RNA. In contrast, additional *Jpx* RNA clouds were observed in female and male Tg(Jpx) transgenic mEFs (Figs. 3.3A and 3.3B), consistent with our finding of increased *Jpx* expression when *Jpx* gene copies are increased (Fig. 3.2). Since the total number of cells expressing *Jpx* remained comparable between wildtype and transgenic (Fig. 3.8B), the data suggest that the increase in *Jpx* expression

measured by qRT-PCR was due to increased *Jpx* expression at the individual cell level. We then quantified the *Jpx* cloud allelic origin in Figure 3.3C and found robust *Jpx* expression from the transgene—on average, 25% of female *Jpx* clouds and 50% of male *Jpx* clouds were transgenic—reaffirming that the BAC transgene contains all regulatory elements sufficient for *Jpx* expression in mice, and that transgenic expression is likely responsible for the observed increase in *Jpx* transcript levels.

Xist expression in Tg(Jpx) E13.5 mEFs was also affected by the increase in *Jpx* copy number (Figs. 3.3A and 3.3B). FISH on transgenic female mEFs revealed only one *Xist* RNA cloud—originating from one of the two endogenous X chromosomes—even in the presence of supernumerary *Jpx* expression (Fig. 3.3A, middle panels). This indicates that Tg(Jpx) E13.5 transgenic females maintain proper dosage compensation with only one silenced X chromosome, which is in agreement with our finding of normal viability in these females (Fig. 3.2B). The increase in *Xist* expression detected by qRT-PCR (Fig. 3.2D) suggests enhanced *Xist* transcription from X_i, likely affected by *Jpx* acting in *trans* from the transgenic site. In comparison, an ectopic *Xist* cloud was observed on the only X chromosome in Tg(Jpx) male cells (Fig. 3.3A, lower panels; Figs. 3.3B and 3.8B). This observation is consistent with the detected *Xist* transcripts and viability reduction observed in such transgenic males (Figs. 3.2B and 3.2D). Overall, by combining RNA and DNA FISH results in the same cells, we confirmed the autosomal integration of transgenes and the allelic association of *Jpx* and *Xist* transcripts. Transgenic *Jpx* induced endogenous *Xist* expression in both male and female mEFs, thus demonstrating a *trans* mechanism of activation in mice.

Jpx *activates* Xist *expression using both* cis *and* trans *mechanisms in Tg(Jpx, Xist) mice*

The Tg(Jpx, Xist) transgene includes *Jpx* and *Xist* genomic sequences in their endogenous *cis* positioning, as illustrated in Figure 3.1A. DNA FISH in Tg(Jpx, Xist) mEFs confirmed the single-site autosomal integration of transgenes, and sequential RNA and DNA FISH resolved the allelic origin of *Jpx* and *Xist* transcripts in individual cells (Fig. 3.4A). As the only two genes contained in Tg(Jpx, Xist), *Jpx* using *cis* mechanisms to regulate *Xist* expression would lead to expression of both genes from the same transgenic allelic locus. Indeed, we observed activation and co-localization of *Jpx* and *Xist* RNA associated with the transgenic site in both female and male Tg(Jpx, Xist) mEFs (Fig. 3.4A: open arrowheads). Significantly more transgenic female cells expressed *Jpx* compared to wildtype controls (Figs. 3.4B and 3.8B). This increase in *Jpx* activity is likely due to expression from the transgenic locus, as approximately 30% of all *Jpx* clouds in Tg(Jpx, Xist) females were transgenic in origin (Fig. 3.4C). Consequently, transgenic *Xist* clouds represented close to 30% of all observed *Xist* clouds in Tg(Jpx, Xist) females (Fig. 3.4C). The percentage of detectable *Jpx* clouds in transgenic male cells was comparable to wildtype, and males maintained a 50/50 split between endogenous and transgenic *Jpx* activation (Figs. 3.4C and 3.8B). Importantly, more than 75% of *Xist* clouds in males were transgenic, contributing to a significantly higher percentage of *Xist* clouds detected in transgenic male cells compared to wildtype controls (Figs. 3.4C and 3.8B). These data are consistent with our observation of increased *Jpx* and *Xist* expression in Tg(Jpx, Xist) males (Fig. 3.2D).

Endogenous *Xist* was also affected in Tg(Jpx, Xist) transgenic mEFs: we observed three *Xist* clouds in a female cell and two *Xist* clouds in a male cell, representing ectopic *Xist* activation on the X chromosome (Fig. 3.4A: arrowheads, Fig. 3.4B). Within one cell, ectopic *Xist* activation from the endogenous X chromosome is consistent with a *trans* regulatory

response from the autosomal transgene, while the concurrent *Xist* and *Jpx* expression from the transgenic allele suggests a *cis* activation of *Xist* by the flanking *Jpx*. We also note that the endogenous *Jpx* may induce transgenic *Xist* expression through a *trans* mechanism in the same cell. When we examined the allelic origin of ectopic *Xist*, as a single *Xist* cloud in the male or a second cloud in the female, we found that an *Xist* cloud was more often associated with the transgene than with the endogenous X chromosome (Figs. 3.8C and 3.8D), suggesting that transgenic *Xist* activation contributes to the increase of *Xist* expression observed in Tg(Jpx, Xist) mice (Fig. 3.2D). Tg(Jpx, Xist) has thus demonstrated *Jpx* activation of *Xist* expression *in vivo*, and revealed the possible mechanism as cooperating both *cis* and *trans* activities.

Ectopic Xist *silences X-linked genes in Tg(Jpx) mice*

We next asked if the observed ectopic *Xist* expression would induce additional XCI and silence X-linked genes in our transgenic animals. We performed quantitative expression analysis (qRT-PCR) for seven X-linked genes, which are located across the length of the X-chromosome at positions of various distance from *Xist* (Fig. 3.5A). Of these seven genes, *Cask, Rnf12, Atrx,* and *Diaph2* are genes subject to XCI in females (Fig 3.5A, boxed grey) while *Kdm6a, Eif2s3x,* and *Mid1* are genes known to escape XCI in mice (Engreitz et al., 2013; Yang et al., 2010). As shown in Figure 3.5B, we observed an overall reduction of X-linked gene expression in Tg(Jpx) E13.5 mEFs from the line 95.4 compared to wildtype mEFs. A significant reduction of *Diaph2* expression was observed in Tg(Jpx) line 95.4 for both female and male mEFs. Particularly in the males, four out of the seven X-linked genes, including *Cask, Rnf12, Diaph2* and *Mid1*, were significantly downregulated in line 95.4. Such a decrease of X-linked gene expression indicates a gene silencing effect, most likely from the ectopic *Xist* expression, in the Tg(Jpx) 95.4 transgenic

animals. An overall downregulation of X-linked genes may lead to developmental disadvantages, which is consistent with the lack of transgenic males observed in line 95.4 (Fig. 3.2B). By contrast, there was no reduction of X-linked gene expression in the mEFs of Tg(Jpx) line 93.7, consistent with a normal survival rate of transgenic animals in this line (Fig. 3.2B). These data demonstrate that ectopic *Xist* expression induced by Tg(Jpx) indeed has functional consequence in silencing X-linked genes, which may lead to physiological defects affecting male viability in mice.

Tg(Jpx, Xist) mEFs did not display the same X-linked gene silencing effect. Instead, an overall increase of X-linked genes was observed in both male and female E13.5 cells from Tg(Jpx, Xist) line 05.2 (Fig. 3.5C). We noted that ectopic *Xist* expression in Tg(Jpx, Xist) mEFs was observed with higher frequency on the autosomal transgene than the endogenous X chromosome (Figs. 3.8C and 3.8D). Therefore, *Xist* upregulation in Tg(Jpx, Xist) cells may preferably affect autosomal genes flanking the transgene integration site rather than silencing the endogenous X chromosome. Transgenic *Xist* in an autosome has been shown to be capable of silencing autosomal genes in *cis* (Loda et al., 2017). At the same time, robust transgenic *Xist* expression can also squelch the endogenous *Xist* (Jeon and Lee, 2011), potentially affecting the X-linked gene silencing. Upregulation of X-linked genes with XCI deficiency is compatible with mouse survival (Yang et al., 2016). This is also consistent with the observed viability of Tg(Jpx, Xist) animals (Fig. 3.2B).

Ectopic Xist *expression in transgenic female and male early embryos*

XCI occurs in the mouse embryo between embryonic days 5.5 (E5.5) and 6.5 (E6.5) (Monk and Harper, 1979). We asked whether the effects of transgenic *Jpx* on *Xist* could be more apparent in the early embryos around the completion of XCI. To address this question, we extracted post-implantation E7.5 and E8.5 embryos, wildtype and transgenic littermates, from Tg(Jpx) lines, 93.7 and 95.8, and Tg(Jpx, Xist) line 04.2 (Figs. 3.6 and 3.9). Specifically, we analyzed cells isolated from the embryo proper, where random XCI occurs (Mak et al., 2004). As shown in Figure 3.6, compared to the wildtype male and female embryonic cells, transgenic male and female E7.5 embryonic cells showed ectopic *Xist* expression. Notably in Tg(Jpx) transgenic female cells, we observed two *Xist* clouds present in up to 25% of cells (Figs. 3.6A and 3.6C). Occurrence of two *Xist* clouds in a cell was never observed in any Tg(Jpx) female E13.5 mEF (Fig. 3.3B). These data further support a *trans*- effect of *Jpx* (from the autosomal transgene) in activating both *Xist* alleles on the X chromosomes, which may lead to cell death during early embryogenesis. Ectopic expression of endogenous *Xist* was also observed in Tg(Jpx) transgenic male E7.5 cells, consistent with the pattern in E13.5 mEFs, which confirms the *trans*- acting effect of *Jpx* on *Xist* activation in these embryos.

Also consistent with the expression pattern of *Jpx* and *Xist* in Tg(Jpx, Xist) E13.5 mEFs, Tg(Jpx, Xist) female and male E7.5 embryonic cells showed expression of both endogenous and transgenic *Jpx* clouds, which were associated with up to two *Xist* clouds, one endogenous and one transgenic (Figs. 3.6B-D; Fig. 3.9A). We note that even with limited cell samples obtained from E7.5 embryos, ectopic *Xist* RNA was clearly present in the early embryonic cells from transgenic mice – confirming our observation of ectopic *Xist* expression in E13.5 transgenic mEFs. Together, these data suggest a mechanism in which *Jpx* is sufficient to induce *Xist*

expression in *trans* (from autosomal transgenic *Jpx* to the endogenous *Xist* on X chromosomes) and is capable of activating *Xist* in *cis* (locally within a transgene).

3.5 Discussion and Conclusion

Our findings suggest a model in which *Jpx* is a competence factor that initiates *Xist* expression in mice (Fig. 3.10). By using a combination of transgenes, we demonstrated that increasing *Jpx* copy number is sufficient to activate *Xist* expression in mice. The *Jpx* transcript is a *trans*-acting factor which, when increased by addition of the Tg(Jpx) transgene in an autosome, is capable of activating endogenous *Xist* on the X chromosome in both male and female mice. In addition, *Jpx* has been described as a member of the *Xist* topologically associated domain (TAD) (Nora et al., 2012; Tsai et al., 2008), indicating *cis* regulatory activity for *Jpx* inducing *Xist* locally within the same chromosomal locus (van Bemmel et al., 2016). This is consistent with our observation of co-localized *Jpx* and *Xist* transcripts from the Tg(Jpx, Xist) transgene in mice, suggesting that *Jpx* activates *Xist* expression in *cis* within the transgene. Together, our observations in Tg(Jpx) and Tg(Jpx, Xist) mice illustrate *Jpx* inducing *Xist* expression, and support *Jpx* as a competence factor directly influencing X chromosome counting and XCI initiation.

To distinguish between *trans*- and *cis*- genetic mechanisms in our mouse models, we emphasize the distinction between *inter*- and *intra*- chromosomal gene regulation. Therefore, an autosomal *Jpx* transgene activating the endogenous *Xist* on the X chromosome is a clear demonstration of *trans*- acting function of *Jpx*; whereas the activation of a transgenic *Xist* by its upstream *Jpx* within the same transgene locus is considered a *cis*- effect of *Jpx*. Our results

suggest that *Jpx* can activate *Xist* locally within the transgene; however, it is possible that *Jpx* RNA moves away from its site of transcription and returns to the target *Xist* locus. At the molecular scale, this mechanism would be considered *trans* acting; whereas the genetic effect is considered *cis* regulation. At the *Xist* promoter, the chromatin insulating factor CTCF has been shown to bind *Jpx* RNA, and together, act in a dose-dependent mechanism for transcriptional initiation of *Xist* in female mESCs (Sun et al., 2013). Titration of CTCF from the *Xist* promoter requires both copies of the *Jpx* gene and *Jpx* RNA transcribed from both X chromosomes in a female cell, consistent with a combination of both *cis* and *trans* mechanisms for *Jpx* RNA. For chromosomal configuration around the *Xist* locus, a change in CTCF occupancy could alter TAD boundary formation, which may facilitate a *cis* interaction between the *Xist* gene and flanking *Jpx*. As recently reported, other proteins in addition to CTCF may also play roles for the formation of TADs in the X chromosome (Barutcu et al., 2018). Additionally, unknown protein factors may be actively directing the *trans* activity of *Jpx* RNA between chromosomes. Future research in identifying *Jpx*-protein binding partners will help elucidate the possible molecular interactions, which are most likely developmentally regulated in mice.

While we observed an overall positive correlation between *Jpx* copy number and expression levels, we did not observe an obvious increase of *Jpx* RNA FISH signals associated with high-copy *Jpx* transgenes, i.e. Tg(Jpx) 93.7 (Fig. 3.3A). A feedback mechanism may regulate the allelic expression of high-copy *Jpx* to inhibit unfavorable allelic overexpression in a cell. This possibility is also supported by the observed *Jpx* allelic expression in transgenic mESCs, in which addition of '*Jpx/Ftx* transgene' actually decreased the endogenous *Jpx* expression (Barakat et al., 2014, Fig. S4A) (Barakat et al., 2014). In addition, the activation of *Xist* within the Tg(Jpx, Xist) transgene could also be complemented by the lack of a functional

Tsix, a suppressor of *Xist* (Lee and Lu, 1999; Tian et al., 2010), which might facilitate a preference of transgenic *Xist* expression over the endogenous *Xist* in the X chromosomes. It is also possible that the endogenous *Jpx trans*- activates the transgenic *Xist*, or works together with the transgenic *Jpx* to cooperate both *trans* and *cis* mechanisms when activating transgenic *Xist* expression in Tg(Jpx, Xist) animals.

High percentages of transgenic *Xist* expression were observed in Tg(Jpx, Xist) E13.5 mEFs (Fig. 3.4C). However, in earlier embryonic cells from E7.5, the majority of *Xist* clouds observed were endogenous in origin (Fig. 3.6D). To understand whether upregulation of the endogenous *Xist* induced XCI in early embryos, we performed qRT-PCR on seven X-linked genes in Tg(Jpx) lines 95.8 and 93.7. As shown in Figure 3.9B-E, there was no obvious decrease of X-linked gene expression in Tg(Jpx) E8.5 or E7.5 embryos. This is in contrast to the significant reduction of X-linked genes observed in Tg(Jpx) E13.5 mEFs (Fig. 3.5). It is possible that the additional silencing effect by ectopic *Xist* was achieved and only obvious at a later stage of the typical XCI developmental timing in mouse embryogenesis.

Overall, our transgenic system provides an example linking *ex vivo* and *in vivo* studies of lncRNA function and mechanism. While gene knockout would be a conventional approach for functional determination, recent reports on the function of lncRNA *Hotair* revealed the complications of lncRNA deletion in mice (Amandio et al., 2016; Li et al., 2013, 2016b; Selleri et al., 2016). The debate on *Hotair*'s molecular mechanism and target genes also advocates for the use of transgenic mice when distinguishing *cis*- and *trans*- actions of lncRNA (Amandio et al., 2016). In this study, our transgenic mouse models help resolve *Jpx*'s function and mechanism while avoiding possible genomic instability brought about by large deletions of lncRNA genes.

Our study thus provides an example of lncRNA functional studies in mice and demonstrates that *Jpx* is sufficient to activate *Xist* expression using *trans* and *cis* mechanisms *in vivo*.

Figure 3.1. *Jpx* transgenes induce *Xist* expression in mESCs using both *trans* and *cis* mechanisms. (A) Map of the X-inactivation center (Xic) with 90kb Tg(Jpx) and 120kb Tg(Jpx, Xist) transgenes and the probes used for Fluorescence *in situ* Hybridization (FISH). (B) Combined RNA-DNA FISH for *Xist* (green, FITC) and *Xpct* (red, Cy3) on female mESC at differentiation days 0, 2, and 4. Top: Control female ESCs transfected with Tg(pSKYneo+), a plasmid that does not contain X-chromosome sequence but provides the same neomycin resistance as Tg(Jpx, Xist); bottom: Tg(Jpx, Xist) transgenic female mESC line #7, which has a single-copy Tg(Jpx, Xist) integrated in an autosome; right: schematic of *Xist* expression at Day 4. Green wavy line, *Xist* RNA; Red dot, *Xpct* (X-Chr.) DNA locus; Open arrowhead: Tg(Jpx, Xist) transgenic site. Scale bar: 2μm. (C) *Xist* cloud frequency throughout differentiation. **, $P<0.01$; ***, $P<0.001$, from a chi-square test comparing total *Xist* cloud counts in wildtype and transgenic cells at each differentiation day. Sample sizes and additional Tg(Jpx, Xist) mESC lines are included in Figure 3.7.

Figure 3.1

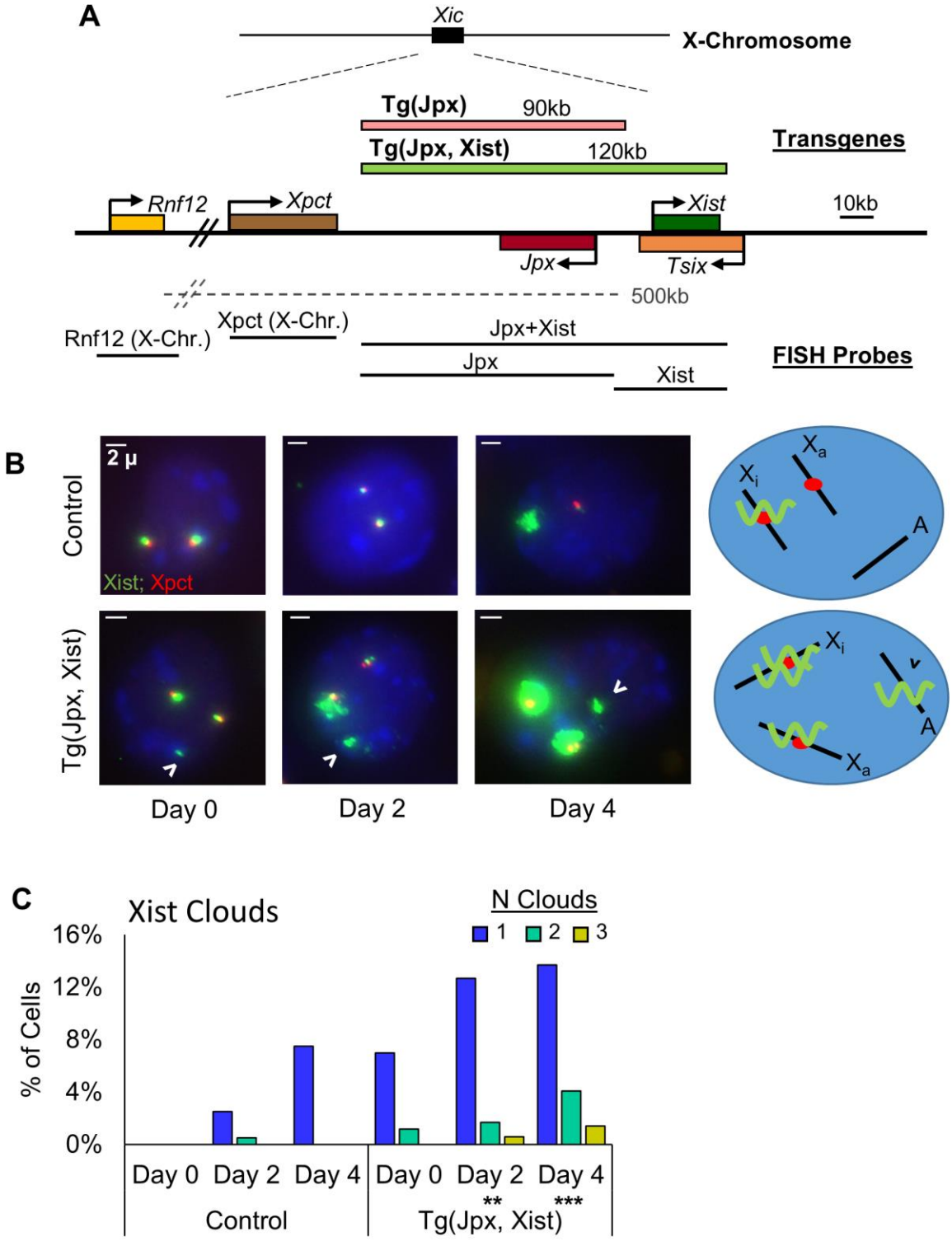
A
Xic
X-Chromosome
Tg(Jpx) 90kb
Tg(Jpx, Xist) 120kb
Transgenes
Rnf12
Xpct
Xist
10kb
Jpx
Tsix
500kb
Rnf12 (X-Chr.)
Xpct (X-Chr.)
Jpx+Xist
Jpx
Xist
FISH Probes
B
2 µ
Control
Xist; Xpct
Tg(Jpx, Xist)
Xi
Xa
A
Day 0
Day 2
Day 4
C
Xist Clouds
N Clouds
1 2 3
% of Cells
16%
12%
8%
4%
0%
Day 0 Day 2 Day 4 Day 0 Day 2 Day 4
**
***
Control
Tg(Jpx, Xist)

Figure 3.2. Transgene copy number is positively correlated with *Jpx* and *Xist* expression. (A) Transgenic Tg(Jpx) and Tg(Jpx, Xist) mouse lines generated in this study. F, female; M, male. In line 03.4, a semicolon separates different transgenic *Jpx* and *Xist* copy numbers. (B) The ratio of transgenic (TG) to wildtype (WT) mice for females and males obtained from five representative transgenic lines, arranged from low to high copy number for each transgene construct.**, $P<0.01$; ***, $P<0.001$, from a binomial test for the expected situation of equal TG and WT animals, independently for males and females. (C) Number of animals included in the analysis. (D) *Jpx* (red bars) and *Xist* (green bars) expression levels in mouse embryonic fibroblasts (mEFs) isolated from female embryos (top) and male embryos (bottom). Left panel: Tg(Jpx) mouse lines. Right panel: Tg(Jpx, Xist) mouse lines. Data plotted are average expression levels normalized to housekeeping gene *Gapdh*, ± standard error of biological replicates. A one-tailed *t*-test was used to compare the expression in transgenic and wildtype samples. *, $P<0.05$; **, $P<0.01$; ***, $P<0.001$. (E) Number of embryos collected and used in the expression analysis. The '+' denotes the number of wildtype animals used when wildtype littermates were unavailable; expression was averaged between such wildtype animals from separate litters.

Figure 3.2

A

	Tg(Jpx)					Tg(Jpx, Xist)				
Tg Line	**93.6**	**93.7**	**95.3**	**95.4**	**95.8**	**03.2**	**03.4**	**04.2**	**04.3**	**05.2**
Transgene Copy Number	2	15	2	1	2	5	12;8	3	3	5
Founder Sex	F	F	M	M	F	M	F	M	F	M

B

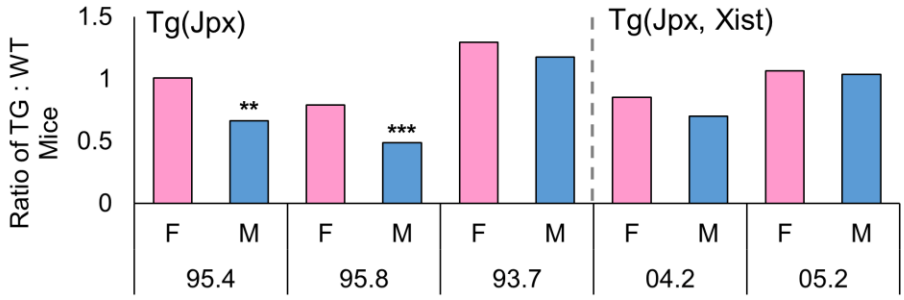

C

Tg Line	95.4		95.8		93.7		04.2		05.2	
Tg Copy Number	1		2		15		3		5	
Sex	F	M	F	M	F	M	F	M	F	M
N WT Postnatal	109	111	62	78	51	45	61	57	26	30
N TG Postnatal	110	74	49	38	66	53	52	40	27	32

D

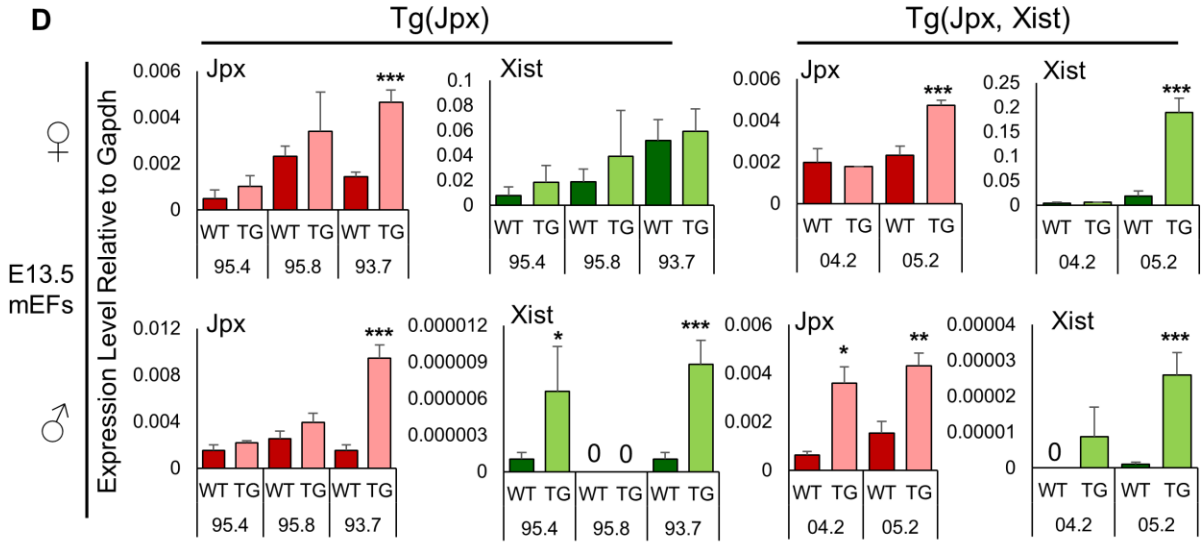

E

Tg Line	95.4		95.8		93.7		04.2		05.2	
Sex	F	M	F	M	F	M	F	M	F	M
N WT Embryos	2	6^{+}	11^{+}	3	5	6^{+}	3	2	11^{+}	6^{+}
N TG Embryos	3	4	3	4	3	2	1	4	5	3

Figure 3.3. *Jpx* utilizes a *trans* mechanism to activate *Xist* expression in Tg(Jpx) mice. (A) RNA FISH (left column) and corresponding DNA FISH (two columns on the right) in wildtype and Tg(Jpx) transgenic mEFs. Representative images shown of ectopic expression patterns observed in cells. Probes are described in Fig. 3.1A. For RNA: *Jpx* (red, Cy3) and *Xist* (green, FITC). For DNA: *Jpx*+*Xist* (red, Cy3) and *Rnf12* (green, FITC). Right column: DNA FISH with two probes to distinguish the endogenous X chromosomal locus (overlapping red and green) from the transgenic insertion site (red only). Closed arrowhead: endogenous RNA transcripts (RNA FISH) and the endogenous X chromosomal loci (DNA FISH). Open arrowhead: transgenic RNA transcripts and the transgenic integration site. Scale bar: 5μm. (B) Percentage of cells with *Jpx* or *Xist* expression categorized by the number of RNA clouds detected. (C) Percentage of endogenous versus transgenic *Jpx* clouds counted in Tg(Jpx) mEFs.

Figure 3.3

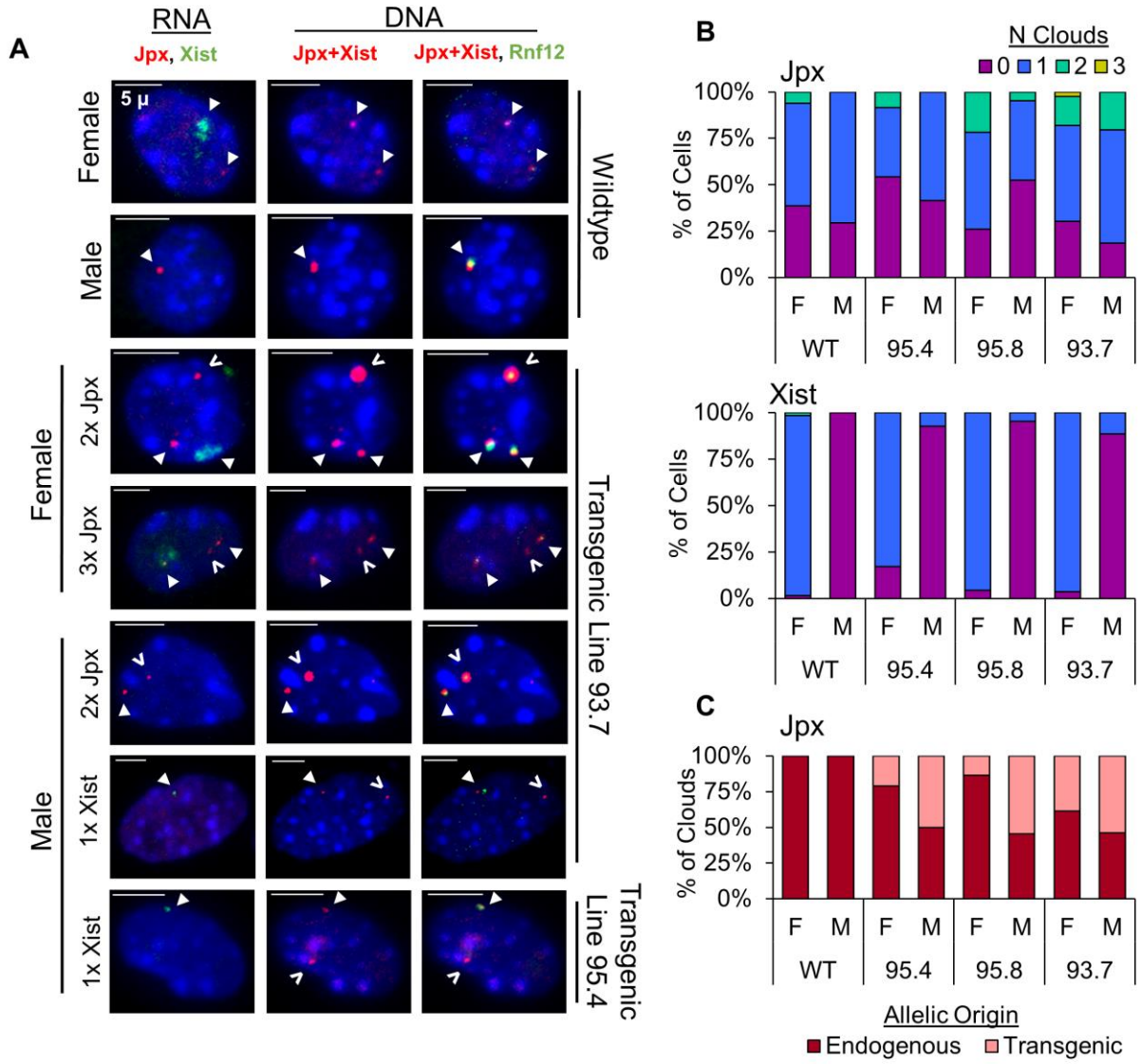
A
RNA
DNA
Jpx, Xist
Jpx+Xist
Jpx+Xist, Rnf12
5 µ
Female
Male
Wildtype
Female
2x Jpx
3x Jpx
Male
2x Jpx
1x Xist
Transgenic Line 93.7
1x Xist
Transgenic Line 95.4
B
N Clouds
0 1 2 3
Jpx
Xist
% of Cells
100%
75%
50%
25%
0%
F M F M F M F M
WT 95.4 95.8 93.7
C
Jpx
% of Clouds
Allelic Origin
Endogenous
Transgenic

Figure 3.4. *Jpx* activates *Xist* expression using both *cis* and *trans* mechanisms in Tg(Jpx, Xist) mice. (A) RNA FISH (left column) and corresponding DNA FISH (two columns on the right) in transgenic Tg(Jpx, Xist) mEFs. Representative images shown of ectopic expression patterns observed in cells. Probes are described in Fig. 3.1A. For RNA: *Jpx* (red, Cy3) and *Xist* (green, FITC); for DNA: *Jpx+Xist* (red, Cy3) and *Rnf12* (green, FITC). Right column: DNA FISH with two probes to distinguish the endogenous X chromosomal locus (overlapping red and green) from the transgenic insertion site (red only). Closed arrowhead: endogenous RNA transcripts (RNA FISH) and the endogenous X chromosomal loci (DNA FISH). Open arrowhead: transgenic RNA transcripts and the transgenic integration site. Scale bar: 5μm. (B) Percentage of cells with *Jpx* or *Xist* expression categorized by number of RNA clouds detected. (C) Percentage of endogenous versus transgenic RNA clouds for *Jpx* and *Xist* in Tg(Jpx, Xist) mEFs.

Figure 3.4

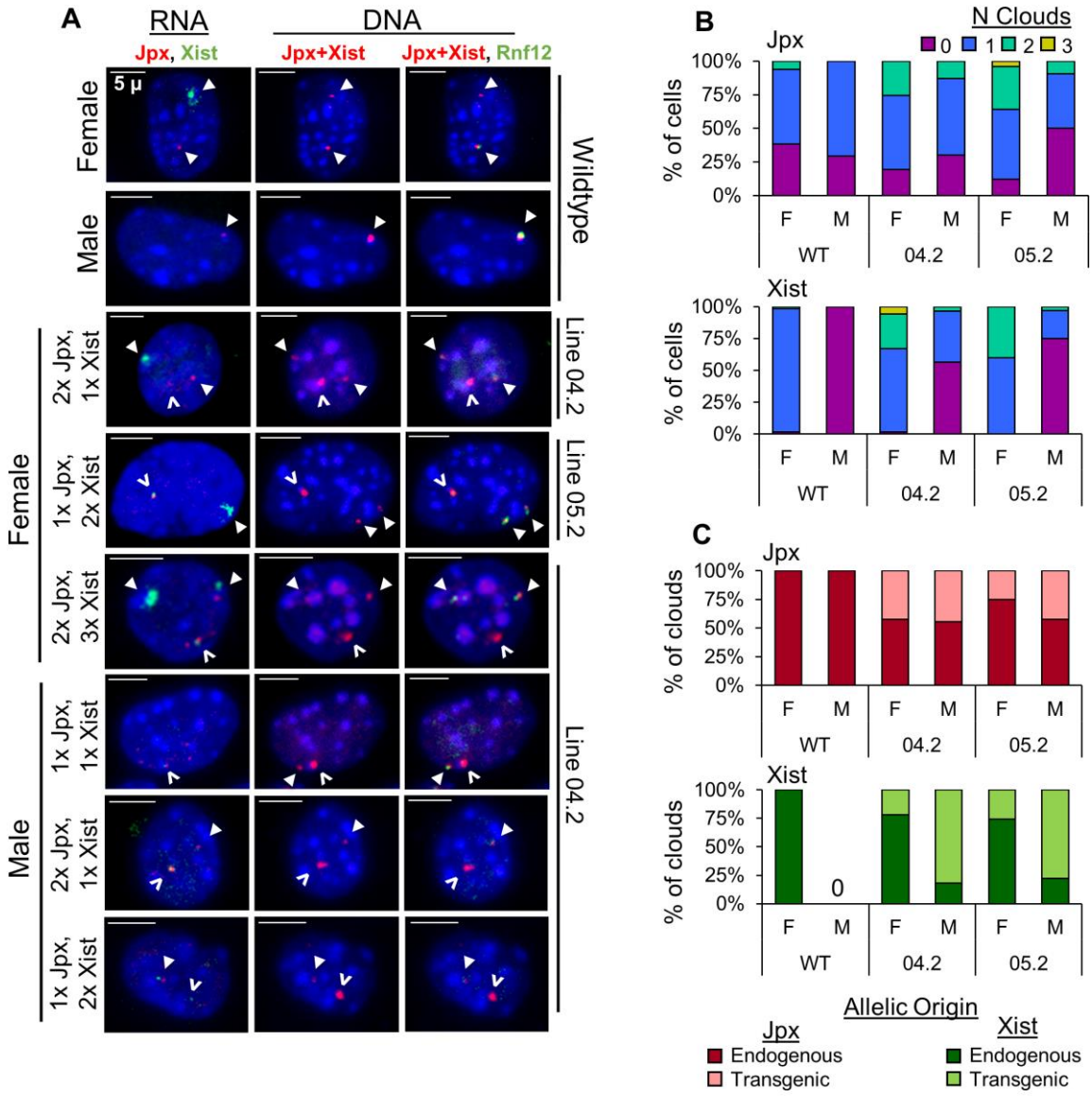
A
RNA
DNA
Jpx, Xist
Jpx+Xist
Jpx+Xist, Rnf12
5 µ
Female
Male
Wildtype
Line 04.2
Line 05.2
2x Jpx, 1x Xist
1x Jpx, 2x Xist
2x Jpx, 3x Xist
1x Jpx, 1x Xist
2x Jpx, 1x Xist
1x Jpx, 2x Xist
B
N Clouds
0 1 2 3
Jpx
Xist
% of cells
100%
75%
50%
25%
0%
F M F M F M
WT 04.2 05.2
C
% of clouds
0
Allelic Origin
Jpx
Endogenous
Transgenic
Xist
Endogenous
Transgenic

Figure 3.5. Ectopic *Xist* silences X-linked genes in Tg(Jpx) transgenic mice. (A) Map of X chromosome and genes for quantitative expression analysis in E13.5 mEFs. Genes boxed in grey (*Cask, Rnf12, Atrx, Diaph2*) are subject to XCI in mice; genes not boxed (*Kdm6a, Eif2s3x, Jpx, Xist, Mid1*) are known to escape XCI in mice. (B) Expression of X-linked genes in wildtype and Tg(Jpx) transgenic mEFs isolated from lines 95.4 and 93.7. Top: Expression in females. Bottom: Expression in males. (C) Expression of X-linked genes in wildtype and Tg(Jpx, Xist) transgenic mEFs isolated from line 05.2. Top: Expression in females. Bottom: Expression in males. Data plotted are average expression levels normalized to housekeeping gene *Gapdh*, ± standard error of biological replicates. A subset of embryos from Fig. 3.2E were used for analysis, N≥2 for each genotype. A one-tailed *t*-test was used to compare the expression in transgenic and wildtype samples. *, $P<0.05$; **, $P<0.01$, ***, $P<0.001$.

Figure 3.5

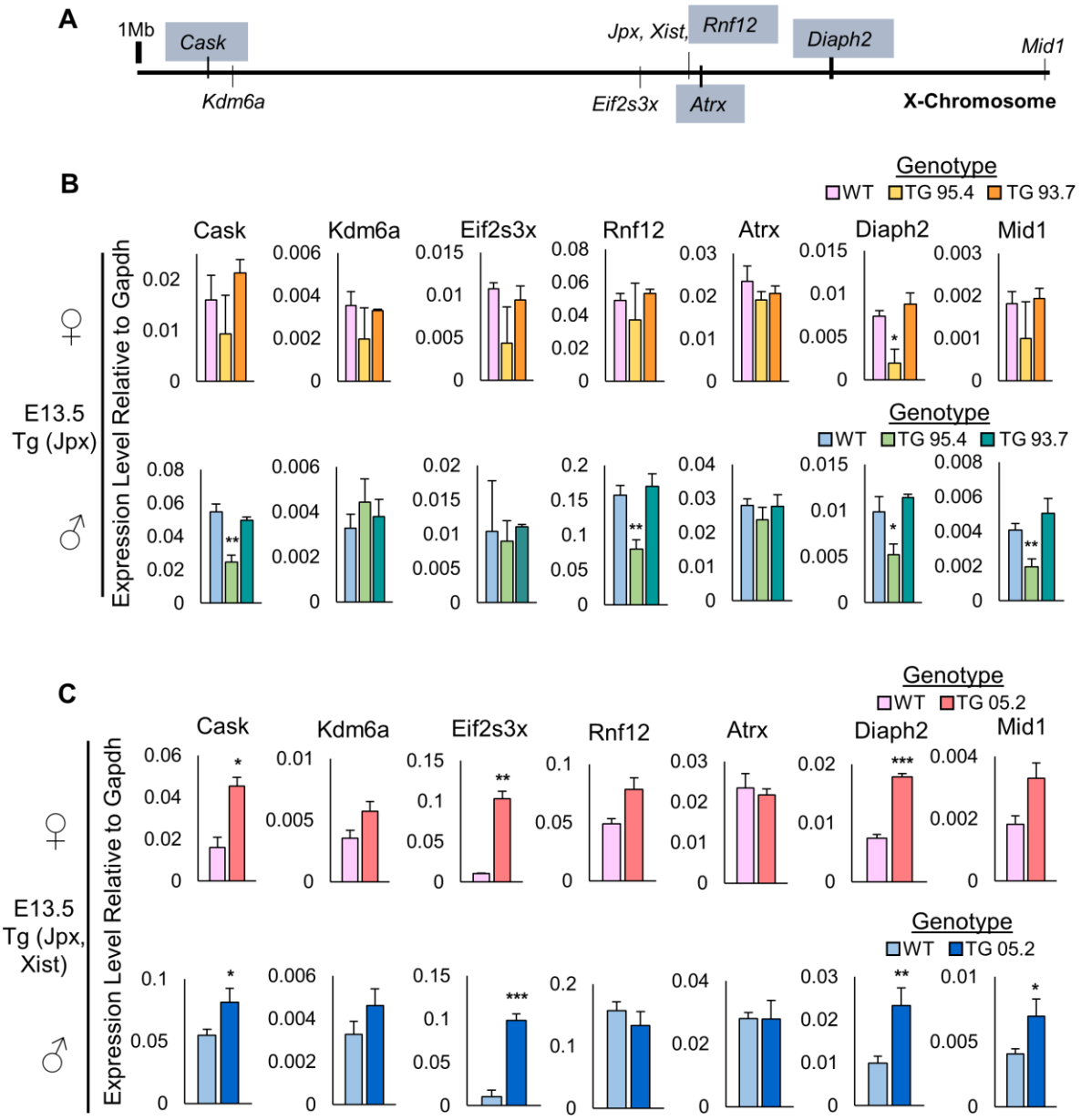
A
1Mb
Cask
Kdm6a
Jpx, Xist,
Rnf12
Eif2s3x
Atrx
Diaph2
Mid1
X-Chromosome
B
Genotype
WT TG 95.4 TG 93.7
Cask
Kdm6a
Eif2s3x
Rnf12
Atrx
Diaph2
Mid1
E13.5
Tg (Jpx)
Expression Level Relative to Gapdh
C
Genotype
WT TG 05.2
E13.5
Tg (Jpx,
Xist)

Figure 3.6. Ectopic *Xist* expression in transgenic female and male early embryos. (A, B) RNA FISH (left column) and corresponding DNA FISH (right column) in wildtype, transgenic Tg(Jpx) (A), and transgenic Tg(Jpx, Xist) embryos (B), extracted at embryonic day 7.5 (E7.5). Representative images shown of ectopic expression patterns observed in cells. Probes are described in Fig. 3.1A. For RNA: *Jpx* (red, Cy3) and *Xist* (green, FITC); for DNA: *Jpx+Xist* (red, Cy3) and *Rnf12* (green, FITC). DNA FISH with two probes distinguishes the endogenous X chromosomal locus (overlapping red and green) from the transgenic insertion site (red only). Closed arrowhead: endogenous RNA transcripts (RNA FISH) and the endogenous X chromosomal loci (DNA FISH). Open arrowhead: transgenic RNA transcripts and the transgenic integration site. Scale bar: 5μm. (C) Percentage of cells with *Jpx* or *Xist* expression categorized by number of RNA clouds detected. (D) Percentage of endogenous versus transgenic RNA clouds for *Jpx* and *Xist* in Tg(Jpx) and Tg(Jpx, Xist) embryos. Number of E7.5 embryos and quantification are included in Figure 3.9A.

Figure 3.6

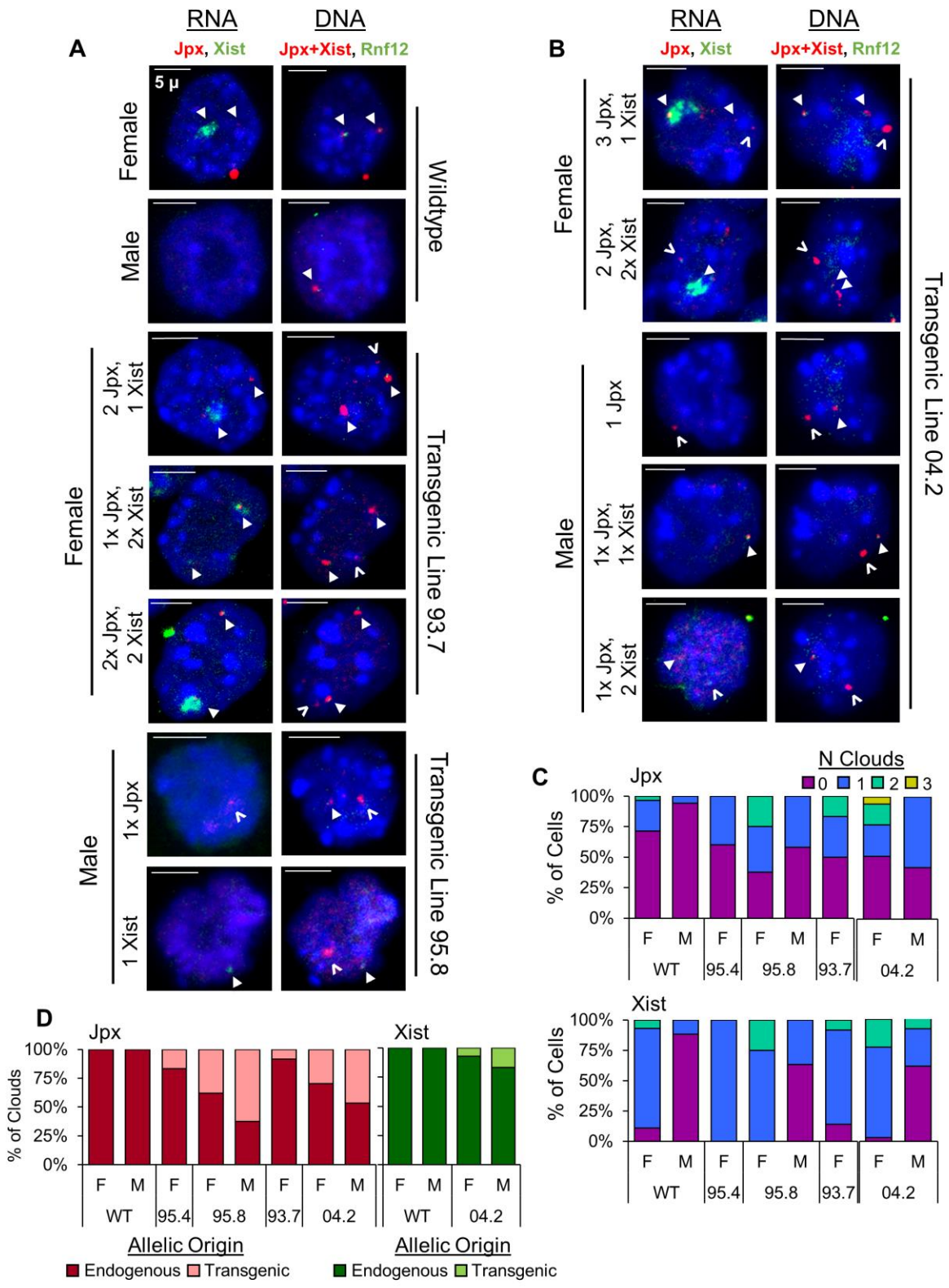
A
RNA
DNA
Jpx, Xist
Jpx+Xist, Rnf12
5 µ
Female
Male
Wildtype
2 Jpx, 1 Xist
1x Jpx, 2x Xist
2x Jpx, 2 Xist
Transgenic Line 93.7
1x Jpx
1 Xist
Transgenic Line 95.8
B
3 Jpx, 1 Xist
2 Jpx, 2x Xist
1 Jpx
1x Jpx, 1x Xist
1x Jpx, 2 Xist
Transgenic Line 04.2
C
Jpx
N Clouds
0 1 2 3
% of Cells
100%
75%
50%
25%
0%
F M F F M F F M
WT 95.4 95.8 93.7 04.2
Xist
D
Jpx
Xist
% of Clouds
F M F F M F F M F M F M
WT 95.4 95.8 93.7 04.2 WT 04.2
Allelic Origin
Endogenous Transgenic
Allelic Origin
Endogenous Transgenic

Figure 3.7. Ectopic *Xist* expression in male and female mESCs transfected with Tg(Jpx, Xist). (A) Quantitative analysis for *Xist* clouds in female Tg(Jpx, Xist) mESC line #7 as shown Fig. 3.1C, and male Tg(Jpx, Xist) mESC lines #5 and #9 as shown in Figs. 3.7 E and F. Charts include corresponding *P* values derived from a chi-square test to determine the difference between cloud counts in wildtype and transgenic cells at each differentiation day. (B) Combined RNA-DNA FISH for control mESCs at differentiation days 0, 2, 4, and 8. Female (top) and male (bottom) mESCs were transfected with a Tg(pSKYneo+) control plasmid. Probes used: *Jpx*+*Xist* (green, FITC) and *Xpct* (red, Cy3), as shown in Fig. 3.1A. (C) Combined RNA-DNA FISH for female Tg(Jpx, Xist) mESCs Line #2, at differentiation days 0, 4, and 8. Probes are as indicated in (B). Open arrowhead: Tg(Jpx, Xist) transgenic site. (D) Combined RNA-DNA FISH for female Tg(Jpx, Xist) mESCs Line #11 at differentiation day 8. Probes are as indicated in (B). Open arrowhead: Tg(Jpx, Xist) transgenic site. (E-F) Sequential RNA and DNA FISH on male Tg(Jpx, Xist) mESCs Line #5 (E) and Line #9 (F) at differentiation day 2. RNA FISH probe: *Xist* (green, FITC), DNA FISH probes: *Xist* (green, FITC) and *Xpct* (red, Cy3), as shown in Fig. 3.1A. Open arrowhead: Tg(Jpx, Xist) transgenic site. Scale bar: 2μm. All Tg(Jpx, Xist) mESC lines are stable transgenic cells with single-copy Tg(Jpx, Xist) transgene integrated in an autosome.

Figure 3.7

A

Female Cell Counts

	Differentiation Day	N Cells	% Cells with Xist Cloud	*P* Value
Control	Day 0	27	0%	-
	Day 2	202	3%	-
	Day 4	53	8%	-
Tg(Jpx, Xist) Line 7	Day 0	85	8%	0.2
	Day 2	173	15%	**0.0001**
	Day 4	73	19%	**0.005**

Male Cell Counts

	Differentiation Day	N Cells	% Cells with Xist Cloud	*P* Value
Control	Day 2	97	2%	-
Tg(Jpx, Xist) Line 5	Day 2	55	84%	**0.0001**
Tg(Jpx, Xist) Line 9	Day 2	82	80%	**0.0001**

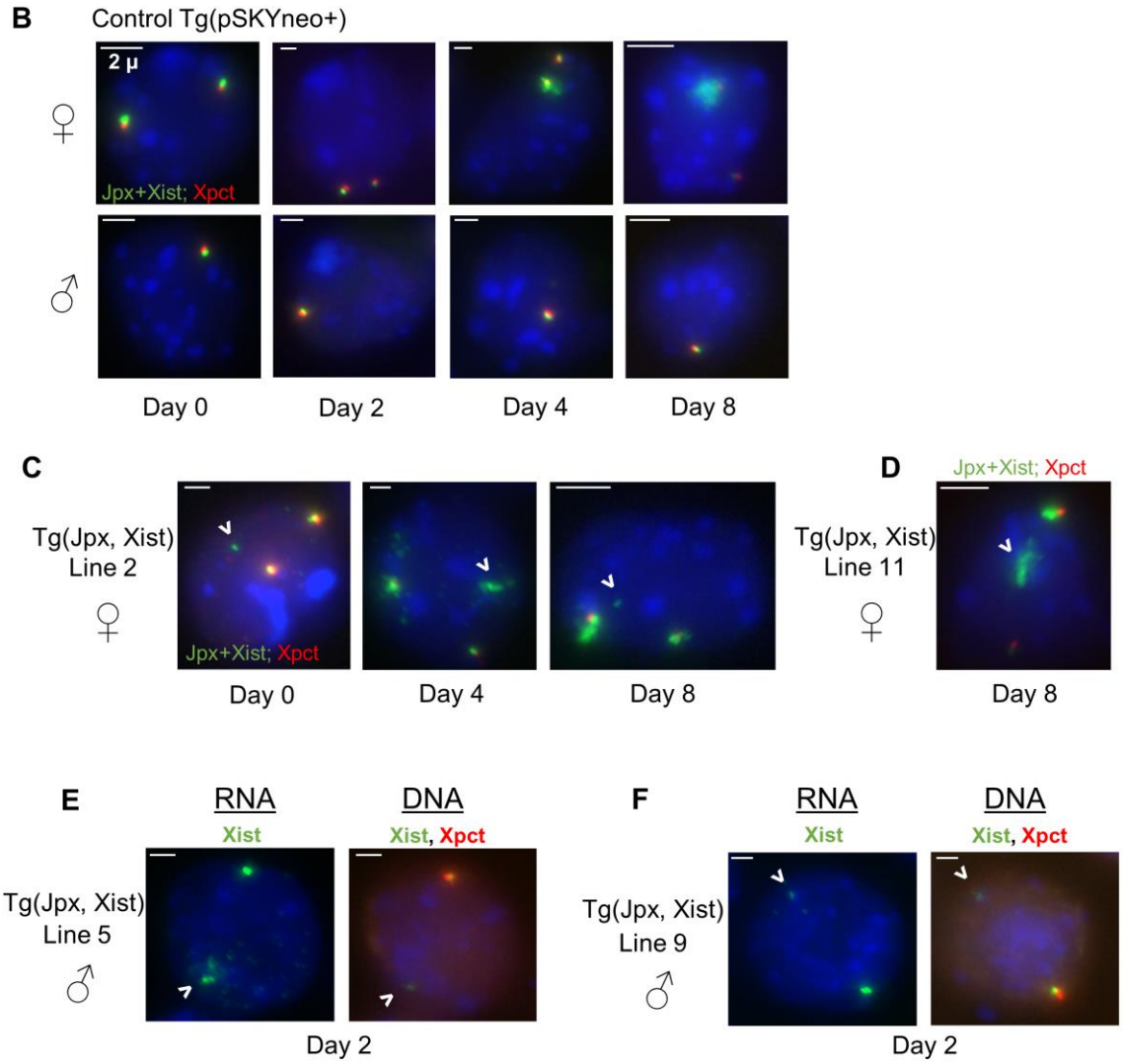

Figure 3.8. *Xist* is expressed from both endogenous and transgenic sites in female and male mEFs. (A) qRT-PCR control reactions for *Gapdh, Jpx,* and *Xist* amplification and Ct values obtained with/without reverse transcriptase enzyme in E13.5 Tg(Jpx) transgenic male mEFs. (B) Number of mEFs included in the FISH analysis for Tg(Jpx) lines as shown in Fig. 3.3, and Tg(Jpx, Xist) lines as shown in Fig. 3.4. *P* value is from a chi-square test comparing the RNA cloud counts between wildtype and transgenic samples in each line. (C, D) Diagram of *Xist* expression patterns observed from transgenic Tg(Jpx, Xist) female (C) and male (D) mEFs. The percentage of observed clouds in each category is listed below the diagram. Cells are counted from two transgenic Tg(Jpx, Xist) lines: 04.2 and 05.2.

Figure 3.8

A RT- Ctl: E13.5 mEFs

Sample	RT Enzyme	**Gapdh** Avg. Ct Value	Std. Dev.	**Jpx** Avg. Ct Value	Std. Dev.	**Xist** Avg. Ct Value	Std. Dev.
Tg(Jpx) Line 93.7 Male	+	21.22	0.04	27.25	0.02	38.42	1.78
	-	31.76	0.29	33.57	2.70	N/A	N/A

B E13.5 mEF FISH cloud counts

Tg Line	Sex	N Cells	% Cells w/ Jpx Cloud	*P* Value	% Cells w/ Xist Cloud	*P* Value
WT	F	65	62%	-	98%	-
	M	41	71%	-	0%	-
95.4	F	35	46%	0.1	83%	**0.007**
	M	41	59%	0.4	7%	0.2
95.8	F	23	74%	0.3	96%	0.5
	M	21	48%	0.1	5%	0.3
93.7	F	83	70%	0.3	96%	0.6
	M	49	82%	0.3	8%	**0.04**

Tg Line	Sex	N Cells	% Cells w/ Jpx Cloud	*P* Value	% Cells w/ Xist Cloud	*P* Value
04.2	F	67	81%	**0.02**	99%	1
	M	117	70%	1	44%	**0.0001**
05.2	F	25	88%	**0.02**	100%	1
	M	32	50%	0.1	25%	**0.0008**

C

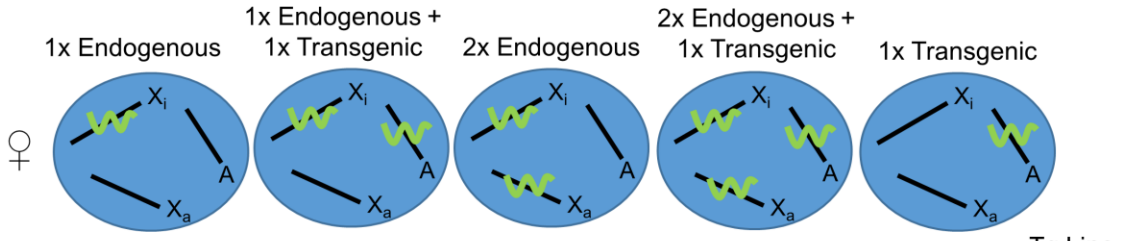

						Tg Line
% Event	69%	23%	3%	5%	0%	04.2
	62%	33%	5%	0%	0%	05.2

D

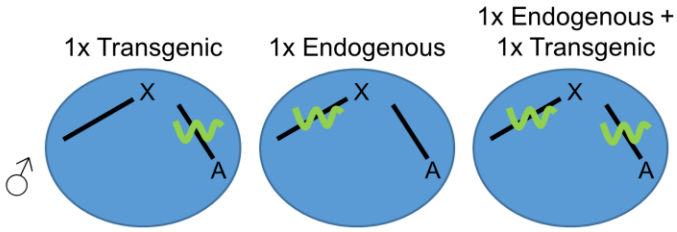

				Tg Line
% Event	78%	11.5%	10.5%	04.2
	86.7%	6.7%	6.7%	05.2

Figure 3.9. X-linked gene expression in early embryos. (A) Number of E7.5 embryonic cells included in the FISH analysis for Tg(Jpx) and Tg(Jpx, Xist) as shown in Fig. 3.6. *P* value is from a chi-square test comparing the RNA cloud counts between wildtype and transgenic samples in each line. (B) Number of embryos obtained as littermates and used for the expression analysis. (C) Map of X-Chromosome and genes for quantitative expression analysis in E7.5 embryos. Genes boxed in grey (*Cask, Rnf12, Atrx, Diaph2*) are subject to XCI in mice; genes not boxed (*Kdm6a, Eif2s3x, Jpx, Xist, Mid1*) are known to escape XCI in mice. (D) Expression of X-linked genes in E8.5 wildtype and Tg(Jpx) transgenic female embryos from line 95.8. (E) Expression of X-linked genes in E7.5 wildtype and Tg(Jpx) transgenic female and male embryos from line 93.7.

Figure 3.9

A FISH cloud counts for E7.5 Embryos

Tg Line	Sex	N Cells	% Cells w/ Jpx Cloud	*P* Value	% Cells w/ Xist Cloud	*P* Value
WT	F	28	29%	-	89%	-
	M	17	6%	-	12%	-
95.4	F	15	40%	0.5	100%	0.5
95.8	F	24	63%	**0.02**	100%	0.2
	M	19	42%	**0.02**	37%	0.1
93.7	F	36	50%	0.1	86%	1
04.2	F	35	49%	0.1	97%	0.3
	M	26	58%	**0.0009**	42%	0.05

B Embryos extracted for qPCR

Tg Line	95.8		93.7	
Timepoint	E8.5		E7.5	
Sex	F	M	F	M
N WT Embryos	1	N/A	1	1
N TG Embryos	3	N/A	2	1

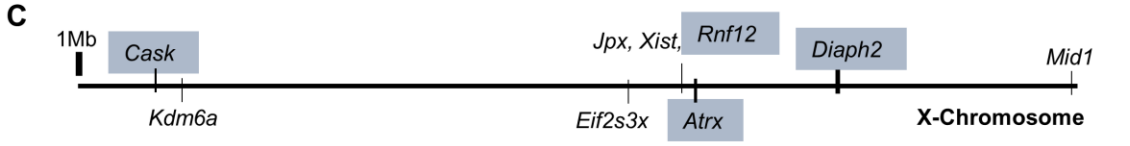

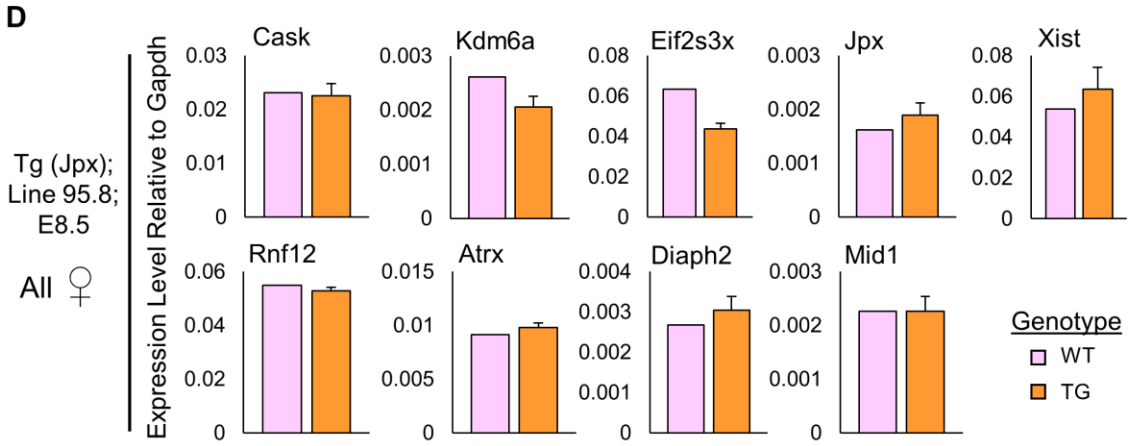

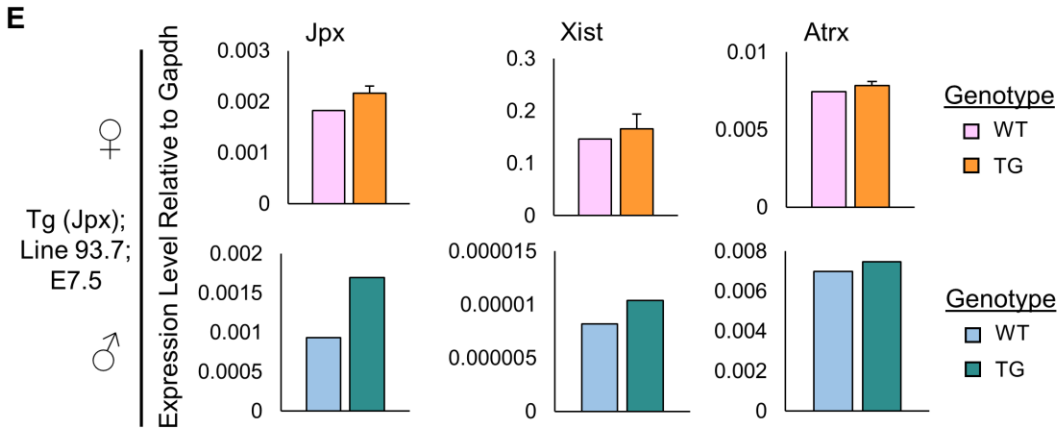

Figure 3.10. *Jpx* activates *Xist* expression in transgenic mice. Summary and model for how *Jpx* activates *Xist* in wildtype (WT) and transgenic mice. The grey dashed arrows in WT represent the proposed mechanisms for *Jpx* activating *Xist*. Up to two endogenous *Xist* clouds were observed in Tg(Jpx) embryos, indicating *trans* activity by *Jpx* (black dashed arrows). In Tg(Jpx, Xist) embryos, up to three *Xist* clouds were observed: two endogenous and one transgenic. This suggests *Jpx* regulation of *Xist* using the proposed *cis* mechanism (grey dashed arrows) in addition to the *trans* mechanisms (black dashed arrows).

Figure 3.10

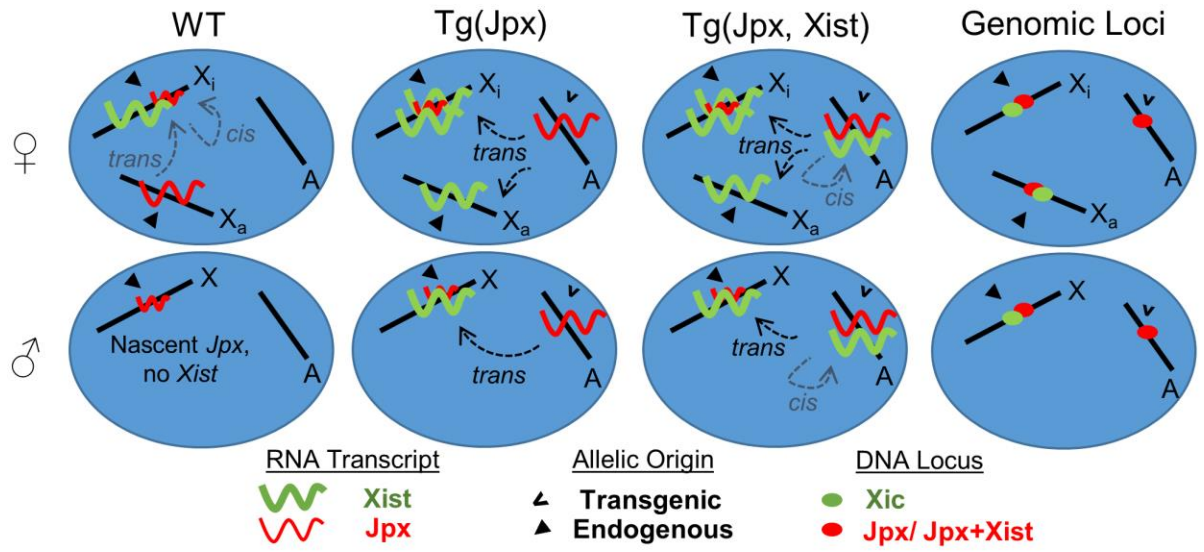
WT
Tg(Jpx)
Tg(Jpx, Xist)
Genomic Loci
♀
♂
Xi
Xa
X
A
cis
trans
Nascent Jpx, no Xist
RNA Transcript
Xist
Jpx
Allelic Origin
Transgenic
Endogenous
DNA Locus
Xic
Jpx/ Jpx+Xist

Table 3.1: List of primers used in the study.

Procedure/ target	Primer name	Direction	Primer Sequence	Reference
BAC8 subcloning	BAC8_68199	F	GGTTTAGGCTCCATTCTTAAGACCTCAT	(Augui et al., 2007; Sun et al., 2015)
	BAC8_68407	R	GGTCTACAGAGCTAGTTCCAAGACACCA	
BAC8 subcloning	BAC8_147016	F	ATCCAGGACACCAGGATTCTCC	(Augui et al., 2007; Sun et al., 2015)
	BAC8_147200	R	CATCTAGAAACACTAGCTTGAGAGG	
Identifying transgenic mice	pBAC4	F	AGTTGGAACCTCTTACGTGCCGAT	(Sun et al., 2015)
		R	ATGTGGTGTGACCGGAACAGAGAA	
Confirming sex of mice	UBEX/Y	F	TGGTCTGGACCCAAACGCTGTCCACA	(Senner et al., 2011)
		R	GGCAGCAGCCATCACATAATCCAGATG	
Jpx gene copy number	JpxEx1	F	GCA CCA CCA GGC TTC TGT AAC	(Tian et al., 2010)
		R	GGG CAT GTT CAT TAA TTG GCC AG	
Xist gene copy number	XistP2Y	F	CTC GAC AGC CCA ATC TTT GTT	(Jeon and Lee, 2011)
	XistP2C	R	ACC AAC ACT TCC ACT TAG CC	
Hprt gene (X-Chr.)	Hprt_12848	F	CTG CTA CTT CAA CTC CTG GTG TGC	(Sun et al., 2015)
	Hprt_12970	R	AGG CGA ATT GGG ATG TAG CTC AG	
Jpx transcript	mJpx76$_{+}$ (Exon 1)	F	TTAGCCAGGCAGCTAGAGGA	(Sun et al., 2013)
	mJpx225- (Exon 2)	R	AGCCGTATTCCTCCATGGTT	
Xist transcript	XistBP2	F	CCCGCTGCTGAGTGTTTGATA	(Payer et al., 2013)
	XistNS33	R	CAGAGTAGCGAGGACTTGAAGAG	(Stavropoulos et al., 2001)
Gapdh transcript	GapdhBP1	F	ATG AAT ACG GCT ACA GCA ACA GG	(Payer et al., 2013)
		R	CTC TTG CTC AGT GTC CTT GCT G	
Mid1	Mid1FY	F	AGCCTGTGGAGTCCATCAAC	(Yang et al., 2010)
		R	GCTTTCAGGCACTCATCACA	
Diaph2	Diaph2_2943F	F	AAGCGCAGGCAAAGTTTCAG	This thesis
	Diaph2_3203R	R	TCCATGTTTACTGTGTTCGGGT	
Atrx	Atrx_264F	F	AGCCCATGAGTGGAAACAAGT	This thesis
	Atrx_368R	R	CAAGTCGTGGAGAAGAACACG	
Rnf12	Rnf12_518F	F	TAAAGAGGGTCCACCACCAC	(Barakat et al., 2014)
	Rnf12_676R	R	GCTCTCCAGGACTGGTTTCC	This thesis
Eif2s3x	EifFY	F	CTTTATCAGGGGCAGAGCAG	(Yang et al., 2010)
		R	AGCCTCAGACACCCAGTGTT	
Kdm6a	Kdm6a_4617F	F	ATCAACATGCTCCTCCATTACCA	This thesis
	Kdm6a_4845R	R	GCTTTACGAGAGTCCTGGCA	
Cask	Cask_2456F	F	TGGTGGCAGGGTAAACTGGA	This thesis
	Cask_2698R	R	TGCTGGCAGTTTGACTACTTCT	

3.6 References

Amandio, A.R., Necsulea, A., Joye, E., Mascrez, B., and Duboule, D. (2016). Hotair Is Dispensible for Mouse Development. PLoS Genet. *12*, 1–27.

Augui, S., Filion, G.J., Huart, S., Nora, E., Guggiari, M., Maresca, M., Stewart, A.F., and Heard, E. (2007). Sensing X Chromosome Pairs Before X Inactivation via a Novel X-Pairing Region of the Xic. Science (80-.). *318*, 1632–1637.

Barakat, T.S., and Gribnau, J. (2012). X chromosome inactivation in the cycle of life. Development *139*, 2085–2089.

Barakat, T.S., Gunhanlar, N., Pardo, C.G., Achame, E.M., Ghazvini, M., Boers, R., Kenter, A., Rentmeester, E., Grootegoed, J.A., and Gribnau, J. (2011). RNF12 Activates Xist and Is Essential for X Chromosome Inactivation. PLoS Genet. *7*, 1–12.

Barakat, T.S., Loos, F., Van Staveren, S., Myronova, E., Ghazvini, M., Grootegoed, J.A., and Gribnau, J. (2014). The trans-activator RNF12 and cis-acting elements effectuate X chromosome inactivation independent of X-pairing. Mol. Cell *53*, 965–978.

Barutcu, A.R., Maass, P.G., Lewandowski, J.P., Weiner, C.L., and Rinn, J.L. (2018). A TAD boundary is preserved upon deletion of the CTCF-rich Firre locus. Nat. Commun. *9*, 1444.

van Bemmel, J.G., Mira-Bontenbal, H., and Gribnau, J. (2016). Cis- and trans-regulation in X inactivation. Chromosoma *125*, 41–50.

Brockdorff, N., Ashworth, A., Kay, G.F., McCabe, V.M., Norris, D.P., Cooper, P.J., Swift, S., and Rastan, S. (1992). The product of the mouse Xist gene is a 15 kb inactive X-specific transcript containing no conserved ORF and located in the nucleus. Cell *71*, 515–526.

Brown, C.J., Hendrich, B.D., Rupert, J.L., Lafrenière, R.G., Xing, Y., Lawrence, J., and Willard, H.F. (1992). The human XIST gene: Analysis of a 17 kb inactive X-specific RNA that contains conserved repeats and is highly localized within the nucleus. Cell *71*, 527–542.

Engreitz, J.M., Pandya-Jones, A., McDonel, P., Shishkin, A., Sirokman, K., Surka, C., Kadri, S., Xing, J., Goren, A., Lander, E.S., et al. (2013). The Xist lncRNA exploits three-dimensional genome architecture to spread across the X chromosome. Science *341*, 1237973.

Gontan, C., Achame, E.M., Demmers, J., Barakat, T.S., Rentmeester, E., van IJcken, W., Grootegoed, J.A., and Gribnau, J. (2012). RNF12 initiates X-chromosome inactivation by targeting REX1 for degradation. Nature *485*, 386–390.

Horvath, J.E., Sheedy, C.B., Merrett, S.L., Diallo, A.B., Swofford, D.L., Green, E.D., and Willard, H.F. (2011). Comparative analysis of the primate X-inactivation center region and reconstruction of the ancestral primate XIST locus. Genome Res. *21*, 850–862.

Jeon, Y., and Lee, J.T. (2011). YY1 Tethers Xist RNA to the inactive X nucleation center. Cell *146*, 119–133.

Jonkers, I., Barakat, T.S., Achame, E.M., Monkhorst, K., Kenter, A., Rentmeester, E., Grosveld, F., Grootegoed, J.A., and Gribnau, J. (2009). RNF12 Is an X-Encoded Dose-Dependent

Activator of X Chromosome Inactivation. Cell *139*, 999–1011.

Lee, J.T. (2012). Epigenetic regulation by long noncoding RNAs. Science (80-.). *338*, 1435–1439.

Lee, J.T., and Lu, N. (1999). Targeted Mutagenesis of Tsix Leads to Nonrandom X Inactivation. Cell *99*, 47–57.

Li, C., Hong, T., Webb, C., Karner, H., Sun, S., and Nie, Q. (2016a). A self-enhanced transport mechanism through long noncoding RNAs for X chromosome inactivation. Sci. Rep. 1–13.

Li, L., Liu, B., Wapinski, O.L., Tsai, M.C., Qu, K., Zhang, J., Carlson, J.C., Lin, M., Fang, F., Gupta, R.A., et al. (2013). Targeted Disruption of Hotair Leads to Homeotic Transformation and Gene Derepression. Cell Rep. *5*, 3–12.

Li, L., Helms, J.A., and Chang, H.Y. (2016b). Comment on "Hotair is dispensible for mouse development." PLoS Genet. *12*.

Loda, A., Brandsma, J.H., Vassilev, I., Servant, N., Loos, F., Amirnasr, A., Splinter, E., Barillot, E., Poot, R.A., Heard, E., et al. (2017). Genetic and epigenetic features direct differential efficiency of Xist-mediated silencing at X-chromosomal and autosomal locations. Nat. Commun. *8*.

Mak, W., Nesterova, T.B., de Napoles, M., Appanah, R., Yamanaka, S., Otte, A.P., and Brockdorff, N. (2004). Reactivation of the paternel X chromosome in early mouse embryos. Science (80-.). *303*, 666–669.

Monk, M., and Harper, M.I. (1979). Sequential X chromosome inactivation coupled with cellular differentiation in early mouse embryos. Nature *281*, 311–313.

Monkhorst, K., de Hoon, B., Jonkers, I., Achame, E.M., Monkhorst, W., Hoogerbrugge, J., Rentmeester, E., Westerhoff, H. V., Grosveld, F., Grootegoed, J.A., et al. (2009). The probability to initiate X chromosome inactivation is determined by the X to autosomal ratio and X chromosome specific allelic properties. PLoS One *4*, 1–14.

Nora, E.P., Lajoie, B.R., Schulz, E.G., Giorgetti, L., Okamoto, I., Servant, N., Piolot, T., van Berkum, N.L., Meisig, J., Sedat, J., et al. (2012). Spatial partitioning of the regulatory landscape of the X-inactivation centre. Nature *485*, 381–385.

Payer, B., and Lee, J.T. (2008). X Chromosome Dosage Compensation: How Mammals Keep the Balance. Annu. Rev. Genet. *42*, 733–772.

Payer, B., Rosenberg, M., Yamaji, M., Yabuta, Y., Koyanagi-Aoi, M., Hayashi, K., Yamanaka, S., Saitou, M., and Lee, J.T. (2013). Tsix RNA and the germline factor, PRDM14, link X reactivation and stem cell reprogramming. Mol. Cell *52*, 805–818.

Selleri, L., Bartolomei, M.S., Bickmore, W.A., He, L., Stubbs, L., Reik, W., and Barsh, G.S. (2016). A Hox-Embedded Long Noncoding RNA: Is It All Hot Air? PLoS Genet. *12*, 8–12.

Senner, C.E., Nesterova, T.B., Norton, S., Dewchand, H., Godwin, J., Mak, W., and Brockdorff, N. (2011). Disruption of a conserved region of Xist exon 1 impairs Xist RNA localisation and X-linked gene silencing during random and imprinted X chromosome inactivation. Development

138, 1541–1550.

Shin, J., Bossenz, M., Chung, Y., Ma, H., Byron, M., Taniguchi-Ishigaki, N., Zhu, X., Jiao, B., Hall, L.L., Green, M.R., et al. (2010). Maternal Rnf12/RLIM is required for imprinted X-chromosome inactivation in mice. Nature *467*, 977–981.

Shin, J., Wallingford, M.C., Gallant, J., Marcho, C., Jiao, B., Byron, M., Bossenz, M., Lawrence, J.B., Jones, S.N., Mager, J., et al. (2014). RLIM is dispensable for X-chromosome inactivation in the mouse embryonic epiblast. Nature *511*, 86–89.

Starmer, J., and Magnuson, T. (2009). A new model for random X chromosome inactivation. Development *136*, 1–10.

Stavropoulos, N., Lu, N., and Lee, J.T. (2001). A functional role for Tsix transcription in blocking Xist RNA accumulation but not in X-chromosome choice. Proc. Natl. Acad. Sci. U. S. A. *98*, 10232–10237.

Sun, S., Del Rosario, B.C., Szanto, A., Ogawa, Y., Jeon, Y., and Lee, J.T. (2013). Jpx RNA Activates Xist by Evicting CTCF. Cell *153*, 1537–1551.

Sun, S., Payer, B., Namekawa, S., An, J.Y., Press, W., Catalan-Dibene, J., Sunwoo, H., and Lee, J.T. (2015). Xist imprinting is promoted by the hemizygous (unpaired) state in the male germ line. Proc. Natl. Acad. Sci. *112*, 14415–14422.

Tian, D., Sun, S., and Lee, J.T. (2010). The long noncoding RNA, Jpx, Is a molecular switch for X chromosome inactivation. Cell *143*, 390–403.

Tsai, C.L., Rowntree, R.K., Cohen, D.E., and Lee, J.T. (2008). Higher order chromatin structure at the X-inactivation center via looping DNA. Dev. Biol. *319*, 416–425.

Wang, F., McCannell, K.N., Bošković, A., Zhu, X., Shin, J.D., Yu, J., Gallant, J., Byron, M., Lawrence, J.B., Zhu, L.J., et al. (2017). Rlim-Dependent and -Independent Pathways for X Chromosome Inactivation in Female ESCs. Cell Rep. *21*, 3691–3699.

Yang, F., Babak, T., Shendure, J., and Disteche, C.M. (2010). Global survey of escape from X inactivation by RNA-sequencing in mouse. Genome Res. *20*, 614–622.

Yang, L., Kirby, J.E., Sunwoo, H., and Lee, J.T. (2016). Female mice lacking Xist RNA show partial dosage compensation and survive to term. Genes Dev. *30*, 1747–1760.

Chapter 4

Summary and Future Directions

4.1 Summary

In summary, I have developed transgenic mouse models to understand the role of lncRNA *Jpx* in mouse X-Chromosome Inactivation. Using transgenic mice with increased *Jpx* copy number, I have determined that *Jpx* is sufficient to activate *Xist* expression *in vivo*. Increasing *Jpx* copy number in mice does not lead to an obvious morphological phenotype. However, reduced viability of transgenic male mice was observed in certain Tg(Jpx) lines. At the molecular level, both *Jpx* and *Xist* expression levels are increased over wildtype levels in transgenic female and male mEFs. This relationship appeared dose-dependent, as increasing transgene copy number led to a corresponding increase of both *Jpx* and *Xist* expression in the five transgenic lines studied. In some transgenic lines, such as Tg(Jpx) line 95.4, ectopic X-linked gene silencing was observed in male and female mEFs. This suggests that XCI may have been triggered in male animals, leading to inappropriate gene silencing and transgenic male death during early embryogenesis. Further, I have observed *Jpx* using both *cis* and *trans* mechanisms to activate *Xist* expression in transgenic mEFs and early embryos. In Tg(Jpx) male cells, I observed *Xist* clouds at the endogenous X chromosomal loci, suggesting that transgenic *Jpx* affected the endogenous *Xist* locus in *trans*. In Tg(Jpx, Xist) female and male cells, I observed *Xist* clouds at both the transgenic and endogenous loci. This suggests that *Jpx* used *cis* mechanisms to activate *Xist* expression locally at the transgenic site and *trans* mechanisms to activate *Xist* at endogenous sites.

My work provides two major contributions to the field: first, I have described evidence for *Jpx* as a competency factor in *Xist* activation within mouse XCI. This addresses a long standing unresolved question in the field regarding which factor is responsible for *Xist* activation and XCI initiation. In mESCs, *Jpx*'s role as an *Xist* activing factor was under debate based on conflicting data from separate groups. This work settles the debate and demonstrates that *Jpx* is able to activate *Xist* expression at the organismal level. Second, I have established the first mouse model in which to study *Jpx* function and mechanism. Prior to the work presented in this thesis, no mouse model existed to study the function of *Jpx in vivo.* Future studies will therefore have a platform to further study *Jpx*'s mechanism, including its regulation, transport, and binding partners.

4.2 Future work

Resolving Jpx *'s genetic mechanism*

Several follow up studies may be proposed following this work. First, direct evidence is still lacking for *Jpx*'s *trans* and *cis* mechanisms *in vivo.* In my study, I have inserted a *Jpx* transgene into the genome and observed transcript activity at specific time points in fixed cells. However, since I was unable to distinguish between endogenous and transgenic *Jpx* transcripts, I had to infer the transcript origin based on corresponding RNA and DNA FISH. Therefore, the evidence I have provided for *Jpx*'s genetic *trans* and *cis* mechanisms in Chapter 3 is indirect. To resolve *Jpx*'s genetic mechanism, I plan to directly observe *Jpx* transcript movement in live cells. Specifically, I will use the PP7 system to observe *Jpx* movement in female mESCs.

LncRNA are generally challenging to study in cells and tissues. Since lncRNA are not translated, we cannot insert a GFP tag and directly track transcript movement or localization. Recently, the MS2 and PP7 systems have provided an opportunity for fluorescent labeling of RNA (Hocine et al., 2013). The PP7 transcript forms a repeating stem-loop pattern which is recognized by the PP7 coat protein (PCP). PCP itself can be coupled to fluorescent molecules such as GFP or mCherry. Ultimately, when an RNA transcript is 'tagged' with PP7, it can be recognized by fluorescent PCP and observed by fluorescence microscopy. Since the repeat region is integrated into each transcript's sequence, live cell imaging is also possible (Lange et al., 2008). Several studies have already reported use of a tagged *Xist*-MS2 construct (which works using the same principles as PP7) to study *Xist* dynamics in cells (Barakat et al., 2014; Ng et al., 2011; Sunwoo et al., 2015). For this experiment, I 'tagged' *Jpx* with PP7, detected the transcript with PCP-mCherry, and observed the transcript movement with live cell imaging.

To begin this study, the PP7 repeat region was cloned into a *Jpx* gene construct. We integrated PP7 into *Jpx*'s exon 3, just after the region necessary for proper CTCF binding and *Xist* activation (Sun et al., 2013). This will ensure that *Jpx*'s primary functional isoform will be modified. CRISPR was then used to insert this PP7 modification into the endogenous *Jpx* locus based on homologous recombination of endogenous and donor DNA. The modification was specifically performed on female *Tsix* TST +/- embryonic stem cells. These ES cells are a hybrid cell line containing X chromosomes from two separate mouse strain origins (X^{129} from *Mus musculus* strain 129S1 mice and X^{cas} from *Mus castaneus* mice). The X^{129} chromosome in this line has a mutated copy of the *Tsix* gene, rendering it inactive. Thus, the X^{129} chromosome will always induce *Xist* and undergo XCI since the *Xist* repressive factor is nonfunctional. This cell line was chosen to easily discern the *Xist* activation site/ *Jpx* target site. CRISPR may target

either *Jpx* on either the X^{cas} or X^{129} for PP7 integration. Therefore, if PP7 was inserted into the X^{cas} chromosome, *Jpx* must act in *trans* to activate *Xist* on the X^{129} chromosome. Alternatively, if PP7 was integrated into the X^{129} locus, *Jpx* would act in *cis* to induce *Xist* expression on the same chromosome.

One challenge with this experimental setup is that PP7 could be inserted into one or both endogenous *Jpx* loci, and we would not know the integration status until confirmation by PCR or live cell imaging. Recently, a method known as SNP-CLING has been developed to perform allele-specific CRISPR modifications (Maass et al., 2018). This technique could be used in the future to specifically integrate PP7 in *Jpx* on either the X^{129} or X^{cas} alleles, allowing for directed study of *Jpx*'s *trans* or *cis* mechanisms. Another downfall of this system is that the PP7 sequence is quite large, which may in turn affect functional properties of the coupled lncRNA by disrupting its folding or targeting (Itzkovitz and Oudenaarden, 2011). Finally, it can be difficult with the PP7 system to discern true signal from background unbound PCP-mCherry proteins, especially in the case of lowly expressed transcripts. Therefore, if need be, a newer system known as RNA Mango has recently been developed and can be used in place of PP7 (Dolgosheina et al., 2014). RNA Mango uses a fluorescently labeled aptamer to bind specific transcript sequences, and has higher affinity than PCP to PP7. Using either method, we should be able to detect the *Jpx* transcript and track its movement in live cells (Autour et al., 2018).

Thus far, the lab has developed the donor plasmid containing PP7 flanked by *Jpx* Exon 3 homologous sequences. As described in Chapter 2, I have transfected this construct into TST ES cells using several strategies (such as a two-day versus one-day transfection) to increase the CRISPR modification efficiency. Once PP7 positive clones were identified by PCR, I transfected the cells with PCP-mCherry for *Jpx* transcript visualization. The cells were differentiated to

specifically study *Jpx* activity at differentiation day 4, the time point when *Jpx* is most active at the start of XCI. My preliminary data suggest that modification and transfection were successful, although I have not yet resolved *Jpx*'s movement through the nucleus. Next, the *Jpx* transcript will be tracked through the cell, specifically comparing the site of transcription and target site, to observe *Jpx*'s genetic mechanism. Based on my FISH data from mouse embryonic fibroblasts, I anticipate that *Jpx* would use both *trans* and *cis* mechanisms to activate *Xist*.

Jpx *movement: passive or active?*

Live cell imaging can also address another question regarding *Jpx*'s movement through the nucleus. Does *Jpx* move to target *Xist* sites by passive diffusion or by an active targeting mechanism? LncRNA are thought to locate and interact with target sites in the genome by a combination of protein binding and 3D proximity (Engreitz et al., 2016). *Xist*, for example, interacts with several proteins (including nuclear lamin proteins to anchor the chromosome and support *Xist* spreading) but is primarily thought to broadly target X chromosomal loci based on the 3D proximity of *Xist* to target genes (Engreitz et al., 2013). Drosophila *roX1/2*, on the other hand, must complex with the CLAMP protein before it can recognize specific sites on the male X chromosome during fly dosage compensation (Quinn et al., 2014; Simon et al., 2011). Transcript abundance and stability are also thought to influence this mechanism. *Xist* is moderately expressed but has low specificity for specific sites (Engreitz et al., 2013; Sunwoo et al., 2015). This may enable its interaction with nearby X-linked genes while limiting spread to distant sites on separate chromosomes. In contrast, low abundant lncRNA such as *HOTTIP* (1 copy of the transcript per cell) likely act locally because they cannot maintain a high enough concentration for efficient diffusion to distant genes (Wang et al., 2011). Therefore, in addition

to lncRNA-protein interactions and the spatial proximity between a lncRNA and its target, transcript abundance and other lncRNA-intrinsic properties likely play a role in localization and transport mechanisms (Engreitz et al., 2016).

For *Jpx*, we can begin to address the mechanisms controlling its movement by observing its localization over time in the cell. For example, is the transcript more diffused (which may suggest a 3D proximity model) or more localized to spatial compartments (suggesting binding to protein cofactors or other restrictions on its movement)? Although primarily qualitative, this data can also give insight into *Jpx*'s relative abundance at the start of XCI. This point has not been specifically addressed in my thesis work since all samples were collected at the completion of XCI or later. To address *Jpx* binding partners (outside of known binding partner CTCF) and identify potential transport mechanisms, we can use chemical crosslinking assays such as CHIRP and RAP. These methods tile the RNA for all possible binding sites, and have been used to identify proteins which interact with *Xist* (Chu et al., 2015; McHugh et al., 2015). Alternatively, depending on the visualization system used, RNA Mango has recently been utilized to purify RNA-protein complexes (Panchapakesan et al., 2015, 2017). Since CTCF is *Jpx*'s only known binding partner, identifying other *Jpx*-binding proteins may uncover new regulatory roles for *Jpx* outside of *Xist* activation. In all, these experiments will help identify the protein binding partners and potential transport mechanisms for *Jpx*.

Functional outcomes of Jpx *and* Xist *expression on autosomal genes*

Another follow up study based on my work is to determine the extent of *Jpx*/ *Xist* activity at the autosomal transgene insertion site. In this thesis we have observed *Jpx* and *Xist* expression

at the autosomal Tg(Jpx, Xist) locus, suggesting that *Jpx* may activate *Xist* expression in *cis*. Interestingly, when we measured X-linked gene expression from Tg(Jpx, Xist) fibroblasts, we saw an increase in gene expression relative to wildtype levels for most genes tested. From this data, we hypothesized that Tg(Jpx, Xist) may be inducing gene silencing locally at the autosomal insertion site rather than on the endogenous X chromosome. In other studies using transgenic *Xist* construct insertions, transgenic *Xist* has been demonstrated as able to silence autosomal genes in *cis* (Jiang et al., 2013; Loda et al., 2017). Further, robust *Xist* expression from a transgene can squelch endogenous *Xist*, potentially leading to an increase in X-linked gene expression (Jeon and Lee, 2011). To understand how transgenic *Xist* may influence autosomal and X-linked silencing in my transgenic mice, I plan to begin with a deeper analysis of autosomal gene expression at the transgene insertion site.

To begin this experiment, we performed RNA-Sequencing on transgenic mouse fibroblasts extracted from a separate transgenic mouse line available in the lab. The "TgBAC8" construct is similar to Tg(Jpx, Xist) but contains a slightly larger region of the Xic (Tg(Jpx, Xist) was originally subcloned from TgBAC8). Specifically, we used fibroblasts from the Tg2087 line of TgBAC8 mice, which has been described in (Sun et al., 2015). As with Tg(Jpx, Xist), the TgBAC8 transgene in this line was also randomly integrated into an autosomal location. In order to determine the transgene integration site and observe the effect on surrounding autosomal gene expression, RNA-Seq was performed in collaboration with the Ali Mortazavi lab at UC Irvine. Relative to wildtype fibroblasts, transgenic fibroblasts displayed significantly reduced gene expression at two loci. DNA FISH will next be used to determine which chromosome and specific locus the transgene has integrated into. Once the transgene integration site has been

confirmed, we can continue our study on surrounding gene expression. Then, we can analyze the transgene's effect on endogenous *Xist* expression and X-linked silencing.

In addition to testing *Jpx*'s *cis* activity and the extent of *Xist* silencing at autosomal loci, this study also aims to identify the region of the Xic which is sufficient for *Xist* expression. A long standing, unresolved aim in the field is to identify the necessary and sufficient regions on the X chromosome which can regulate *Xist* expression and induce XCI. In a previous recent study (Loda et al., 2017), the authors inserted a 300kb Xic transgene into an autosome and were able to observe *Xist* expression and autosomal silencing. Here, TgBAC8 is 194kb and appears to contain all necessary regulatory elements for *Xist* expression and function. TgBAC8 contains five lncRNA genes (*Jpx, Xist, Tsix, Xite, Tsx*) which are associated with both positive and negative regulation of *Xist*. Once we have described the function of TgBAC8, we can continue this study by characterizing the Xic and *Xist* function in the Tg(Jpx, Xist) transgene, which is 120kb and contains only the *Jpx* and *Xist* genes. We can begin studying Tg(Jpx, Xist) in a similar way as TgBAC8, by RNA-Seq on mouse fibroblasts to determine how *Xist* influences autosomal gene silencing. In all, these experiments narrow down the Xic to determine which region is sufficient to induce *Xist* expression and gene silencing.

4.3 Broader directions

4.3.1 Achieving *Jpx* deletion in the mouse through a conditional knockout

More broadly, while I have tested the sufficiency of *Jpx* in mouse XCI, it remains unknown if *Jpx* is also necessary for *Xist* activation in the mouse. The necessity of *Jpx* in XCI is unclear based on mESC knockout models, with arguments both for (Tian et al., 2010) and

against (Barakat et al., 2014) a necessary role for *Jpx* as an *Xist* activator. To resolve this debate, I propose developing a *Jpx* knockout mouse model. Specifically, I plan to conditionally knock out *Jpx* in the mouse embryo proper at the start of XCI. LncRNA knockouts are not trivial to perform or interpret in mice. Some of the relevant challenges and strategies for developing this mouse model are described below.

Challenges with interpreting lncRNA loss-of-function data

A variety of strategies for accomplishing lncRNA loss-of-function have been described in mice, including genomic locus deletion, promoter deletion, and use of RNAi to knock down transcript levels (Bassett et al., 2014). Some of the first studies disrupting the *Xist* and *H19* loci in mice accomplished loss-of-function by replacing all or part of the genomic locus with a neomycin expression cassette (Marahrens et al., 1997; Ripoche et al., 1997). Broad phenotypes were reported in the *Xist* knockout, such as female embryonic lethality (Marahrens et al., 1997). Later, another study utilized a different strategy, locus inversion, for knocking out *Xist* and similarly reported embryonic lethality (Senner et al., 2011). Together, these studies argued that *Xist* is necessary for dosage compensation in female mice.

While broad phenotypes were observed in both of these studies, lncRNA deletions often display no phenotype, making functional analysis particularly challenging (Sauvageau et al., 2013). For example, three separate loss-of-function strategies have been described for *Malat1*: genomic deletion of the entire gene locus, LacZ reporter insertion and premature transcriptional termination, and deletion of a region containing the promoter and first exon (Eissmann et al., 2012; Nakagawa et al., 2012; Zhang et al., 2012). In all three cases, however, no phenotype was

observed at the organismal level. This might suggest that, despite strong evidence for function at the molecular level, lncRNA make a relatively small contribution to animal development.

Alternatively, a lncRNA may be functionally redundant. In this case, a single gene knockout would not show a phenotype because its function is being compensated by another, possibly undiscovered, lncRNA. Cases of functional redundancy in lncRNA have been described in zebrafish (Ulitsky et al., 2011) and in fruit flies. Specifically for the Drosophila dosage compensation system, lncRNA *roX1* and *roX2* are functionally redundant, and a double knockout is required to abolish dosage compensation mechanisms (Franke and Baker, 1999). Therefore, lack of a phenotype at the organismal level does not necessarily indicate the lack of an overall function for lncRNA. As observed with miRNA functional studies, it may be necessary to knock out the complete biogenesis machinery, rather than a single lncRNA in the system, to uncover significant functions for lncRNA (Park et al., 2010).

Reproducibility and off-target effects

Intriguingly, recent reports on the function of lncRNA *Hotair* in mice have questioned the reproducibility of lncRNA deletion studies, and added a level of complexity to experimental design and analysis. The function of mouse *Hotair* was originally determined by a conditional knockout of the mouse *Hotair* gene (Li et al., 2013). Based on this knockout, *Hotair* was understood to regulate homeotic body patterning by influencing homeobox genes at distant loci in *trans*. In particular, homeotic transformations of the mouse spine and wrist were observed (Li et al., 2013). In a second study which replaced *Hotair* exons with a LacZ construct, homeotic skeletal transformations were also observed (Lai et al., 2015). However, when the original

Hotair knockout allele was analyzed in a different, mixed mouse genetic background, separate spinal transformations were observed (Amandio et al., 2016). In this mouse model, *Hotair* was also found to influence neighboring homeobox genes in *cis*, with little *trans* influence on genes in separate hox loci. The dispute regarding *Hotair*'s function has not been resolved, but prompts further analysis particularly of technical parameters such as the genetic mouse background, deletion strategy, and data analysis.

Mouse background has been shown to influence the expression pattern of lncRNA genes (Gomez et al., 2013) and knockout phenotypes of protein coding genes (Threadgill et al., 1995). Therefore, the genetic background used in future lncRNA knockout studies should be carefully selected and reported. Ideally, to eliminate the possibility of strain-specific phenotypes, knockout mouse phenotypes should be analyzed in multiple backgrounds: by inbred mouse lines and genetically crossed lines. This control was performed during the deletion and functional analysis of *Rnf12* in the mouse epiblast, in which the authors used an inbred mouse line and two mixed background crosses to confirm their results (Shin et al., 2014). Such a detailed analysis may not practical given the time and resources necessary. If using a single strain of mice, we should be cognizant of strain-specific phenotypes or off-target effects.

Repeating the *Hotair* deletion using a mixed mouse background produced both targeted and off-target effects. While the deletion did lead to a targeted defect in spinal morphology, the affected vertebrae differed between the original and repeat experiments (Amandio et al., 2016; Li et al., 2013). Further, several new transcripts were identified in the repeat study (Amandio et al., 2016). These off-target noncoding RNA transcripts arose from new sequences spanning the *Hotair* deletion locus. They were transcribed from formerly uncharacterized promoters, or allowed to continue transcription based on a missing transcription termination sequence within

the deleted sequence. Strand-specific RNA-sequencing identified novel transcripts, including 'Ghost of Hotair' (*Ghostair*) on the sense strand and both short and long anti-*Hotair* (*AHotair* and *LAHotair*) transcripts on the antisense strand (Amandio et al., 2016). These novel transcripts are functionally independent of *Hotair*, and may impact gene expression in the same locus or at distant genomic loci. Therefore, both *trans* and *cis* mechanisms should be considered when profiling for off-target effects, especially for a lncRNA like *Jpx* which has been shown to use both mechanisms to influence target gene expression.

Conditional knockouts

LncRNA are highly tissue specific and are developmentally regulated. Therefore, I expect conditional knockouts that induce loss-of-function at the time and tissue in which the lncRNA is expressed to most accurately resolve a lncRNA's function. This technique has recently been used to target *Xist* function during early embryogenesis. Specifically, a Sox2-driven Cre recombinase was used to conditionally delete the *Xist* promoter region and exons 1-3 from the mouse epiblast, resulting in female homozygous *Xist*-null progeny (Yang et al., 2016). This specific, targeted knockout allowed for study of *Xist* specifically in the developing embryo, which would not have been possible with a simple cross of heterozygous *Xist*-null mice, since *Xist* is required for both random XCI (rXCI) in the embryo and imprinted XCI (iXCI) in extraembryonic tissues (Wutz, 2011). Surprisingly, the female homozygous *Xist* null mouse was viable, and further analysis revealed the presence of an entirely new, *Xist*-independent method of dosage compensation (Yang et al., 2016). Therefore, conditionally knocking out *Xist* has allowed for more specific study of its function and brought forth new questions about its role in XCI.

A Sox2-Cre allele has also been used to conditionally knockout *Rnf12* in the mouse embryo. Prior to this knockout, *Rnf12* deletions in mESCs demonstrated that RNF12 is required for *Xist* activation (Barakat et al., 2011). However, when conditionally deleted from the mouse epiblast, *Xist* was still expressed and XCI proceeded. rXCI was thus found to proceed in an *Rnf12*-independent manner, while iXCI was dependent on *Rnf12* function (Shin et al., 2010, 2014; Wang et al., 2017).

Based on this knowledge, I propose a conditional deletion of *Jpx* from the mouse embryo using the same Sox2-Cre allele. By deleting *Jpx* specifically at the start of XCI, when the gene is actively transcribed, I would be analyzing *Jpx*'s function at the most relevant time point. This method is also expected to most efficiently target *Jpx* while eliminating off-target effects, such as those which may arise from deleting *Jpx* from extraembryonic tissues. Further, this knockout strategy can distinguish between functional roles for *Jpx* in rXCI and iXCI, as observed with the *Rnf12* conditional knockout (Wang et al., 2017). Although I expect that *Jpx* is necessary for *Xist* expression during random XCI, which is the system modeled by differentiating mESCs and by my transgenic mouse fibroblasts, it is unknown if *Jpx* will also hold a functional role in iXCI. To develop the *Jpx* knockout mouse model, CRISPR could be used to quickly and efficiently flox the *Jpx* gene in mice (Wang et al., 2013; Yang et al., 2014). Once *Jpx* has been conditionally deleted, I would extract embryos at time points throughout XCI (E3.5, 5.5, 7.5 for before, during, and after XCI) and look for morphological defects in transgenic embryos, as well as measure *Jpx* and *Xist* expression. In all, a conditional *Jpx* knockout will determine if *Jpx* is necessary for *Xist* activation in mice, and may uncover a new role for *Jpx* in iXCI. Further, this *Jpx* loss-of-function mouse model will complement the gain-of-function data presented earlier in this thesis, rounding out the study of *Jpx*'s function and mechanism in mice.

4.3.2 Investigating *JPX* function in human XCI

Finally, the role of *JPX* in human XCI remains entirely unknown. The *Jpx* gene sequence is relatively conserved between mouse and human (Chureau et al., 2002). Yet *Xist* gene regulation likely differs between the two systems because no functional *Tsix* lncRNA has been detected in the human for negative *Xist* regulation (Chureau et al., 2002; Horvath et al., 2011; Migeon et al., 2001). Does *JPX* function as an *XIST* activator in the human system, as *Jpx* does in the mouse?

Human *JPX* function can be studied in several ways. First, human stem cells (or iPSCs) can serve as model systems for analyzing *JPX* function over the course of XCI and generally at different developmental stages. Next, since *XIST* is dysregulated in many cancers, cancer cell lines may provide relevant information on altered *JPX* levels and corresponding *XIST* expression. Finally, mouse models can also be utilized to study functional homology between mouse and human *Jpx/ JPX*. For these experiments, I propose knocking out *Jpx* in the mouse (using techniques described in the previous section) and replacing it with human *JPX*. This will determine if *JPX* is functionally homologous to mouse *Jpx* at the organismal level. The same knockout and replacement experiment can be performed using cultured mESCs, particularly using the *Jpx* knockout cell line described in (Tian et al., 2010). These cells display an obvious morphological phenotype when one copy of *Jpx* is removed, so it would be relatively easy to observe a rescue by human *JPX* if it is functionally homologous. In addition, functional roles for *JPX* outside of an *XIST* activator should be monitored. Since human *XIST* is under different regulatory control than *Xist* in the mouse, the function of *JPX* may have also diverged. In all, these experiments will determine a functional role for *JPX* in human XCI. This will aid in our

understanding of lncRNA functional evolution and will give insight into our own, human X-Chromosome Inactivation mechanisms.

4.4 Perspective

Dosage compensation mechanisms are essential for balancing X-linked gene products between the sexes. The functions of the lncRNA regulating these processes have been well studied and are often used as model systems to broadly understand lncRNA function, mechanism, regulation, and evolution. However, the function of most lncRNA remain unknown, and specific questions remain in each model system. In this thesis, I have provided a detailed functional and mechanistic study of the lncRNA *Jpx* in mouse X-Chromosome Inactivation. This work resolves a long standing argument in the field regarding *Jpx*'s role as an *Xist* activating factor. While it is still unclear what the primary, necessary *Xist* activator is in mice, the future directions presented in this thesis will examine if *Jpx* is necessary for *Xist* activation *in vivo.*

Many questions remain regarding *Jpx*'s mechanisms and XCI in general, some of which have been described above. For example: What is the trigger that initiates XCI, and how does *Jpx* copy number contribute to X chromosome counting? Perhaps the *Jpx* transcript dosage plays a role via cross talk between *Jpx* loci. To address this, we could begin by studying how *Jpx* moves through the nucleus: if either by passive diffusion or actively towards target loci (see future directions above). Understanding which proteins bind *Jpx* will also help determine *Jpx*'s molecular mechanism in mice. In mESCs, *Jpx* specifically binds CTCF protein at the *Xist* promoter. Does *Jpx* bind other proteins in mESCs or mice? Further, how does *Jpx* maintain specific affinity for this CTCF molecule when CTCF is ubiquitous throughout the genome?

Conceivably, a more detailed analysis of the *Jpx* transcript secondary structure will provide biochemical reasoning to explain this specificity. Other protein co-factors which may bind *Jpx* can also provide specificity to the interaction. Outside of random XCI in the embryo, does *Jpx* play a role in imprinted XCI as well? To answer this question, we would need to specifically isolate *Jpx*'s function in rXCI vs iXCI. This could be achieved using the conditional knockout model proposed in the future directions section. Finally, how do *Jpx*'s mechanisms translate to human XCI? Some features of the Xic are divergent between mouse and human, including the *TSIX* gene. Without knowledge of a functional repressor, *XIST* gene regulation will need to be revisited in humans. It would be intriguing to delete *JPX* in human cancer cell lines and observe if *XIST* expression decreases. This would describe a similar role for *JPX* as an *XIST* activator in human XCI.

For lncRNA in general, which lncRNA are essential, and what are their functions and mechanisms? How are lncRNA functions conserved across species? How does genetic background affect lncRNA function? What is the best strategy for resolving functional discrepancies? This last question is especially important for lncRNA research moving forward. A combination of loss-of-function and gain-of-function models, as well as a full understanding of the biogenesis pathway in which the lncRNA participates, will be a step in the right direction.

My work has contributed valuable insight into the mechanisms regulating *Xist* gene expression and ultimately XCI initiation. I have resolved the function and mechanism of *Jpx* within XCI, and established mouse models to continue exploring lncRNA mechanisms in the future. This work shapes the course of XCI research in terms of *Xist* activating factors and their functions *in vivo*.

4.5 References

Amandio, A.R., Necsulea, A., Joye, E., Mascrez, B., and Duboule, D. (2016). Hotair Is Dispensible for Mouse Development. PLoS Genet. *12*, 1–27.

Autour, A., Jeng, S.C.Y., Cawte, A.D., Abdolahzadeh, A., Galli, A., Panchapakesan, S.S.S., Rueda, D., Ryckelynck, M., and Unrau, P.J. (2018). Fluorogenic RNA Mango aptamers for imaging small non-coding RNAs in mammalian cells. Nat. Commun. *9*, 1–12.

Barakat, T.S., Gunhanlar, N., Pardo, C.G., Achame, E.M., Ghazvini, M., Boers, R., Kenter, A., Rentmeester, E., Grootegoed, J.A., and Gribnau, J. (2011). RNF12 Activates Xist and Is Essential for X Chromosome Inactivation. PLoS Genet. *7*, 1–12.

Barakat, T.S., Loos, F., Van Staveren, S., Myronova, E., Ghazvini, M., Grootegoed, J.A., and Gribnau, J. (2014). The trans-activator RNF12 and cis-acting elements effectuate X chromosome inactivation independent of X-pairing. Mol. Cell *53*, 965–978.

Bassett, A.R., Akhtar, A., Barlow, D.P., Bird, A.P., Brockdorff, N., Duboule, D., Ephrussi, A., Ferguson-Smith, A.C., Gingeras, T.R., Haerty, W., et al. (2014). Considerations when investigating lncRNA function in vivo. Elife *3*, 1–14.

Chu, C., Zhang, Q.C., da Rocha, S.T., Flynn, R.A., Bharadwaj, M., Calabrese, J.M., Magnuson, T., Heard, E., and Chang, H.Y. (2015). Systematic Discovery of Xist RNA Binding Proteins. Cell *161*, 404–416.

Chureau, C., Prissette, M., Bourdet, A., Cattolico, L., Jones, L., Avner, P., and Duret, L. (2002). Comparative Sequence Analysis of the X-Inactivation Center Region in Mouse, Human, and Bovine. Genome Res. *12*, 894–908.

Dolgosheina, E. V, Jeng, S.C.Y., Panchapakesan, S.S.S., Cojocaru, R., Chen, P.S.K., Wilson, P.D., Hawkins, N., Wiggins, P.A., and Unrau, P.J. (2014). RNA Mango Aptamer-Fluorophore: A Bright, High-Affinity Complex for RNA Labeling and Tracking. ACS Chem. Biol. *9*, 2412–2420.

Eissmann, M., Gutschner, T., Hämmerle, M., Günther, S., Caudron-Herger, M., Gross, M., Schirmacher, P., Rippe, K., Braun, T., Zörnig, M., et al. (2012). Loss of the abundant nuclear non-coding RNA MALAT1 is compatible with life and development. RNA Biol. *9*, 1076–1087.

Engreitz, J.M., Pandya-Jones, A., McDonel, P., Shishkin, A., Sirokman, K., Surka, C., Kadri, S., Xing, J., Goren, A., Lander, E.S., et al. (2013). The Xist lncRNA exploits three-dimensional genome architecture to spread across the X chromosome. Science *341*, 1237973.

Engreitz, J.M., Ollikainen, N., and Guttman, M. (2016). Long non-coding RNAs: spatial amplifiers that control nuclear structure and gene expression. Nat. Rev. Mol. Cell Biol. *17*, 756–770.

Franke, A., and Baker, B.S. (1999). The rox1 and rox2 RNAs are essential components of the compensasome, which mediates dosage compensation in Drosophila. Mol. Cell *4*, 117–122.

Gomez, J.A., Wapinski, O.L., Yang, Y.W., Bureau, J.F., Gopinath, S., Monack, D.M., Chang, H.Y., Brahic, M., and Kirkegaard, K. (2013). The NeST long ncRNA controls microbial susceptibility and epigenetic activation of the interferon-γ locus. Cell *152*, 743–754.

Hocine, S., Raymond, P., Zenklusen, D., Chao, J.A., and Singer, R.H. (2013). Single-molecule analysis of gene expression using two-color RNA labeling in live yeast. Nat. Methods *10*, 119–123.

Horvath, J.E., Sheedy, C.B., Merrett, S.L., Diallo, A.B., Swofford, D.L., Green, E.D., and Willard, H.F. (2011). Comparative analysis of the primate X-inactivation center region and reconstruction of the ancestral primate XIST locus. Genome Res. *21*, 850–862.

Itzkovitz, S., and Oudenaarden, A. Van (2011). Validating transcripts with probes and imaging technology. Nat. Methods *8*, S12–S19.

Jeon, Y., and Lee, J.T. (2011). YY1 Tethers Xist RNA to the inactive X nucleation center. Cell *146*, 119–133.

Jiang, J., Jing, Y., Cost, G.J., Chiang, J.-C., Kolpa, H.J., Cotton, A.M., Carone, D.M., Carone, B.R., Shivak, D.A., Guschin, D.Y., et al. (2013). Translating dosage compensation to trisomy 21. Nature *500*, 296–300.

Lai, K.M.V., Gong, G., Atanasio, A., Rojas, J., Quispe, J., Posca, J., White, D., Huang, M., Fedorova, D., Grant, C., et al. (2015). Diverse phenotypes and specific transcription patterns in twenty mouse lines with ablated lincRNAs. PLoS One *10*, 1–21.

Lange, S., Katayama, Y., Schmid, M., Burkacky, O., Brauchle, C., Lamb, D.C., and Jansen, R.-P. (2008). Simultaneous Transport of Different Localized mRNA Species Revealed by Live-Cell Imaging. Traffic *9*, 1256–1267.

Li, L., Liu, B., Wapinski, O.L., Tsai, M.C., Qu, K., Zhang, J., Carlson, J.C., Lin, M., Fang, F., Gupta, R.A., et al. (2013). Targeted Disruption of Hotair Leads to Homeotic Transformation and Gene Derepression. Cell Rep. *5*, 3–12.

Loda, A., Brandsma, J.H., Vassilev, I., Servant, N., Loos, F., Amirnasr, A., Splinter, E., Barillot, E., Poot, R.A., Heard, E., et al. (2017). Genetic and epigenetic features direct differential efficiency of Xist-mediated silencing at X-chromosomal and autosomal locations. Nat. Commun. *8*.

Maass, P.G., Barutcu, A.R., Shechner, D.M., Weiner, C.L., Melé, M., and Rinn, J.L. (2018). Spatiotemporal allele organization by allele-specific CRISPR live-cell imaging (SNP-CLING). Nat. Struct. Mol. Biol. *25*, 176–184.

Marahrens, Y., Panning, B., Dausman, J., Strauss, W., and Jaenisch, R. (1997). Xist-deficient mice are defective in dosage compensation but not spermatogenesis. Genes Dev. *11*, 156–166.

McHugh, C.A., Chen, C.-K., Chow, A., Surka, C.F., Tran, C., McDonel, P., Pandya-Jones, A., Blanco, M., Burghard, C., Moradian, A., et al. (2015). The Xist lncRNA interacts directly with SHARP to silence transcription through HDAC3. Nature *521*, 232–236.

Migeon, B.R., Chowdhury, A.K., Dunston, J.A., and McIntosh, I. (2001). Identification of TSIX, Encoding an RNA Antisense to Human XIST, Reveals Differences from its Murine Counterpart:

Implications for X Inactivation. Am. J. Hum. Genet. *69*, 951–960.

Nakagawa, S., Ip, J.Y., Shioi, G., Tripathi, V., Zong, X., Hirose, T., and Prasanth, K. V. (2012). Malat1 is not an essential component of nuclear speckles in mice. RNA *18*, 1487–1499.

Ng, K., Daigle, N., Bancaud, A., Ohhata, T., Humphreys, P., Walker, R., Ellenberg, J., and Wutz, A. (2011). A system for imaging the regulatory noncoding Xist RNA in living mouse embryonic stem cells. Mol. Biol. Cell *22*, 2634–2645.

Panchapakesan, S.S.S., Jeng, S.C.Y., and Unrau, P.J. (2015). RNA complex purification using high-affinity fluorescent RNA aptamer tags. Ann. N. Y. Acad. Sci. *1341*, 149–155.

Panchapakesan, S.S.S., Ferguson, M.L., Hayden, E.J., Chen, X.I.N., Hoskins, A.A., and Unrau, P.J. (2017). Ribonucleoprotein purification and characterization using RNA Mango. RNA *23*, 1592–1599.

Park, C.Y., Choi, Y.S., and Mcmanus, M.T. (2010). Analysis of microRNA knockouts in mice. Hum. Mol. Genet. *19*, 169–175.

Quinn, J.J., Ilik, I.A., Qu, K., Georgiev, P., Chu, C., Akhtar, A., and Chang, H.Y. (2014). Revealing long noncoding RNA architecture and functions using domain-specific chromatin isolation by RNA purification. Nat. Biotechnol. *32*, 933–940.

Ripoche, M.A., Kress, C., Poirier, F., and Dandolo, L. (1997). Deletion of the H19 transcription unit reveals the existence of a putative imprinting control element. Genes Dev. *11*, 1596–1604.

Sauvageau, M., Goff, L.A., Lodato, S., Bonev, B., Groff, A.F., Gerhardinger, C., Sanchez-Gomez, D.B., Hacisuleyman, E., Li, E., Spence, M., et al. (2013). Multiple knockout mouse models reveal lincRNAs are required for life and brain development. Elife *2013*, 1–24.

Senner, C.E., Nesterova, T.B., Norton, S., Dewchand, H., Godwin, J., Mak, W., and Brockdorff, N. (2011). Disruption of a conserved region of Xist exon 1 impairs Xist RNA localisation and X-linked gene silencing during random and imprinted X chromosome inactivation. Development *138*, 1541–1550.

Shin, J., Bossenz, M., Chung, Y., Ma, H., Byron, M., Taniguchi-Ishigaki, N., Zhu, X., Jiao, B., Hall, L.L., Green, M.R., et al. (2010). Maternal Rnf12/RLIM is required for imprinted X-chromosome inactivation in mice. Nature *467*, 977–981.

Shin, J., Wallingford, M.C., Gallant, J., Marcho, C., Jiao, B., Byron, M., Bossenz, M., Lawrence, J.B., Jones, S.N., Mager, J., et al. (2014). RLIM is dispensable for X-chromosome inactivation in the mouse embryonic epiblast. Nature *511*, 86–89.

Simon, M.D., Wang, C.I., Kharchenko, P. V, West, J.A., Chapman, B.A., Alekseyenko, A.A., Borowsky, M.L., Kuroda, M.I., and Kingston, R.E. (2011). The genomic binding sites of a noncoding RNA. Proc. Natl. Acad. Sci. *108*, 20497–20502.

Sun, S., Del Rosario, B.C., Szanto, A., Ogawa, Y., Jeon, Y., and Lee, J.T. (2013). Jpx RNA Activates Xist by Evicting CTCF. Cell *153*, 1537–1551.

Sun, S., Payer, B., Namekawa, S., An, J.Y., Press, W., Catalan-Dibene, J., Sunwoo, H., and Lee, J.T. (2015). Xist imprinting is promoted by the hemizygous (unpaired) state in the male germ

line. Proc. Natl. Acad. Sci. *112*, 14415–14422.

Sunwoo, H., Wu, J.Y., and Lee, J.T. (2015). The Xist RNA-PRC2 complex at 20-nm resolution reveals a low Xist stoichiometry and suggests a hit-and-run mechanism in mouse cells. Proc. Natl. Acad. Sci. *112*, E4216-4225.

Threadgill, D.W., Dlugosz, A.A., Hansen, L.A., Tennenbaum, T., Lichti, U., Yee, D., Lamantia, C., Mourton, T., Herrup, K., Raymond, C., et al. (1995). Targeted Disruption of Mouse EGF Receptor: Effect of Genetic Background on Mutant Phenotype. Science (80-.). *269*, 230–234.

Tian, D., Sun, S., and Lee, J.T. (2010). The long noncoding RNA, Jpx, Is a molecular switch for X chromosome inactivation. Cell *143*, 390–403.

Ulitsky, I., Shkumatava, A., Jan, C.H., Sive, H., and Bartel, D.P. (2011). Conserved function of lincRNAs in vertebrate embryonic development despite rapid sequence evolution. Cell *147*, 1537–1550.

Wang, F., McCannell, K.N., Bošković, A., Zhu, X., Shin, J.D., Yu, J., Gallant, J., Byron, M., Lawrence, J.B., Zhu, L.J., et al. (2017). Rlim-Dependent and -Independent Pathways for X Chromosome Inactivation in Female ESCs. Cell Rep. *21*, 3691–3699.

Wang, H., Yang, H., Shivalila, C.S., Dawlaty, M.M., Cheng, A.W., Zhang, F., and Jaenisch, R. (2013). One-Step Generation of Mice Carrying Mutations in Multiple Genes by CRISPR / Cas-Mediated Genome Engineering. Cell *153*, 910–918.

Wang, K.C., Yang, Y.W., Liu, B., Sanyal, A., Corces-Zimmerman, R., Chen, Y., Lajoie, B.R., Protacio, A., Flynn, R.A., Gupta, R.A., et al. (2011). A long noncoding RNA maintains active chromatin to coordinate homeotic gene expression. Nature *472*, 120–124.

Wutz, A. (2011). Gene silencing in X-chromosome inactivation: advances in understanding facultative heterochromatin formation. Nat. Rev. Genet. *12*, 542–553.

Yang, H., Wang, H., and Jaenisch, R. (2014). Generating genetically modified mice using CRISPR/Cas-mediated genome engineering. Nat. Protoc. *9*, 1956–1968.

Yang, L., Kirby, J.E., Sunwoo, H., and Lee, J.T. (2016). Female mice lacking Xist RNA show partial dosage compensation and survive to term. Genes Dev. *30*, 1747–1760.

Zhang, B., Arun, G., Mao, Y.S., Lazar, Z., Hung, G., Bhattacharjee, G., Xiao, X., Booth, C.J., Wu, J., Zhang, C., et al. (2012). The lncRNA malat1 is dispensable for mouse development but its transcription plays a cis-regulatory role in the adult. Cell Rep. *2*, 111–123.